MODELING, SIMULATION & CONTROL OF PHOTOVOLTAIC REVERSE OSMOSIS DESALINATION SYSTEM

BY

MOHAMMED RIAZ AHMED

A Thesis Presented to the

DEANSHIP OF GRADUATE STUDIES

KING FAHD UNIVERSITY OF PETROLEUM & MINERALS

DHAHRAN, SAUDI ARABIA

In Partial Fulfillment of the
Requirements for the Degree of

MASTER OF SCIENCE

In

SYSTEMS ENGINEERING

NOVEMBER 2013

KING FAHD UNIVERSITY OF PETROLEUM & MINERALS

DHAHRAN- 31261, SAUDI ARABIA

DEANSHIP OF GRADUATE STUDIES

This thesis, written by **MOHAMMED RIAZ AHMED** under the direction of his thesis advisor and approved by his thesis committee, has been presented and accepted by the Dean of Graduate Studies, in partial fulfillment of the requirements for the degree of **MASTER OF SCIENCE IN SYSTEMS ENGINEERING.**

Dec 30, 13

Dr. Fouad Al Sunni
Department Chairman

Dr. Salam A. Zummo
Dean of Graduate Studies

6/1/14

Date

M. El Sh.

Dr. Moustafa El Shafei
(Advisor)

Anwar Khalil Sheikh

Dr. Anwar K. Sheikh
(Member)

Dr. Abdul Wahid Al-Saif
(Member)

IN THE NAME OF ALLAH, THE MOST GRACIOUS, THE MOST MERCIFUL

DEDICATED

TO

MY FAMILY

ACKNOWLEDGMENTS

All praise is due only to ALLAH subhana wa ta' aala, the sustainer of the worlds, the most merciful for granting me patience, health and knowledge to complete this work.

I would like to thank King Fahd University of Petroleum and Minerals for providing me the opportunity and financial assistance for pursuing MS program.

I acknowledge my sincere appreciation and thanks to Dr. Moustafa El Shafei for his supervision and guidance throughout this research. I am grateful to my committee, Dr. Anwar K. Sheikh and Dr. Abdul Wahid Al- Saif for their guidance and cooperation. I am also indebted to the Department Chairman, Dr. Fouad Al Sunni and other faculty members especially Dr. Abdur Rahim and Dr. Magdi S. Mahmoud for their support. I acknowledge the efforts and guidance of Mr. Naseer and Mr. Sabih and thank them whole heartedly.

I would also like to thank all my friends back home and at KFUPM for their encouragement, support and the fun-filled memories shared with them.

Last but the most special thanks are for two of the most important people in my life, my parents, for their unconditional love, sacrifices, efforts, prayers and constant encouragement without which I would be nothing and consider myself extremely lucky to have got the best parents in the world.

TABLE OF CONTENTS

LIST OF TABLES

LIST OF FIGURES

ABSTRACT (ENGLISH)

Full Name : [Mohammed Riaz Ahmed]

Thesis Title : [Modeling Simulation and Control of Photovoltaic Reverse Osmosis Desalination System]

Major Field : [SYSTEMS ENGINEERING]

Desalination is the process of removal of salts from seawater or brackish water to produce fresh water. There are various desalination techniques that are available but the most popular is the reverse osmosis desalination which is based on membrane separation. This work presents the performance evaluation, system identification and control of a small-scale reverse osmosis desalination system which is intended to be used with solar panels but the solar energy is utilized to charge the batteries with MPPT (Maximum power point tracking). The RO system then operates on batteries at night, at steady pressure to ensure smooth and trouble-free operation of the system which is not guaranteed when the system is operated on solar energy. For the purpose of performance evaluation, the system is run at steady state for certain duration of time and corresponding current and voltage is measured every second. Other performance evaluation parameters namely the salt rejection, the recovery ratio and the specific energy consumption in kWh/m3 are also studied. Three discrete time models namely ARX, ARMAX and Output Error model are estimated using system identification and compared against each other. The data for identification is collected for the product water flow rate considering the pump motor control voltage as the manipulated variable. The models are also validated with a separate experimental dataset. Two state-space models are also developed using subspace identification and prediction error method and their performance is evaluated using optimal linear quadratic regulator. The best model was further investigated for different control penalties. Model predictive controller is also evaluated for the state-space model obtained from subspace identification. The model predictive control was investigated for the unconstrained and the constrained case and the robustness was also studied by considering disturbance in the input variable. Simulation results show that the constrained model predictive control is more suited for the given system. The optimal and model predictive control algorithms were developed and simulated using MATLAB.

ABSTRACT (ARABIC)

تعرف عملية إزالة الأملاح من مياه البحر أو المياه المالحه عموما لإنتاج الماء العذب بالتحلية. تختلف عمليات التحلية في أشكالها و طرقها غير أن أشهرها تلك التي تعتمد على الخاصية الإسموزية العكسية المعتمدة على أختلاف التركيز على جانبي الغشاء المنفذ.يتلخص العمل في هذه الرسالة بتقييم كفاءة وحدة تحلية صغيرة، تعمل على الطاقة الشمسية أعتمادا على الخاصية الإسموزية العكسية ، إلى جانب تحديد العلاقات الرياضية التي تخضع لها من أجل التحكم بها. يتم إستخدام الخلايا الشمسية وفق قانون تتبع الطاقة القصوى لتوفير أكبر كمية من الطاقة الضوئية المتاحة في زمان و مكان معينين حيث تستخدم هذه الطاقة لشحن البطاريات المستخدمة في هذه الوحدة الصغيرة حتى يتسنى تشغيلها ليلا تحت ضغط مستقر لتجنب المشاكل المترتبة على أستخدامها نهارا باستخدام طاقة الشمس المباشرة.

يتم تشغيل هذا النظام بشكل مستقر لوقت محدد و يتم في أثنائه أخذ قراءات كل من التيار و فرق الجهد في كل ثانية من الزمن وذلك لتسهيل تحديد كفاءة هذا النظام و التي يمكن إجمالها في إيجاد نسبة التخلص من الأملاح و سرعة التعافي و كمية الطاقة النوعية المستهلكة بوحدة KWh/m^3.

أما بالنسبة لتحديد العلاقات الرياضية التي تخضع لها هذه الوحدة، فقد تم هذا باستخدام ثلاثة نماذج و هي: ARX و Output Error و نموذج ARMAX حيث تمت مقارنة نتائجها جميعا بعضها ببعض، حيث تم تدوين معدل تدفق الماء العذب و جعل مقدار فرق الجهد الكهربائي على محرك المضخة هو المتغير الأساسي. وأيضا تمت مقارنة هذه النتائج بمجموعة من البيانات التجريبية. إضافة إلى النماذج السابقة، فقد تم بناء نموذجين إضافيين إعتمادا على State-Space Models و تمت مقارنة أدائهما باستخدام Prediction Error Method و Subspace Identification إستخدامهما في طريقتي Model Predictive Controller حيث ومن ثم فحص الأفضل منهما تحت ظروف تحكم مختلفة و استخدامه لعمل LQR تم فحص الأخير لتعرف على كفائته تحت ظروف محددة و غير محددة حيث بينت نتائج المحاكاة أن استخدام هذا المتحكم في الظروف المحددة هو الأنسب لهذا النظام.

أخيرا ، فقد تم عمل محاكاة باستخدام برنامج MATLAB لكل من Optimal Controller و Model Predictive Controller. و جمع النتائج و عرضها

Chapter 1

INTRODUCTION

1.1 Water Scarcity around the World

Water is a priceless commodity for human beings for their day-to-day use. It is highly important to provide safe drinkable water to the growing population and also for agricultural and industrial growth. It is a known fact that ninety-seven percent of all water is in the form of oceans, two-percent is in the form of ice mass, and the rivers and lakes form the remaining percentage. However the ever-increasing need for safe drinking water and low-saline water for the industries cannot just be fulfilled by these water sources. It is a known fact that there are many regions in the world which are facing enormous water shortages especially the Arab world, the North African countries and those located in deserts [1]. Lack of good use of water resources leading to water scarcity is one of the most crucial challenges faced by the world in 21st century. The latest UN analysis states that almost 25,000 people die each day due to starvation, and more than700 million are malnourished. Hence the need to increase food production will obviously mean an increase in water demand, as additional water supply would be needed for irrigation, to meet the challenge of more food production. The degradation in water quality has also contributed significantly to a number of problems of global concern, like humans consuming contaminated water, which often causes disease and can lead to early deaths. As per the latest UN analysis, around 1 billion human populations do not have access to clean drinking water, and 2.5 billion do not have basic sanitation services. Every day, almost 2 million tons of human waste is disposed of in rivers and streams which leads to serious degradation in the quality of water. This has pushed the humans to search for alternate fresh water source to avoid this grave condition of

water scarcity. Some of the other reasons that contribute to water scarcity, which cannot be ignored, are the ever-growing population around the world and the increasing water demands for industry and tourism lead to further water shortages. Pollution as well as the exploitation of natural sources of freshwater is equally responsible for the significant decrease in the quality and the quantity of available clean drinking water, worldwide [2].

But the most obvious reason for the deterioration in water-quality is the salinization of water resources. Salinization is a serious issue and is the sole reason for many water bodies across the world becoming unsuitable for drinking purpose because of the high amounts of salinity present in them. The salinity problem has had some serious negative consequences on the political and socio-economical relations of the countries that are sharing the cross-boundary basins [3].

As illustrated in Fig.1.1, the Middle East, North African countries (MENA), the southern European Mediterranean Islands (SEMI) are the areas facing the physical and economic water scarcity. The physical water scarcity refers to the condition when more than 75% of a region's river flows are used for agriculture, domestic or industrial purposes. Economic water scarcity is when human and financial uses limit the access to water, even where water is locally available.

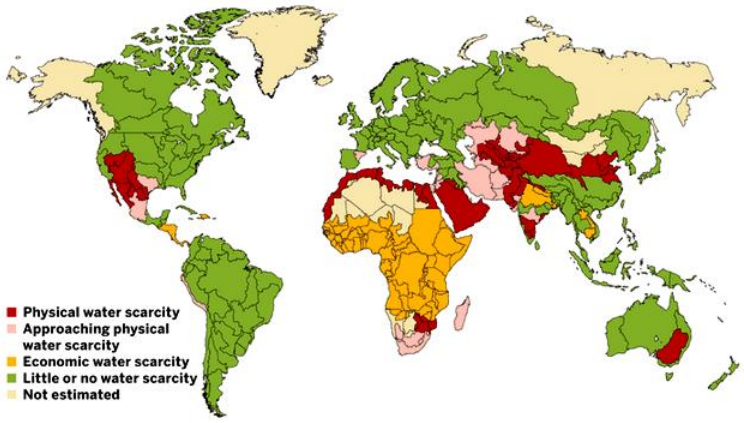

Figure 1.1: Areas of physical and economic water scarcity [4]

There are many countries around the world that are facing huge shortages in the supply of fresh and potable water and definitely Arab world is also a representative of such countries. The interest in water resources is highest for the Arab since they are situated in the driest part of the world and also obviously due to the increasing demand for water to be used for agricultural, industrial and house purposes. As a result we see the Arab countries making continuous efforts for improving their water resources so that they can supply fresh and usable water to villages for agriculture and also to the urban centers to fulfill their water demands. However, the scarcity of water resources has created an imbalance between the water resources that are available and the fresh water demand. Hence in today's times, the fresh water has also become a very critical commodity for the Arab countries, just like electricity. As evident from the projections in Fig.1.2, Middle East is likely to face the problem of water scarcity even in 2025.

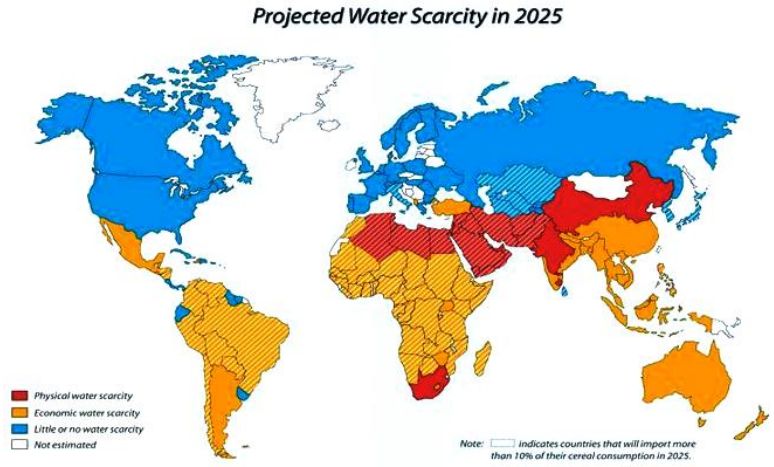

Figure 1.2: Projected Water Scarcity in 2025 [4]

Certainly, the Middle-East is facing the most difficult challenge to fulfill the demand of its communities to supply fresh and potable water. It represents ten-percent of the world's geographical area and five-percent of the world's fresh water consumption and the scenario gets even harder with the ever-increasing population growth which in turn calls for higher amounts of

fresh-water consumption. Hence, the need of the hour is to increase the number of water resources, not just in the Arab countries but in all the developing countries, in general.

1.2 Salinity, Water Classification & Health Guidelines

Salinity, defined as the total dissolved salt content in water, is expressed in terms of the chloride content i.e. mg/L or ppm or total dissolved solids content (TDS). Based on salinity, water can be classified into three groups: 0 to 500 mg/L(ppm) is generally considered as Fresh Water. Brackish Water has salinity between 500 and 30,000 mg/L(ppm) and Seawater has salinity greater than 30,000 mg/L, normally, in the range of 30,000- 50,000 ppm in the form of total dissolved salts whereas majority of the water available on earth has salinity up to 9,000 ppm. Figure 1.3gives a pictorial representation of classification of water based on salinity. World Health Organization (WHO) standard is that, water is suitable for drinking when the TDS level is less than500 ppm and up to 1000 ppm based on taste consideration (special cases).However, no specific health guideline has been proposed due to the fact that there is no data available that one can rely on in order to identify the possible deteriorating effects on health related to the intake of Total Dissolved Solids (TDS) in drinking water.

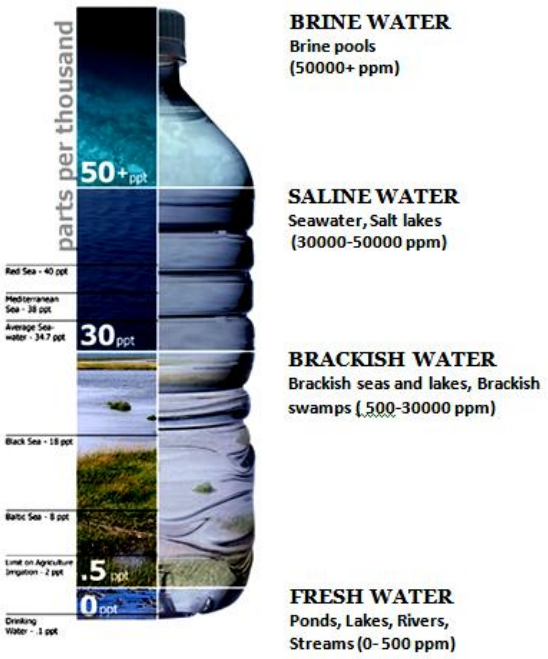

Figure 1.3: Water Classification based on Salinity [5]

However, the intake of brackish water has been associated with health diseases, including diarrhea, diabetes, kidney and gastric disorders. The other pollutants of water that cause salinity are sulphate, fluoride, sodium, selenium etc. In China, Africa and India, for example, high quantity of fluoride in ground water has been the reason for causing a lot of dental problems.

1.3 Desalination- The Answer to Water Scarcity

Approximately, 97% of water on earth is in the form of oceans and therefore qualified as seawater. Of the 3% of planets fresh water, close to 70% is in the form of snow and ice and 30% is in the form of rivers, lakes and ground water. So even though the volume of water available on earth is large, less than 1% of it is suitable for drinking only after using the conventional water treatment only. This is where desalination comes into picture by providing means of utilizing the world's main water resource – the ocean, to obtain fresh water [6]. Hence today, we see that the

use of desalination techniques have increased leaps and bounds around the world especially in Middle East, to reduce the problem of water scarcity.

Desalination, is a natural process which has come about on earth since thousands of years. One such phenomenon is when the sea water freezes near the polar region where the pure water is formed in the form of ice crystals without any salt content. The other phenomenon is the evaporation of water from sea which condenses to form pure water in the form of rain.

But the last two to three decades, have seen immense growth and development in desalination technology which has improved leaps and bounds especially in driest parts of the globe like the Arab world and the Mediterranean. As a result, we see the installation of desalination plants in more than hundred countries around the globe. According to International Desalination Association, till 2009, there were about 14,000 desalination plants worldwide with production capacity of 16,000 million gallons per day.

Today, we have a number of desalination techniques that are available and are accepted as the source that provides fresh water by removing salts from saline water. However, on the flip side, the costs for these desalination techniques can be relatively high because of its rigorous use of energy, but still the cost is less than other alternative energy resources that are available. Hence, we see a widespread increase in the use of desalination processes around the world, to obtain fresh quality of water which is suited for human consumption and for other purposes and this trend is expected to increase continuously in the coming years especially in the Arabian countries and parts of Africa. A visual depiction of the desalination plants installed all over the world is shown in Fig. 1.4.

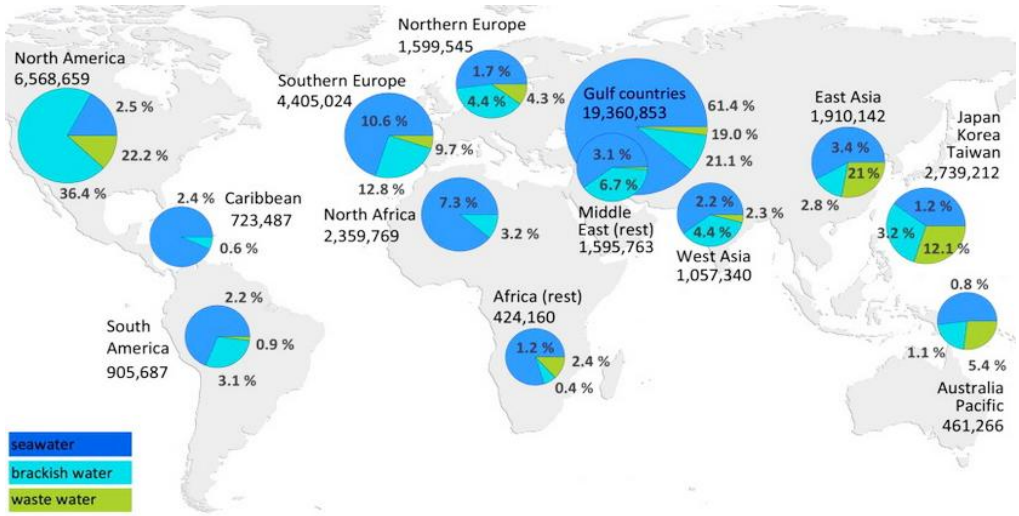

Figure 1.4: Global Desalination capacities in cubic meter per day [7]

As evident in Fig. 1.4, the installed capacity in Middle East is 19,360,853 m3/day. The figure also includes the various source water types as seawater, brackish water and waste water respectively with seawater indicated by color blue. Seawater desalination accounts for majority of water production in Middle East, followed by brackish water and waste water plays a very minor role. The percentage figures given inside the pie diagrams indicate the contribution to the water production globally. Hence the seawater desalination capacity in Middle East represents a whopping 61.4% of the total seawater desalination capacity across the globe. The brackish water capacity represents 21.1% of the worldwide brackish water desalination capacity [7].

Fig.1.5 shows the installed desalination capacity related to the various sources of feed water that are available. The seawater desalination is the most popular, being applied at63% of all the installed desalination units' worldwide and brackish water accounting for 19% of all the installed desalination capacity globally.

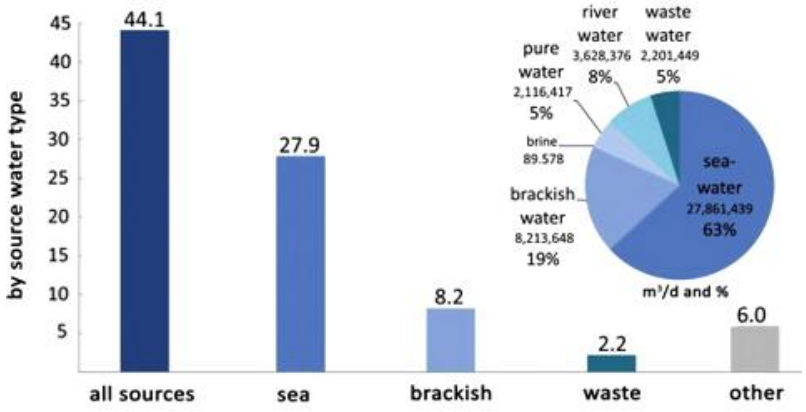

Figure 1.5: Globally installed desalination capacity by feed water sources [8]

1.4 Desalination Techniques

Desalination means producing fresh water from saline water. For this, many methods have been proposed. Fig.1.6 shows the various desalination techniques that are available which have been divided into two main types namely the phase-change which is based on thermal and membrane separation which is based on filtration. Multi-stage flash (MSF), Multiple effect distillation (MED) etc fall under phase-change category whereas Reverse osmosis (RO), Membrane distillation (MD) and Electro dialysis fall under membrane separation desalination techniques. The main desalination processes are shown in Figure.6 and are explained in detail in Chapter .2.

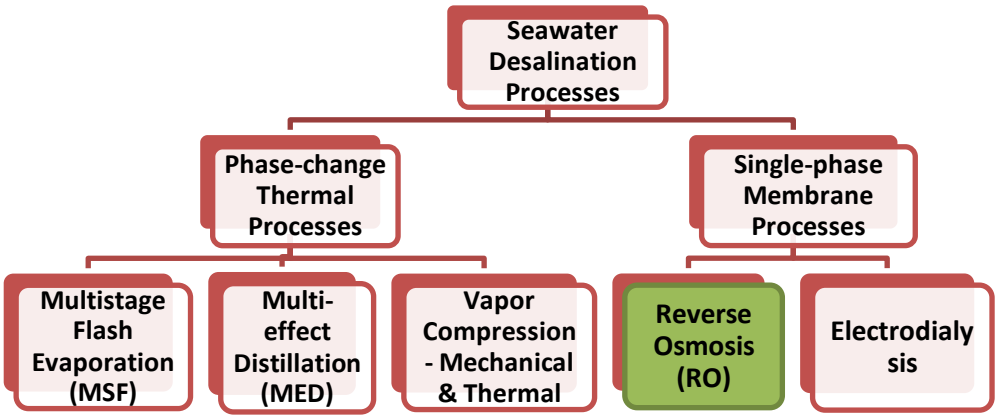

Figure 1.6: Types of desalination processes [9]

Based on installed capacity for all source water types included, more than 80% of the world's desalination capacity is provided by two technologies: Multi-stage flash (MSF), and Reverse Osmosis(RO) (Fig.1.7). The MSF process represents more than 93% of the thermal process production while RO process represents more than 88% of membrane processes production [2].

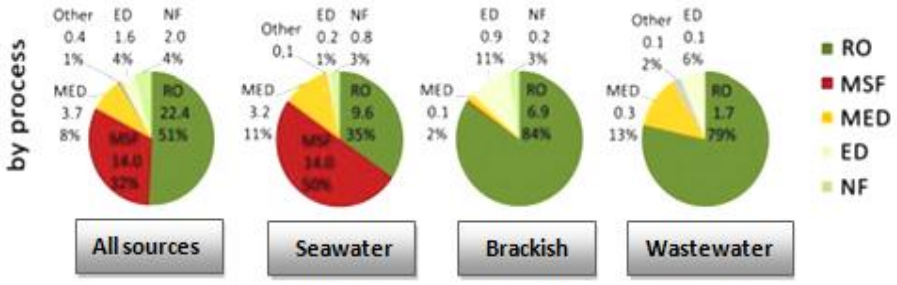

Figure 1.7: Globally installed desalting capacity by process [9]

1.5 Reverse Osmosis – The Most Popular in Desalination

It is a known fact that desalination by reverse osmosis has turned out to be the leader amongst the desalination types mentioned above, mainly because it is available in a range of sizes and has low specific energy consumption (SEC), about 3-8 kWh of electric energy per m3 of freshwater

produced from seawater, as compared to multi-effect distillation and vapor compression techniques. Other advantages of RO systems include low maintenance costs and investment costs and the flexibility of the location of site make it the best alternative amongst the other desalination techniques, especially for applications in remote areas with small and medium local water demand.

1.6 Reverse Osmosis – The Principle

To understand the principle of reverse osmosis, it is important to understand the principle behind osmosis. Osmosis is a natural flow through a semi-permeable membrane. The direction of flow through the membrane is determined by the chemical potential of the solvent, which is a function of pressure, temperature, and concentration of dissolved solids. If there is pure water on either sides of an ideal semi-permeable membrane at equal pressure and temperature, then no flow occurs through the membrane because of the equal chemical potential on both sides. If we add salt to one of the sides of the semi-permeable membrane, then its chemical potential will reduce. As water flows from higher potential to lower potential, there is flow of water from the pure water side (permeate) to the saltwater side (concentrate). This is known as osmotic flow, as depicted in Fig.1.8, and will continue to happen until the chemical potential on both sides is equal again. In order to explain the principle of reverse osmosis, we consider the application of an external pressure to the salt solution side, greater than the osmotic pressure. This causes flow of solvent from the salt water side (concentrate) to the pure water side (permeate), because the pure water now has lower chemical potential. This phenomenon is known as Reverse Osmosis, better depicted in Fig. 1.8.

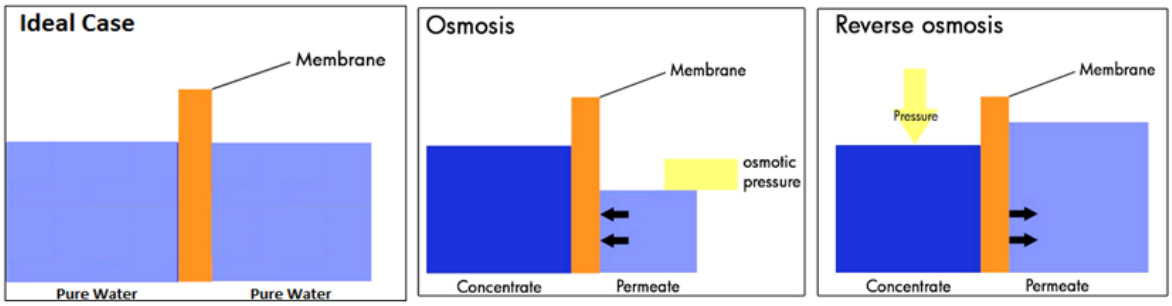

Figure 1.8: Osmosis and Reverse Osmosis Principle [10]

1.7 Energy recovery devices for Reverse Osmosis& their Importance

As mentioned earlier, the disadvantage associated with the reverse osmosis desalination is the high operating costs because of its rigorous use of energy. However, a very important point to be noted is that, once the desalination takes place, along with the fresh water that is produced, a large quantity of brine discharge (wastewater) also takes place. The notable point here is that the pressure drop across the feed-brine channel is 1-2 bar. As a result, the discharged brine carries large part of the energy in the feed water and can be recovered, and reused to minimize the overall energy cost for seawater desalination.

There have been vast improvements in developing the energy recovery equipments to utilize the high-pressure brine in order to reduce the use of power to desalinate water, thereby improving the overall efficiency of the desalination system. However amongst all the desalination technologies, reverse osmosis desalination has the lowest energy requirements per unit of permeate that is produced. Proper term for this energy is the Specific Energy Consumption (SEC) measured in kWh/m3 and is used to determine the overall efficiency of the reverse osmosis desalination system. Correct implementation of the energy recovery systems can reduce the power consumption from 100kWh per 1000 gallons in 1980 to 10kWh per 1000 gallons of fresh water today.

And in today's times, when energy is also a big problem that the world is facing, utilizing the energy recovery systems to bring down the total energy consumption of desalination system by almost 10 times is a very productive step. Considering the fact that that the cost of power consumption is typically 20 to 30 percent of the total cost of desalinated water, these technological innovations contribute greatly to the reduction of the overall cost of seawater desalination. Novel energy recovery systems that work based on the pressure exchange principle are currently available in the market and use of these technologies is expected to further reduce the desalination power costs with 10 to 15 %.

Hence in view of this major advantage that the energy recovery systems provide, we see that the usage of these systems in large-scale reverse osmosis desalination plants is a common practice but sadly the energy recovery systems are ignored when it comes to small-scale RO systems. Instead, they have needle valves that dissipate the energy in the concentrate and provide the necessary backpressure for the process. But such systems have a lot of wastage of energy and are pretty expensive to run.

The main reason for the energy recovery devices not being used for small-scale applications is because the energy recovery practices are neglected at this level. Scaling down devices that are successful at the large scale does not work because clearances, tolerances and losses become more significant in smaller devices. Hence, positive displacement devices, pumps with built-in energy recovery system and Clark Pump, a pressure intensifying device, were used for the small-scale RO systems.

Researchers at Fraunhofer ISE, Germany developed a tool to analyze and compare the performance of various energy-recovery options in small-scale RO systems. Their results,

illustrated in Fig.1.9, clearly indicate how less the specific energy consumptions are when energy recovery devices are used in small-scale systems as compared to the case when the energy recovery devices are not implemented in RO systems. An example of energy conversion device would be a device that uses shaft like a hydraulic motor, pressure exchanger refers to devices like PX Pressure Exchanger and DWEER, pressure intensifiers refers to devices with pistons with variable effective areas, like a Clark Pump.

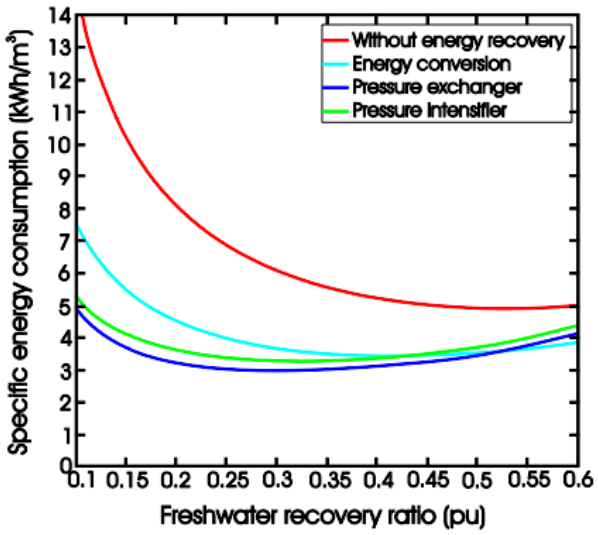

Figure 1.9: Specific Energy Consumption for various energy recovery options [11]

1.8 The Clark Pump

The energy recovery device used in this work is Clark pump from Spectra Water makers, which is basically a pressure intensifying device. It is powered by a flow of relatively low-pressure water from a separate pump (well or feed-water pump).Fig. 1.10 gives a schematic of the Clark Pump.

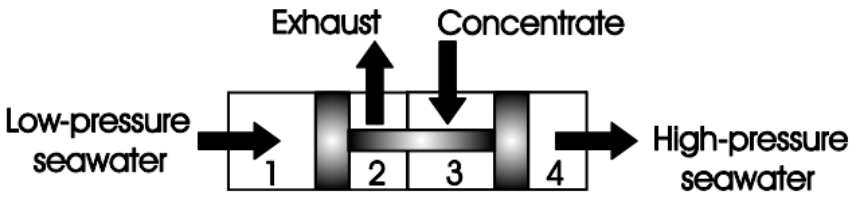

Figure 1.10: Clark Pump Schematic [12]

It uses the reciprocating motion of two pistons connected by a rod inside a cylindrical housing, to recover energy from brine (wastewater). The water from the feed water pump reaches the driving cylinder and pushes the rod to go through the pressurizing cylinder, which has the driven piston. As the rod pushes the driven piston, it circulates water on top of it, through the reverse osmosis membrane. The high energy-brine that is produced is fed back to the same cylinder where the rod is entering, thereby providing additional energy to push the rod through the cylinder.This way, the high-energy present in the brine is utilized to increase the pressure of feed water.A more detailed explanation of the working of Clark Pump in reverse osmosis desalination is given in Chapter .2, along with a real time picture of the Clark Pump that is used in this work.

1.9 Reverse Osmosis Desalination Experimental Set-up

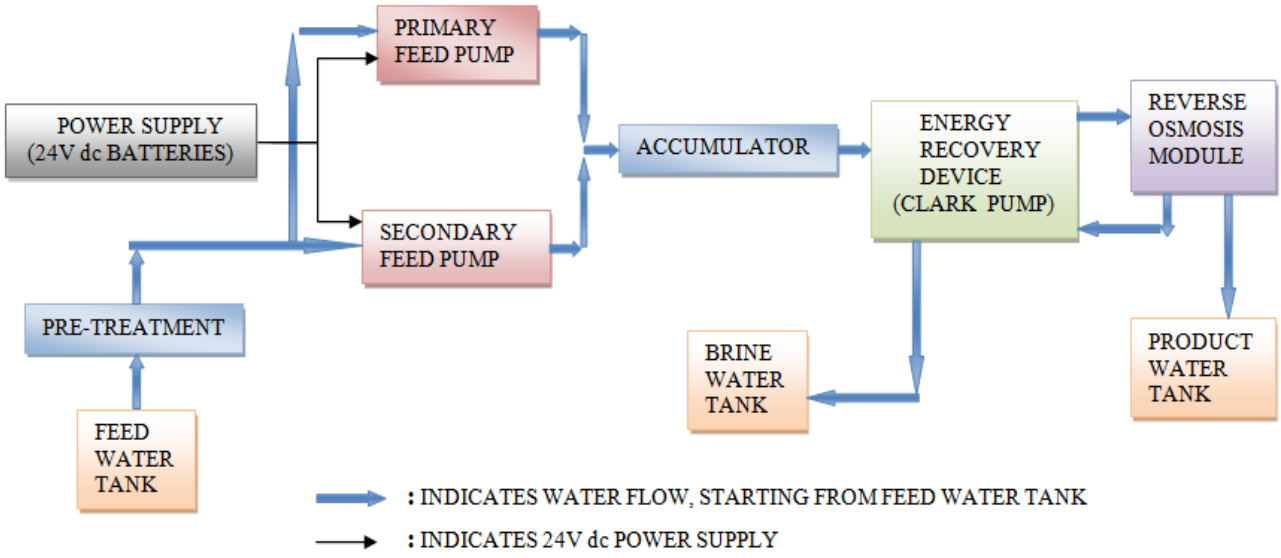

Figure 1.11: Process flow diagram of Reverse Osmosis Desalination System

Fig.1.11 shows the process flow diagram of reverse osmosis desalination system. The process of water desalination is composed of several stages as shown in the figure. The two pumps (primary and secondary) suck water from the source into the system. Water, first passes through a pre-filter which removes large particles from the feed water before it is circulated through the system. It is then distributed into two branches to be pressurized by the two pumps. After being pressurized by the pumps, water is passed to water accumulator which supplies high-pressure water as per the system's demand. From the accumulator, the water goes to the pressure intensifying device called Clark Pump which pumps it across the reverse osmosis module. The module desalinates the feed water thereby producing fresh water. The brine(waste water) produced is of very high pressure and is therefore pumped back to the Clark Pump to utilize the high energy of the brine, before pumping it out of the system. The pure water produced is stored in product tank and its conductivity is measured using a TDS meter. Fig.1.12 shows the small-scale experimental RO setup at KFUPM. More detailed explanation of all the individual components is done in Chapter .3.

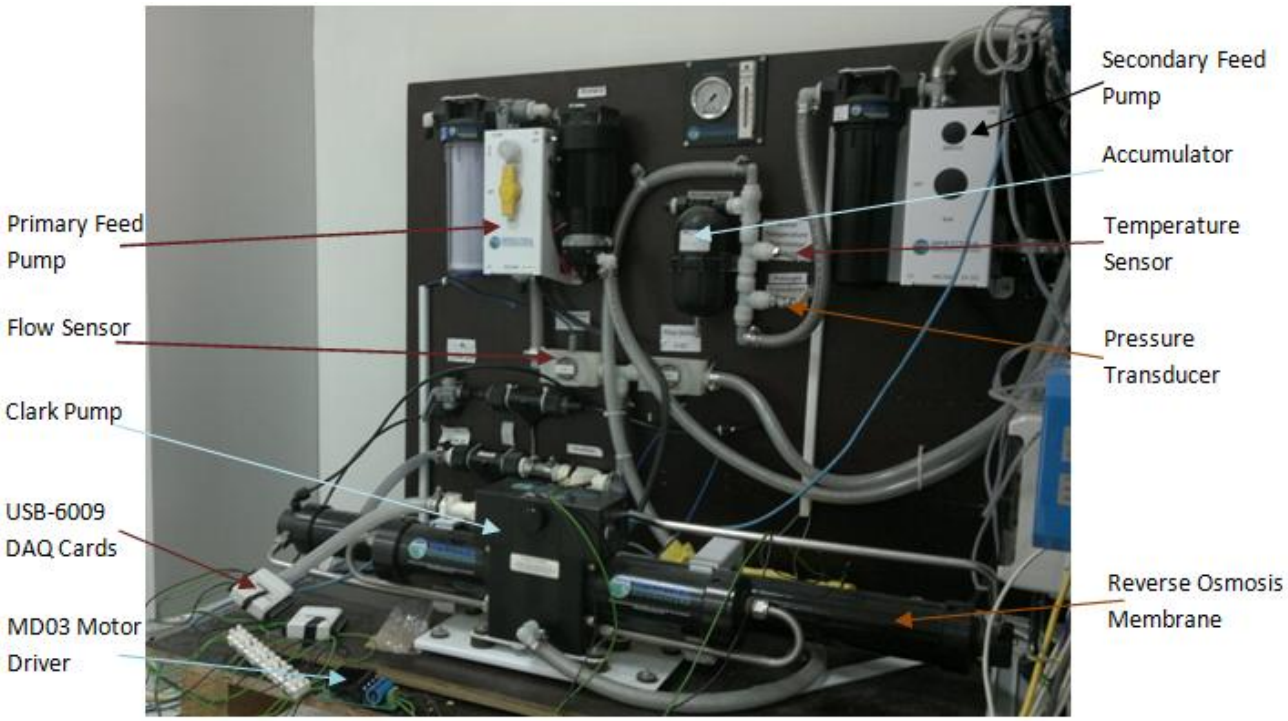

Figure 1.12: The small scale experimental RO setup at KFUPM

Another important aspect of the experimental setup is that the motors driving the two feed pumps, have their voltages being controlled by a device called motor driver which enables us to vary the motor voltage on a scale of 0 to 5 volts, means that the 5v on the motor driver corresponds to maximum voltage on the driven motor and hence maximum pump speed. Motor Driver details and specifications are also explained in Chapter .3.

Chapter 2

TECHNOLOGY AND LITERATURE REVIEW

2.1Seawater desalination technologies

There are basically two ways to achieve seawater desalination, either through thermal methods or by the use of membranes. However, the industry saw the development of thermal desalination first, followed by the development of membrane desalination in the second half of the last century. Fig.2.1 shows the relative growth of thermal and membrane desalination plants worldwide, in terms of the installed capacity, since the 80s and results clearly show that even though membrane technologies came after thermal technologies, the former has clearly overtaken the thermal methods and the trend is expected to remain the same in the near future.

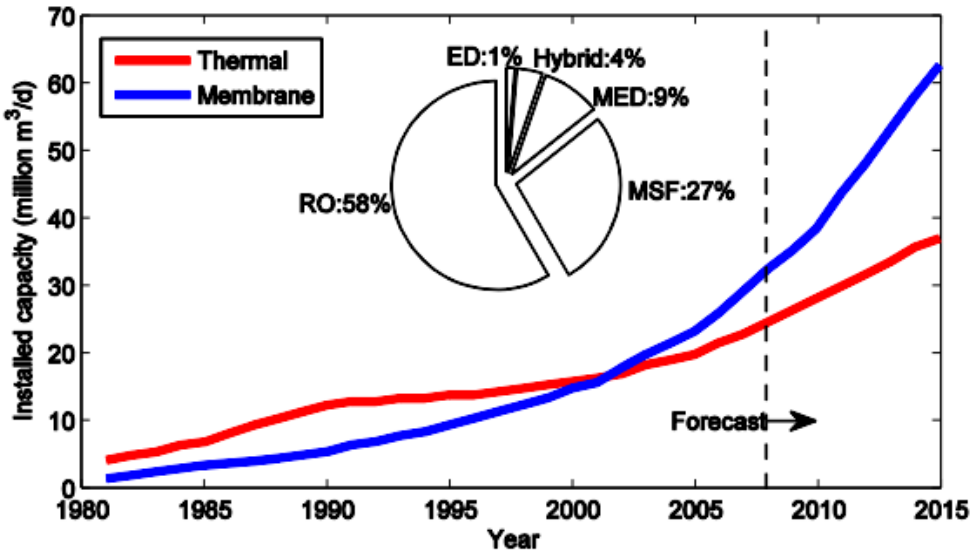

Figure 2.1: Membrane and thermal desalination - Installed capacity worldwide. [13]

2.1.1 Desalination by Evaporation

Evaporation is the easiest method of desalination. In this process, heat is supplied to seawater to produce water vapor which is later condensed and collected in the form of fresh water leaving behind concentrated brine, similar to the natural water cycle. The heat that is required for water evaporation is close to 600 kWh per cubic meter of freshwater produced [14].However, the disadvantage associated with this method of desalination was, the inability to recover heat as the heat required to condense water vapor was being transferred to a cooling medium. Industry was quick to identify this and later developed methods to recover heat, resulting in the technologies presented below.

2.1.2 Multi-effect Distillation

Multi-effect (ME) distillation, as compared to vapor compression has the advantage that it produces large quantity of fresh water from sea. This process makes use of series of vessels and decreasing the pressure of the complete setup is the principle used. The heat is provided to the initial stage only and the heating that takes place in the following stages is without any additional heating that is provided to the stages after the initial stage. Fig. 2.2 shows the schematic of Multi-effect distillation. The vapor formed in the first effect transfers heat to the next stage where condensation as well as evaporation takes place inside the tubes and the procedure remains the same for the subsequent stages.

For quick evaporation and boiling, water is sprinkled on the evaporator. The larger the stages of evaporation the lesser the heat needed. The main advantage of MED is the energy recuperation which makes it a better option as compared to evaporation.

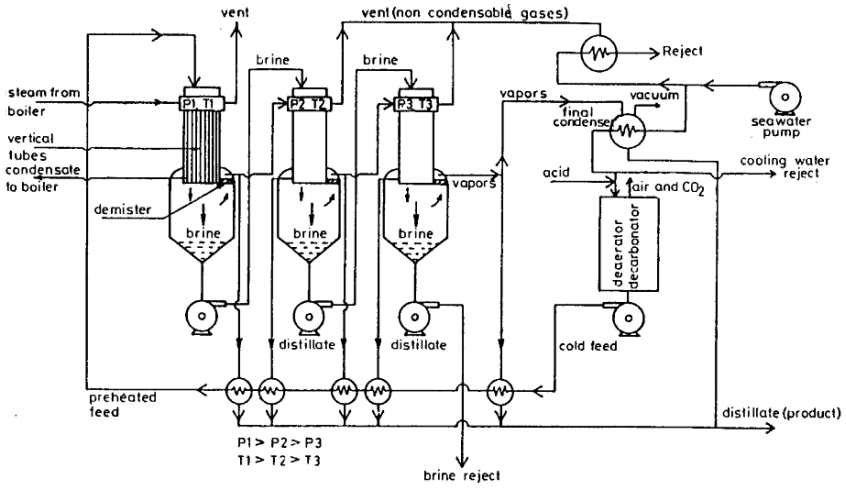

Figure 2.2: Schematic of Multi-effect Desalination Plant (Khan, 1986) [14]

2.1.3 Multi-stage Flash Distillation (MSF)

This process also involves evaporation but the evaporation will occur only when the feed water passing through the first stage of evaporation has pressure which is smaller compared to the pressure needed for saturation. MSF also consists of a number of cascading stages at progressively lower pressure, but energy recovery is done in a different way compared to MED.

In MSF, the seawater is heated up to the saturation level and then enters the first stage through a valve, where its pressure reduces below the saturation pressure. This results in rapid boiling (flashing) of seawater without any additional supply of heat, unlike MED. The brine produced in the first stage is passed on to the next stage via another valve, resulting in further flashing and so on. The steam is condensed in the same stage where it was produced using the incoming seawater before it enters the first stage. Since no heat is exchanged with the brine, scale formation is reduced. In this way, condensation of seawater takes place

Desalination plants using Multi-stage flash technology have the highest percentage of thermal desalination plants installed globally and are the second biggest of all desalination technologies after reverse osmosis (RO).

2.1.4 Vapor Compression

Vapor-compression desalination method makes use of mechanical energy instead of thermal energy. The basic principle involved is that the saline water is sprayed on the outside of an evaporator tube bundle. This leads to the formation of vapor which is passed through compressor for required amount of compression, leading to an increase in the temperature of condensation and also the pressure which leads to decrease in volume. The compressed vapor is then passed through the evaporator bundle, where it undergoes condensation leading to the formation of distilled water. The condensed heat can also be used to evaporate more brine.

This desalination process has very low specific energy consumption due to which the overall costs associated is also on the lower side. However, the disadvantage is that its size is very small, and also the quality of water that is produced is of lower quality compared to the other distillation processes.

The other classification of Desalination techniques is based on membrane separation which has two sub-types namely Electro dialysis and Reverse Osmosis.

2.1.5 Electro dialysis

This technique makes use of two cases of membranes are used namely, the action membrane allows only positive ions and the second type of membrane which is anion allows negative ions. Both these membranes are held parallel to each other in the sea water with the sea water being subjected to current flow. This leads to the cations being attracted to the cathode, and the anions to the anode. And the water that passes between these two membranes is split into two flows first

being the fresh water and the second is waste water also known as the brine. This process is considered to be better at desalinating brackish water. Fig. 2.3 illustrates the electro dialysis principle.

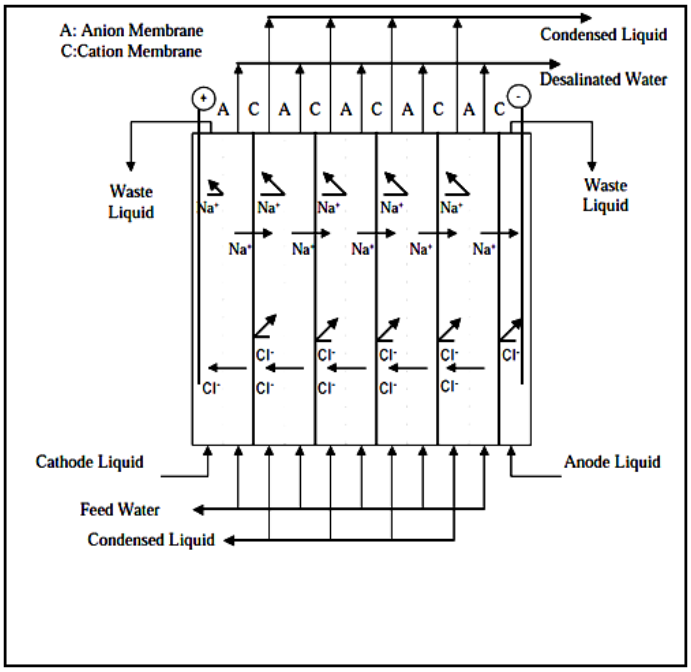

Figure 2.3: Electro dialysis Principle [14]

2.1.6 Reverse Osmosis

Reverse Osmosis is the process where water consisting of inorganic salts, suspended particles, soluble and insoluble solvents, aquatic organisms and other water contaminants are forced under pressure through a semi permeable membrane.

A membrane is in essence a selective barrier. When two water solutions of different concentration such as pure water and saltwater are separated by a semi permeable membrane which allows the water to pass through at a very high rate, but opposes the flow of other constituents of water like salt. Water flows through the membrane naturally from the pure

waterside (high water concentration) to the saltwater side because the latter is at lower water concentration. This phenomenon is Osmosis.

When water flows through the semi permeable membrane, naturally, the volumes of the two solutions change too and there is a hydrostatic pressure difference that develops. Water continues to flow until the equilibrium state is achieved. Whatever the pressure difference is, when the process reaches equilibrium, is known as Osmotic Pressure. At this point the net flow of water through the semi permeable membrane is zero.

If pressure is applied on the saltwater side greater than the osmotic pressure that develops due to osmosis, the direction of the natural osmosis flow, through the membrane, is reversed and water starts flowing from the saltwater side to the pure water side. This phenomenon is Reverse Osmosis which enables the separation of salts from salt water to produce fresh water. When seawater is used as the feed water, the osmotic pressure difference of 25 bar and above is found. Hence, this is the minimum pressure that must be applied to the seawater for reverse osmosis to take place [15].

Conventional v Cross-flow Filtration

In conventional filtration techniques, the feed water flow is perpendicular to the surface of the semi permeable membrane as shown in Fig. 2.4. This perpendicular flow causes quick build up of solids on the membrane surface leading to a decrease in permeate flux. To overcome this drawback, modern reverse osmosis processes use a cross-flow approach, also shown in Fig. 2.4, wherein the feed water is pushed along the membrane surface in a sweeping type of action. This type of cross flow reduces the buildup of suspended solids on the membrane surface enabling large water flux and improves the overall membrane efficiency. Only a small portion of the feed

water goes through the membrane as freshwater. The rest of the feed water flows along the membrane surface along the feed-brine channel, flushing the salts out of the membrane. This flow is referred to as the brine or reject.

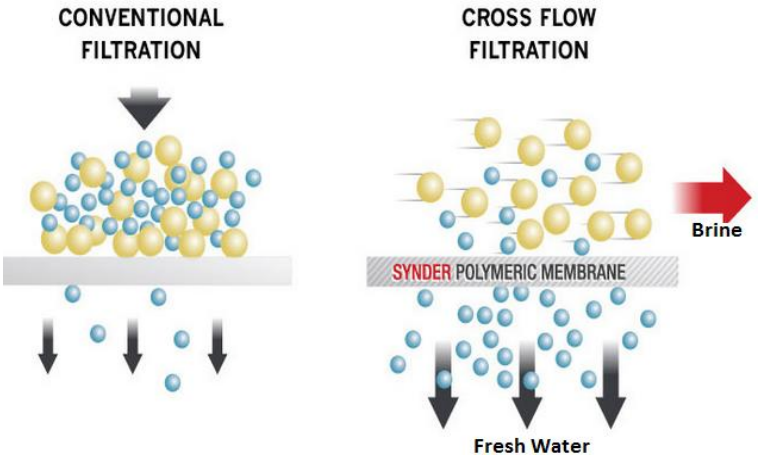

Figure 2.4: Cross flow filtration [15]

Hence, the process requires a reverse osmosis membrane for separation of salts and a high-pressure pump to raise the pressure of the feed water to typically 50 bar or higher. The complete schematic of Reverse Osmosis process depicting the cross-flow as well is shown in Fig. 2.5.

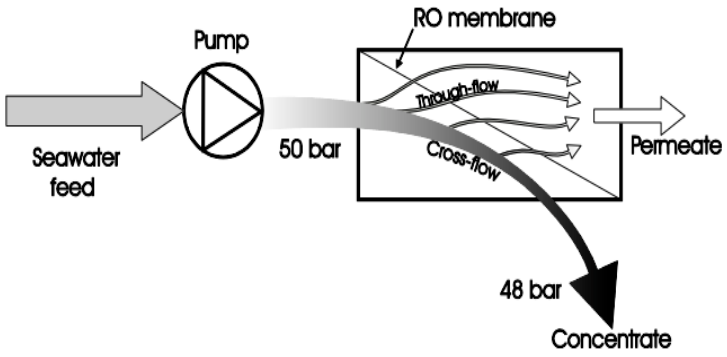

Figure 2.5: Schematic diagram of Reverse Osmosis Process [15]

2.2 Performance Evaluation Parameters

The various performance evaluation parameters for Reverse Osmosis system is the Osmotic Pressure, Net-driving pressure required for reverse osmosis to take place, Permeate Recovery Ratio and the Salt rejection ratio.

2.2.1 Water flow through Reverse Osmosis Membranes

Ideally the water flow through the reverse osmosis membrane should be free and should completely stop the salts from passing through. However, in practical, the reverse osmosis membranes are not so perfect and offer some resistance to the flow of water through them. This implies that in addition to the minimum energy that is required for the separation of salts from water, an additional amount of energy is required i.e. pressure, to push the water through the membrane. Hence, the flow of product water through the membrane is proportional to the net pressure that is applied, which should be above the osmotic pressure. Eqn.1 represents the relationship between product flow rate and the net driving pressure across the reverse osmosis membrane.

$$\text{Product flow (Qp)} = (\Delta P - \Delta\pi) * K * A \quad (1)$$

Where, Q_p – Product water flow rate, K – water permeability coefficient, A- Membrane area, $\Delta\pi$ is the differential osmotic pressure across the membrane, ΔP is the difference of feed water and permeate (product water) pressures. $(\Delta P - \Delta\pi)$ represents the net driving pressure required for reverse osmosis to occur.

2.2.2 Permeate Recovery Rate

Another very important performance evaluation factor for a reverse osmosis desalination system is the recovery ratio, which is given by the ratio of product flow and the feed water flow. It is expressed in terms of percentage.

$$\text{Recovery Ratio} = 100\% \left(\frac{\text{Product flowrate}}{\text{Feedwater flowrate}} \right) \quad (2)$$

For seawater, the plant recovery ratio is in the range of 30-45%.It is the selection of an appropriate recovery ratio which is a criteria since it involves a compromise between the amount of water to be produced, the salinity, energy consumption and life of the system especially the reverse osmosis membranes.

From Eqn. 1, it can be seen that an increase in the feed water pressure would result in an increase in product water flow (Qp) and hence, high recovery ratio as per Eqn. 2. However, the relationship between the applied pressure and the recovery ratio is not that simple since increasing the recovery ratio means decreasing the feed water flow rate which implies an increase in the salt concentration on the feed-brine side and thereby increase in the salt flow across the membrane. This increase in salt concentration on feed brine side results in an increase in the osmotic pressure,which reduces $(\Delta P - \Delta \pi)$ term in Eqn.1 reducing the net driving pressure across the membrane and decreases the product flow rate.

2.2.3 Salt passage in Reverse Osmosis

Ideally the RO membranes should completely stop the passage of salts through them but in reality they do not completely stop the passage of salt. However, the data sheets of modern seawater membranes shows salt rejection in excess of 99% . [16,17,18,19]

The rate of flow of salt through the membrane is driven by the concentration gradient across the RO membrane and is given by Eqn. 3.

$$Qs = K_s * A * (C_{avg} - C_p) \quad (3)$$

Where, Q_S is the salt flow through the membrane, Ks is the salt permeability coefficient of the membrane, C_{avg} is the average salt concentration in feed-brine, C_p is the product concentration.

Therefore, the final salt concentration in the product water or permeate is the ratio of salt flow and the water flow through the membrane given by Eqn.4.

$$\text{Salinity of product water} = {Q_s}/{Q_p} \quad (4)$$

Another important performance evaluation parameter, apart from Recovery Rate is the Salt Rejection ratio which is calculated using the salinity of product water and the salinity of feed water. It is given by the expression given in Eqn.5.

$$\text{Salt Rejection} = 100\% \left(1 - {Xp}/{Xf}\right) \quad (5)$$

Where Xp represents the product water salinity and Xf represents the feed water salinity. Salt rejection is usually expressed in terms of percentage.

2.3 Review & Evolution of Reverse Osmosis

The evolution of reverse osmosis started in late-1950s when Reid et al., (1959) [20]showcased the compressed membranes made of cellulose acetate to decelerate the dispersion of salts through the membranes while allowing the dispersion of water. Based on

this, Loeb et al., in 1960s worked towards building the first cellulose acetate membrane which is asymmetric, for reverse osmosis [21]. Then the evolution of reverse osmosis saw polyamide composite membranes being developed during the 70s and 80s [14][22].In terms of the source water that reverse osmosis was tested on, it was the brackish water and later was used for the treatment of sea water in the late 1970s when for the first time, the commercial RO membranes were presented [21][23].It was in mid 1980s that Reverse osmosis started becoming increasingly popular and was a tough competition to the thermal desalination [24].

Since its beginning, reverse osmosis of both sea water and brackish water has seen giant strides in terms of its development, in the form of higher product flux, better salt rejection, less energy consumption and reduction in overall costs associated with RO desalination. Fig. 2.6 shows how product flux and salt rejection varied from 1978 to until 2004. The product water flux was more than double in 2004 compared to 1978. Salt passage continuously decreased and was found to be just 20% in 2004 of the value in 1978.

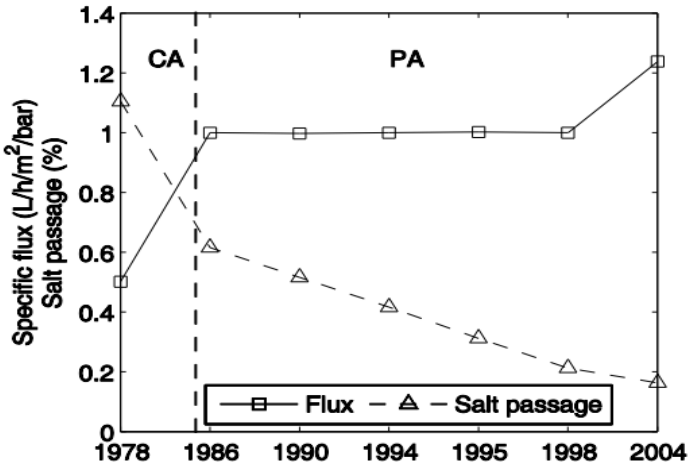

Figure 2.6: Specific flux and salt passage for seawater membranes.[22]

There has been significant reduction in the net driving pressure that is required for reverse osmosis as presented in Fig. 2.7 which shows the evolution of net driving pressure from 1969 to 2004.From Fig.2.6 and 2.7, it is clear that polyamide membranes have had a significant role in the evolution and development of reverse osmosis.

Apart from the developments discussed, advanced engineering of RO membranes has improved the membrane's resistance to fouling (fouling is discussed later), which naturally increases the life time of a membrane and at the same time reduces the maintenance costs related to its cleaning and replacement [25].

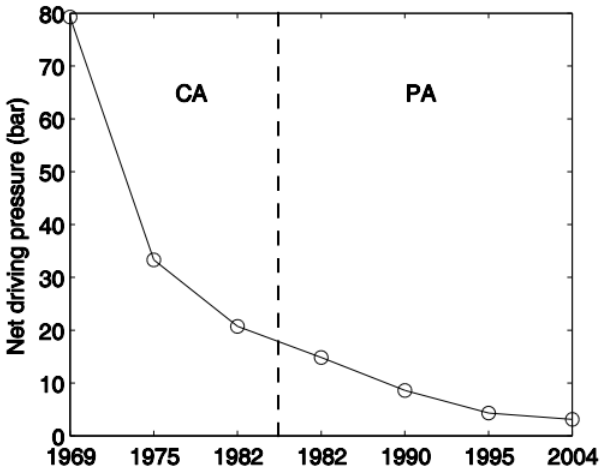

Figure 2.7: Net driving pressure – evolution - for brackish water membranes [22]

Altogether, the advantages and the evolution of membrane technology and the development of other important reverse osmosis desalination components such as the energy recovery devices (Clark Pump, being used in this work), have led to significant reduction in the total energy consumption of reverse osmosis desalination system, which is extremely important since electricity is costly and as scarce as the water around the world. Hence, we see today that large volumes of high-quality pure water can be produced with very less specific energy consumption. Fig. 2.8 shows the evolution or the decrease in specific energy consumption of reverse osmosis

systems from 1980 to 2005. It can be seen that, the reverse osmosis used in 2005 consumes a quarter of the energy consumed in 1980 [26][27].

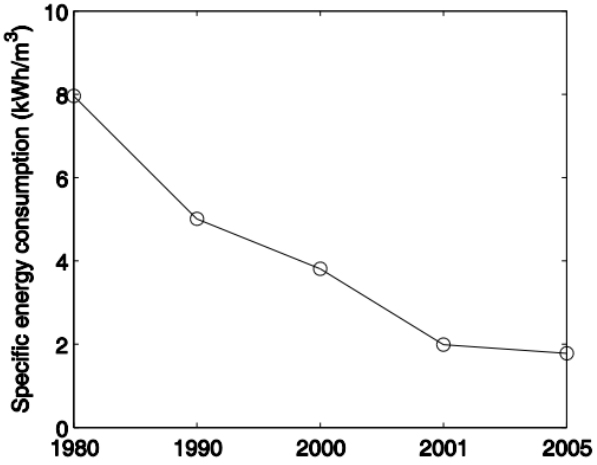

Figure 2.8: Evolution of Specific Energy Consumption [26]

2.4 RO Membrane Materials

2.4.1 Cross-flow filtration

As mentioned earlier, the first reverse osmosis membranes that were used were made of cellulose acetate. Later on, since 1980s polyamide membranes dominated the desalination industry. In order to withstand high pressures that are needed in desalination, the membranes should have high physical strength and should have rigid supporting structure too.

2.4.2 Cellulose Acetate Membranes

As mentioned earlier, the first cellulose acetate membranes were developed in the late 1950's by Loeb and Sourajan. It was made from the polymer of cellulose diacetate. The latest CA membranes are a mixture of cellulose diacetate and triacetate. The method followed for construction of the membranes is a complex process which includes casting which is responsible for the partial removal of solvent by the process of evaporation, cold bathing is responsible for

removal of whatever solvent that is left after casting and lastly, annealing, at very high temperatures in the range of 70-100°C, is done to better the semi-permeability of the membrane, bringing about a substantial improvement in the ability of the membrane to reject the salt flow. As far as the structure of the CA membranes goes, it is very asymmetric and the rest of the membrane is highly porous due to which the water permeability is higher. Better salt rejection results can be obtained by increasing the length (time) of annealing.

2.4.3 Polyamide Membranes

Polyamide membranes are supported on a polysulfone layer which is highly porous. The thickness of these assemblies is about 0.2 mm, wherein the polyamide membrane skin thickness is of the order of hundred nanometers and the polysulfone supporting layer has thickness between 0.03-0.045 mm. The remainder of the polyamide membrane is polyester whose main purpose is to improve the mechanical properties of the membrane [22]. Fig. 2.9 illustrates the schematic of polyamide membranes.

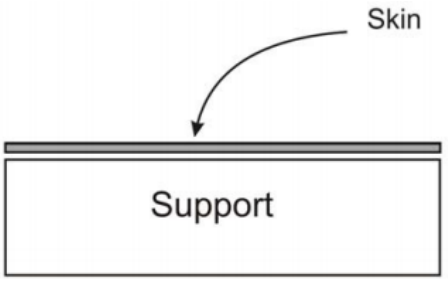

Figure 2.9: Schematic of Polyamide Membrane [22]

Since the membrane skin thickness is small compared to the support layer, the resistance offered is less and higher water flow is expected because of this reason, compared to CA membranes.

2.4.4 Comparison of Membrane Materials

1) The salt rejection capability and the water flow through a polyamide membrane is much better than cellulose acetate membrane, which means low working pressure and less specific energy consumption.

2) The disadvantage associated with polyamide membranes is that they are prone to degradation by the presence of chlorine whereas the cellulose acetate membranes can withstand chlorine up to certain level.

3) The cellulose acetate membrane has a polished surface as compared to polyamide membrane.

Hence, CA membranes perform better than polyamide membranes in cases where the feed water has high chlorine content and has high fouling rate such as the surface water whereas polyamide is more suited for applications where regular disinfection is done, like food industry.

2.5 Membrane Modules

There are basically four membrane configurations that are available namely, tubular, plate type, hollow fiber and spiral wound. The spiral wound and hollow-fiber configurations are the most popular whereas the tubular and plate-type are mostly used in food industries.

2.5.1 Plate-type membrane configuration

The most important part of the plate-frame module is the supporting plate that is sandwiched between two flat sheet membranes. The membranes are sealed to the plate, to make it rigid and to have high resistance, through the use of locking devices, glue or directly bonded. The plate is porous from inside and provides a channel for the flow of permeate which is picked up from a tube on the side of the plate. The grooves present on the surface of the plate are to provide a side flow channel for the feed water. The height of the feed channel varies from 0.31 to 0.8 mm.

However, such type of an arrangement would result in low area-to-volume ratios, making the configuration very bulky. Hence, these membranes are mostly used in industrial applications [28]. The advantage associated is that they are easy to dismantle for proper inspection and maintenance. Fig. 2.10 shows the plate-frame type membrane configuration.

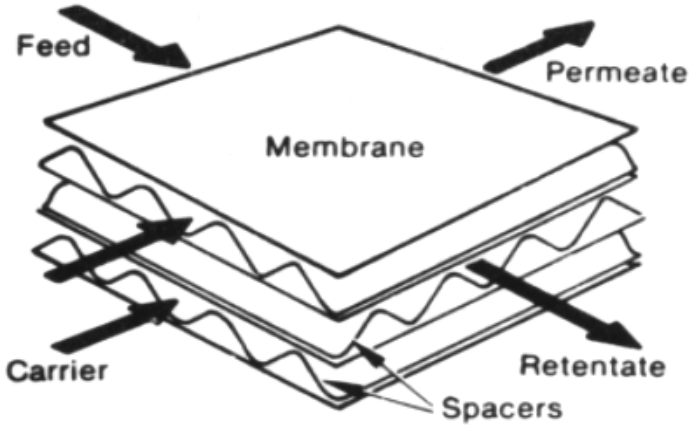

Figure 2.10: Plate-frame membrane configuration [28]

2.5.2 Tubular Membranes

These modules go a step ahead of the plate-frame module configuration by increasing the surface are of the membrane along with all the advantages associated with plate-frame type. In this configuration, many tubular membranes are packed inside a tube of larger diameter which is porous. Such a structure is to withstand high pressures of the feed water. These membranes allow tangential, or cross-flow, where in the feed water is pushed along the membrane surface in a sweeping type action. These cross flow operate at velocities around 6-7m/sec and reduces the shaping of a concentration polarization layer on the membrane surface, enabling large water flux and easy maintenance. The tubular membrane configuration has many advantages, apart from their rigid construction; they have the advantage of processing suspended particles, without plugging. Some tubular membranes can be cleaned with the help of sponge balls which provide good level of cleaning and takes very less time. The typical applications where these types of

membrane configurations are used are the pulp and paper industry waste, waste water treatment, waste from oil industry etc. The life time of the tubular membranes, range from 3 up to 10 years. Fig. 2.11 shows few tubular membranes.

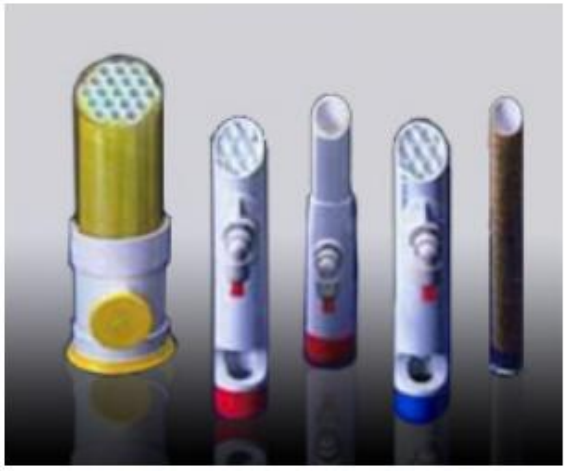

Figure 2.11: Tubular membrane pictures [29]

The above two configurations where used when reverse osmosis was in its early stages. They are not used much in today's' time except for the food industry and waste water treatment which have high membrane fouling potential. These membranes have become obsolete because of their high costs and are replaced by the hollow-fiber and spiral wound membrane configurations.

2.5.3 Hollow-fiber Module

The hollow fiber module is made up of millions of hollow fibers (in a tubular module configuration), as thin as 100micrometers and as long as 2.4meters, are kept in a large pipe. The membrane skin which is responsible for salt-rejection is on the outside of the fiber and the feed water flows in radial direction through the walls of the tubes to the inside which is hollow. The major difference between the hollow-fiber configuration and the other two configurations discussed before it is that the hollow-fiber module does not need any supporting structure because the fibers itself are so strong that they can easily tolerate the high pressure of the feed

water that is required for reverse osmosis to take place. The reason for such ruggedness of the fibers is because their outside diameter is large (90 – 150 micrometer) compared to the inside diameter (30 – 70 micrometer) [22][28].

To obtain the module configuration, the fiber bundle is folded to half its original length and a feed water plastic tube with holes on its surface is inserted in between the folded bundle of fibers, thereby increasing the length of the whole bundle. To firmly hold the fiber bundle, it is sealed at both its ends in an epoxy cap. The caps at one of the two ends of the fiber bundle is cut perpendicularly to the fibers to allow the product water that permeates through the walls of the fibers, to flow out of the fibers. Finally the whole arrangement (fiber bundle with its end caps and the water plastic tube (distributor tube)) is put inside a cylindrical housing. Appropriate external connections to the cylindrical housing are fitted to collect the product water (permeate), the waste water (brine) and to supply the feed water toplastic tube. Fig.2.12 shows assembly.

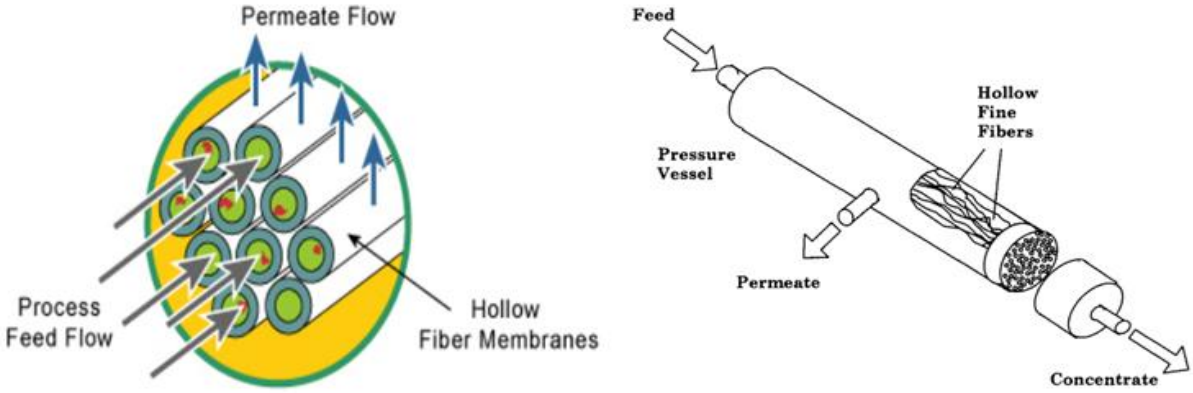

Figure 2.12: Hollow-fiber flow pattern and assembly [29][30]

The various advantages associated with such membrane configurations is that it occupies less space because of its compact design, less man-power required, high quality fresh water is produced and the benefits of hollow fiber membranes include the tangential flow along the surface of the membrane which reduces the chances of membrane fouling, membrane back-

flushing can be done to remove suspended solids from the inside of the membrane, high amount of fresh water production because of the compact structure. Fig. 2.13 shows the pictures of hollow-fiber module with end-caps.

Figure 2.13: Hollow-fiber modules with end caps [29]

2.5.4 Spiral-wound Module

To create a standard spiral wound membrane, we construct the flat sheet membrane using automated casting equipment. The process begins with polyester fabric support base and coated with micro-porous polysulfone layer. This provides additional support for the top 0.2 micron thick membrane skin (membrane barrier layer). This top barrier layer makes the actual separation to purify the feed water. The semi-permeable polyamide membrane consists of thin film of polymeric material formed on porous supporting material. The semi-permeable membrane skin is formed on the polysulfone substrate by interfacial polymerization of molecules containing amine and carboxylic acid chloride functional groups. The combination of these three layers makes a durable membrane flat sheet that is used in each spiral wound element.

The membrane flat sheet is folded into half and then combined with the sheet of feed channel spacer. This provides turbulence and creates space between the membrane sheets to allow uniform flow of the water to the entire membrane surface. The leaves of membrane and feed

channel spacer are then combined with a sheet of permeate spacer which provides open-flow channels for permeate even at high pressures. The leaves are glued along each of the three exposed sides and then rolled around the core tube connected on the fourth side for permeate exit.

With the back of the membrane completely sealed to the edges of the permeate spacer, the feed water is forced through the feed channel spacer contacting the barrier layer (front) of the membrane. Clean water or permeate passes through the membrane surface into the membrane channel and then flows in a spiral direction to the center of the element and is collected in the core tube. The spiral wound membranes are then loaded into pressure vessels and interconnected with additional membrane elements to fulfill any number of design specifications. Once the pressure vessels are sealed, the feed water can be introduced and treated. The feed water that does not permeate becomes enriched in salts as it travels through the feed channel spacer due to permeate water being removed. The permeate water flows at the end of the vessel and is collected as the product. Fig. 2.14 gives a detailed illustration of the spiral wound membrane configuration and it's working.

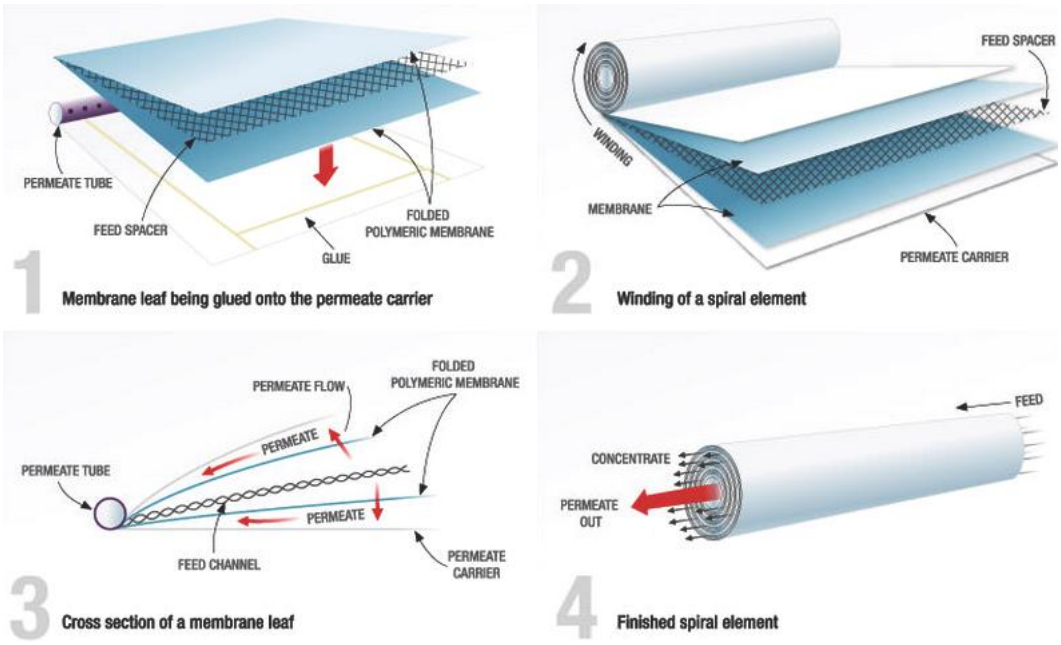

Figure 2.14: Spiral wound membrane construction and working principle [31]

Spiral wound membranes occupy large membrane area packed in a small volume which enables higher permeate flux and low costs. The two major reasons why the spiral wound configuration is not prone to membrane fouling are that it works at lower operating pressures and secondly, there is enough space between the membrane sheets. Due to this reason, the spiral wound can easily handle feed water of very poor quality.

Spiral wound membrane is currently the most popular of all the membrane configurations and is dominating the reverse osmosis desalination industry and would continue to do so in the near future as well.

2.6 Concentration polarization

Whenever reverse osmosis takes place, the freshwater permeates through the membrane but the salt is rejected due to which a boundary layer of high salt concentration develops adjacent to the

membrane surface. This phenomenon is known as concentration polarization and understandably has a number of serious effects on the desalination process [22][28].

The major disadvantages associated with concentration polarization are as follows:

1) Due to the development of salt boundary layer near the membrane surface, the osmotic pressure at the membrane surface increases, decreasing the net driving pressure $(\Delta \boldsymbol{P} - \Delta \boldsymbol{\pi})$ across the membrane.

2) Due to the decrease in Net Driving Pressure (NDP), the product water flow through the membrane decreases as per the product flow equation given in Equation .1.

$$\text{Product flow (Qp)} = (\Delta P - \Delta \pi) * K * A \qquad \text{(Eqn. 1, Page .41)}$$

3) The concentration gradient across the membrane, which is the difference of the average salt concentration ($C_{avg)}$ in feed-brine channel and product concentration (C_p), increases with concentration polarization. Hence the salt flow through the membrane which is dependent on concentration gradient also increases as per the equation,

$$Qs = K_s * A * (C_{avg} - C_p) \qquad \text{(Eqn. 3, Page .42)}$$

The salinity of product water which is the ratio of salt flow and water flow through the membrane also increases due to increase in salt flow and decrease in water flow through the membrane.

4) High level of concentration polarization can reduce the life of the membrane by causing membrane fouling discussed in next segment.

2.7 Membrane Fouling

The main reason that contributes to the decrease in membrane performance and its life is the membrane fouling. Hence when designing the RO system, the various ways and techniques for avoiding or at least good efficient management of fouling, is considered, since this determines how frequently the membranes need cleaning or replacement if possible. Fouling mainly occurs due to poor feed water quality and poor pre-treatment.

Fouling is of many types like particle fouling, organic and inorganic fouling and scaling (soluble salts get deposited on the membrane surface). The various negative effects caused by membrane fouling is the decrease in performance and life of membrane, decrease in net driving pressure due to various particles getting deposited on the membrane surface, decrease in product flow, increase in salt flow through the membrane, increase in product water salinity, high specific energy consumption and high operating costs. Hence to overcome membrane fouling, good and efficient membrane pre-treatment should be considered which is explained in next segment.

2.8 Reverse Osmosis Membrane Pretreatment

Reverse Osmosis membranes are designed to remove compounds that are soluble like the mineral ions. The membrane structure is such that they cannot remove the large amount of suspended particles or solids that accumulate on its surface. If the membrane is kept in the feed water with these suspended particles on its surface, it will cause membrane fouling i.e. blocking the membrane surface, leading to a discontinuous and unsteady desalination process. Hence it is very important to remove these suspended solids before they reach the RO membranes. Hence this process of removal of suspended particles before the feed water reaches the membrane is known as pretreatment. The various membrane pretreatment techniques used today include

granular media filtration and membrane ultra filtration and micro filtration. Granular media filtration is basically used for small to medium sized desalination plants and ultra and micro filtration is mostly used in large desalination plants. Fig. 2.15 shows the pretreatment that is done before the feed water is passed through the membrane for reverse osmosis to take place.

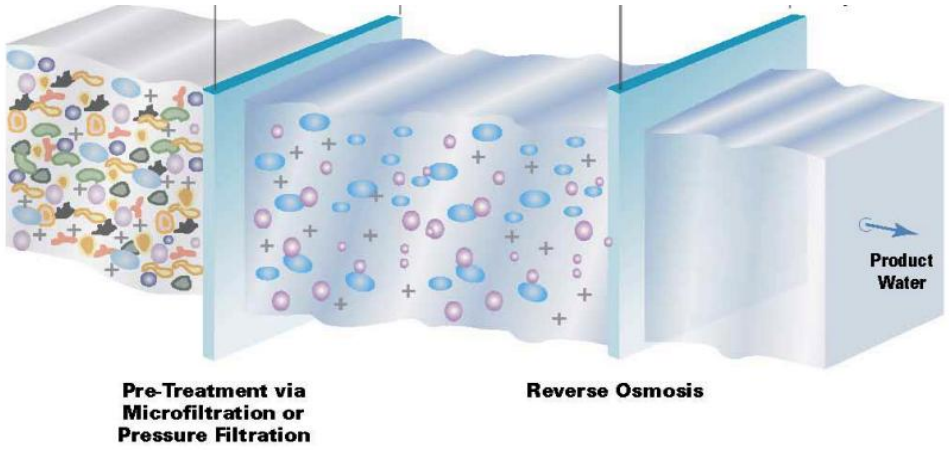

Figure 2.15: RO Membrane Pretreatment [6]

The feed water has various types of suspended particles, bacteria, viruses, colloids, dissolved ions, organic and inorganic molecules, metals, salts etc before it goes through the pretreatment where large amount of suspended particles and solids are removed before it is passed to the reverse osmosis membrane where desalination takes place to produce fresh water as the product.

2.9 Brine stream energy recovery and its types

As discussed earlier, the disadvantage associated with the reverse osmosis desalination is the high operating costs because of its rigorous use of energy. This is overcome by utilizing the high energy present in brine water, for pushing the water through RO membrane, thereby minimizing the energy consumption of RO system. This utilization of brine-energy is done with the help of an energy recovery device. The use of a proper energy recovery device can bring down the energy consumption by 10 times simultaneously improving system's efficiency.

Apart from improving the overall system's efficiency, brine-stream energy recovery systems have a major effect on the economics related to reverse osmosis process. While it reduces the specific energy consumption and therefore, the running costs of the RO plant, it also increases the set-up costs as well. The trade-off between these two important points is dependent on various factors like type and the size of the application; it is used for, the amount of energy that is needed, the overall cost of the system and the energy. For large RO plants, for their long-term running operations, the energy recovery is critical and is therefore used as it reduces the specific energy consumption and improves the overall efficiency of the plant. On the contrary, small RO systems are purchased based on the available capital costs and therefore they rarely use the energy recovery device.

The first energy recovery systems were developed for large-scale desalination plants. Devices like the Pelton wheel and hydraulic pressure booster were used as energy-recovery devices. These devices use a rotating shaft for the transfer of energy from brine to the feed water. Later on, devices that use pistons for the transfer of energy like DWEER (Dual work exchanger energy recovery), Clark pump, both using two pistons and Pressure Exchangers using three pistons respectively, came into existence and were also very successful. Some of these devices are explained next.

2.9.1 Pelton Wheel

Pelton wheel energy recovery devices are mostly used in large RO plants. They are simple, easy to understand and reliable but imperfect. They make use of the high-pressure brine by feeding it to the pelton wheel's turbine. The turbine has a wheel with cup-shaped blades fixed on its perimeter. When the brine is directed towards pelton wheel, it hits the cups which in turn rotate the wheel. This rotation of wheel/turbine (coupled to the feed pump's shaft) produces rotating

power output, which is used to serve the main electric motor in driving the high-pressure feed pump to pressurize the feed water. There are basically two energy conversions taking place in Pelton: first, the hydraulic energy associated with brine to kinetic energy of the rotating shaft and second, from this kinetic energy of the shaft back to the hydraulic energy in feed water pump.

Pelton wheels are generally considered to be simple and robust. They were first used for energy recovery in RO systems in the late 1980s but in spite of it having high efficiency in hydroelectric generation plants, they turned out to be inefficient in RO plants mainly because of the high speeds of the pump shaft that they are coupled to and the poor quality of the cups on the wheel, in a bid to reduce the set-up costs [33].

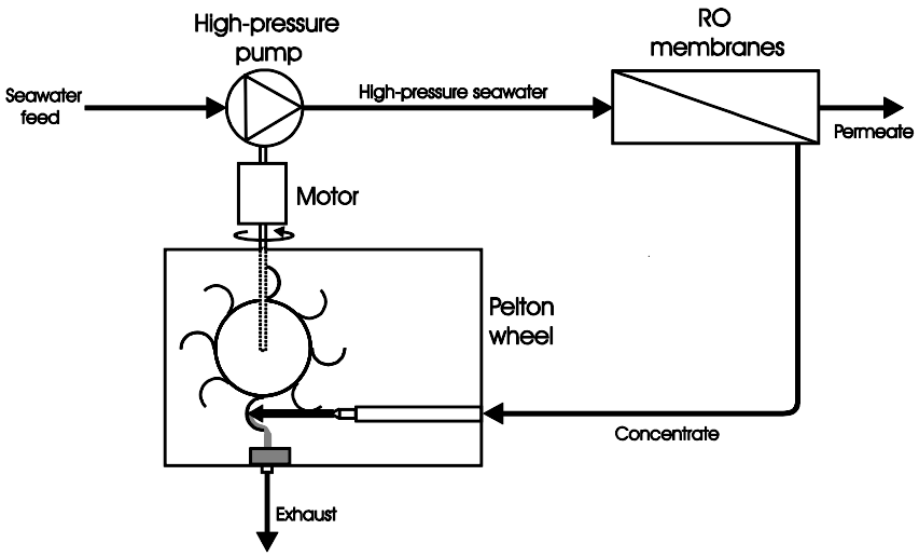

Figure 2.16: Pelton wheel energy recovery schematic [34]

2.9.2 Hydraulic turbo booster

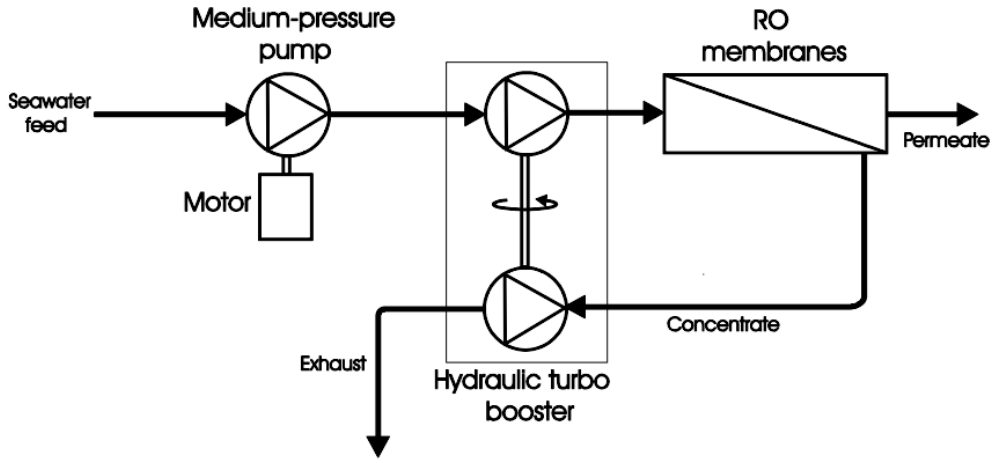

Figure 2.17: Hydraulic turbo booster Schematic [34]

Oklejas and Oklejas [35] in the year 1990 patented the use of the turbocharger in Reverse Osmosis applications, for energy recovery from brine. The various commercially available hydraulic turbo boosters are the ones manufactured by Fluid Equipment Development Company (http://www.fedco-usa.com, accessed 11August 2013) and by Pump Engineering (http://www.pumpengineering.com, accessed 11August 2013). The hydraulic turbo booster, as the name suggests makes use of hydraulic energy and transfers it from the high pressure brine to the feed water in RO applications. It basically consists of a turbine to be driven by the high pressure brine and a centrifugal pump impeller mounted on the same shaft without any motor. This unit is totally free from the feed water motor driven medium pressure pump as evident in Fig. 2.17. The concentrate stream, known as the brine, is directed to the turbine and produces a rotating power output which is used to drive the centrifugal pump, mounted on the same shaft, to increase the medium-pressure of the seawater to high pressure prior to entering the RO membranes.

The turbo charger also has a bypass around it which allows the user to control the flow. This comes in very handy when the required brine pressure is more than what is required to boost the

feed water pressure. However the disadvantage associated is that the efficiency is the product of efficiencies of turbine and the centrifugal pump. Hence the device operates only at peak efficiency when pressure and flow is less. Fig. 2.18 shows real-time picture of turbo booster.

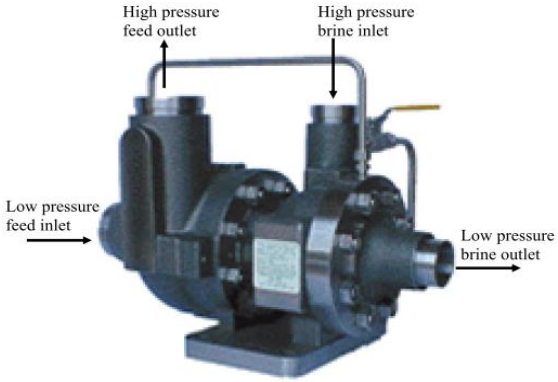

Figure 2.18: Turbo Booster Unit [34]

2.9.3 DWEER Pressure Exchanger Energy Recovery

DWEER makes use of the principle of positive displacement for the energy recovery in RO systems. It makes use of two cylinders, each with a piston inside them. The use of DWEER in RO process is shown in Fig. 2.19.

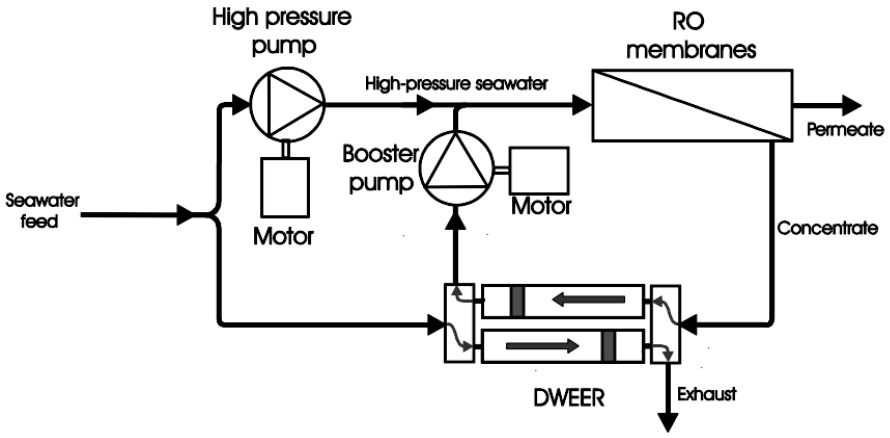

Figure 2.19: RO system with DWEER [34]

During one stroke, the high-pressure concentrate from RO membrane is fed to one of the two cylinders, where it pushes the cylinder's piston due to which the pressure of the feed water present on the other side of the piston increases. At the same time, the feed water is fed to the other cylinder where it pushes the cylinder's piston due to which the old brine (from the previous stroke) present on the other side of the piston is ejected out of the system. The pistons reverse roles on the next stroke, with the help of valves which are used to coordinate the flow of water in the two cylinders. A more detailed representation of DWEER is shown in Fig. 2.20.

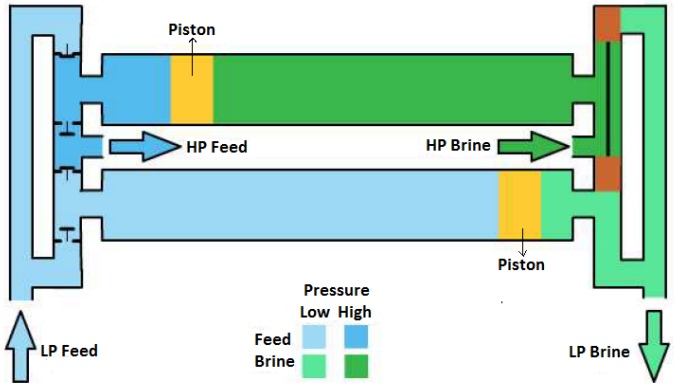

Figure 2.20: DWEER Unit Schematic [34]

The advantage associated with the DWEER Pressure exchanger is that it transfers the pressure in brine (concentrate) to feed water pressure, through a piston, where the chances of the brine and feed waters getting mixed is very minimum. Hence the energy transfer is almost 100% in this scheme. Hence, such devices are considered to be much more efficient than centrifugal devices like the pelton wheel and turbo booster which rely on shaft for the transfer of power.

In RO systems, there is a pressure drop between the feed water entering the RO membrane and the brine exiting the membrane and entering the DWEER. Because of this pressure drop, the exhaust from the DWEER cannot flow to the feed water. Another notable feature of DWEER, is the requirement of a booster pump, driven by a separate motor (indicated in Fig. 2.19), to boost

the feed water from the DWEER to match the discharge pressure of the high-pressure feed water pump [36].

2.9.4 PX Pressure Exchanger

This device uses twelve cylinders located around the circumference of a ceramic rotor, with no pistons in them. The arrangement of these cylinders is like the bullet holes in a revolver. The ceramic rotor is the only moving part in this device. Surrounding the rotor are two end covers fitted firmly to form a tight seal preventing the pressure from escaping. The rotation of the ceramic rotor is due to the flow of water through the device, spinning at about 1200 rotations per minute. The use of PX Pressure Exchanger in RO process is shown in Fig. 2.21 where the low pressure feed water enters the PX and gets exposed to high-pressure concentrate entering from the opposite end of the device, leading to transfer of pressure from concentrate to feed water. The used concentrate then leaves the rotor at low pressure, pushed out by fresh feed water [37].

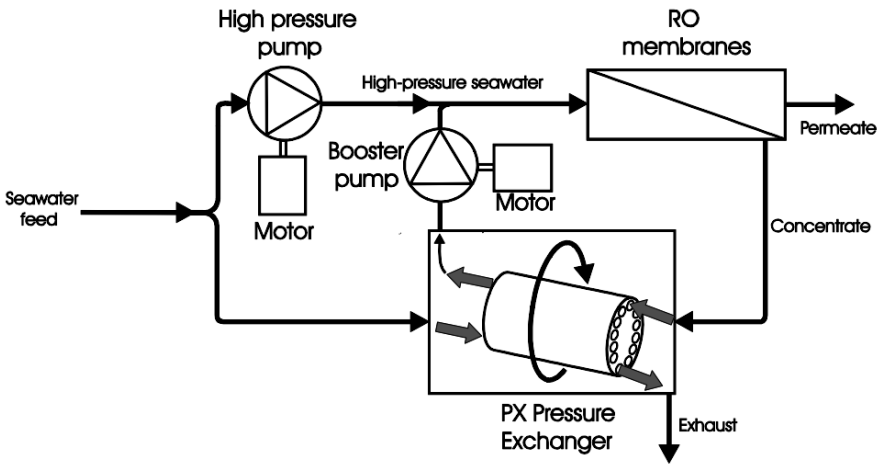

Figure 2.21: RO Process with PX Pressure Exchanger [37]

The absence of piston in this device may lead to slight mixing of concentrate and feed water which in turn might increase the feed water concentration but this is minor and can be managed. However, this mixing can further be reduced by increasing the speed of rotation of the ceramic

rotor. Like DWEER, a booster pump is used in PX too, to boost the feed water from RX to match the pressure of the feed water coming from high pressure pump.

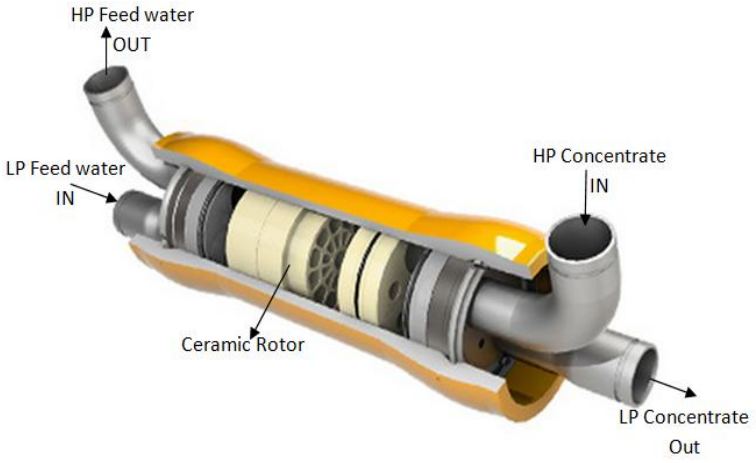

Figure 2.22: PX S Series Cutaway View [37]

The cross-sectional view of a PX S Series pressure exchanger is shown in Fig. 2.22 wherein the water inlets and outlets and the ceramic rotor are clearly indicated. A very illustrative animation video showing the working of PX Pressure Exchanger is given under PX Pressure Exchanger Devices in [37].

2.9.5 Energy recovery devices for small-scale RO plants

It is a known fact that energy recovery systems play a very important role in reducing the specific energy consumption of Reverse Osmosis process thereby reducing the overall costs of the system. Hence in view of this, we see that the implementation of energy recovery devices in large RO plants is a common practice. The problem is with small-scale RO systems as they do not have energy recovery systems. They use needle valves that provide the required back pressure for the RO process but it involves huge wastage of energy and thus is very expensive.

Scaling down the large-scale energy recovery systems to make them suitable for small-scale RO process does not really work because of the clearances and the tolerances that are involved. The

energy recovery incorporation (ERI) that manufactures large-scale pressure exchangers did produce small-scale pressure exchangers but found them to be prone to fouling because of lesser clearances. This led to the development of pumps with built-in energy recovery systems, by Bowie Keefer in 1980s, for use with small-scale RO systems. However, due to excessively high manufacturing costs, this promising idea was discontinued

2.9.6 Hydraulic motor

Hydraulic motors devices that transfer energy from high-pressure oil to rotary motion and are considered to be very efficient. Apart from the oil-driven hydraulic motors, the water-driven hydraulic motors are also used especially in food industry where a small leakage of oil can prove to be extremely harmful. Danfoss (accessed Aug 12 2013) manufactured high-pressure water-hydraulic pumps for various industrial applications like reverse osmosis, fire fighting and wood processing. The hydraulic motors are used for brine-stream energy recovery to drive the electric motor of high-pressure pump similar to the Pelton wheel arrangement shown in Fig. 2.16 .

2.9.7 Clark Pump

The Clark Pump is very similar to the dual work exchanger explained in section 2.9.3, except that the two cylinders are next to each other (inline) and their respective pistons are connected by a single rod. The rod and therefore the pistons reciprocate inside the cylinders as one unit as shown in Fig. 2.23 by the bi-directional arrow. It is also known as the pressure intensifying device, manufactured by Spectra Water makers. The working mechanism is explained with the help of an animation in [12].

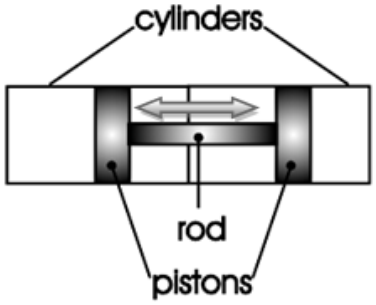

Figure 2.23: Clark Pump unit - Schematic

It was Clark Permar who developed the Clark Pump, named after him, working in collaboration with a company called Spectra Water makers. He then gave the license to the company to manufacture the Clark Pump for onboard yachts and the late 1990s saw the first implementation of Clark Pump.

Working Principle

The Clark pump is powered by a flow of relatively low-pressure water from a separate pump (well or feed-water pump). It uses the reciprocating motion of two pistons connected by a rod inside a cylindrical housing as shown in Fig. 2.23, to recover energy from brine (wastewater). During a stroke, one cylinder functions as driving cylinder and the other functions as pressurizing cylinder and on the next stroke, the cylinders switch roles. Both the strokes are depicted in Fig. 2.24

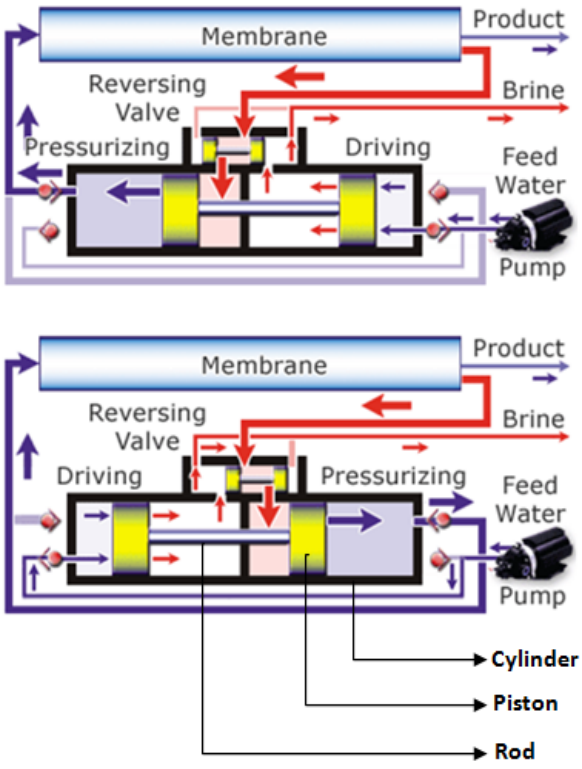

Figure 2.24: Clark Pump & Stages of compression [11]

First, the water from the feed water pump reaches the driving cylinder and pushes its piston. This driving piston in turn pushes the rod to go through the center block into the pressurizing cylinder, which has the driven piston. As the rod pushes the driven piston, it circulates water on top of it, through the reverse osmosis membrane. The high energy-brine that is produced is fed back to the reversing valve which directs it to the same cylinder where the rod is entering, thereby providing additional energy to push the rod through the cylinder. As the rod enters the pressurizing cylinder, it pushes the water on top of the piston and since this water has no place to go, this leads to rise in pressure to the point where reverse osmosis can take place in the membrane to produce fresh water. The amount of fresh water that is produced is proportional to the volume of the rod entering the pressurizing cylinder. When the driven piston touches the base of its cylinder, the process is instantly reversed by the reversing valve, with pressurizing cylinder

now working as the driving cylinder and vice-versa. The brine water under the driving piston, which had entered its cylinder on the previous stroke, is ejected out. This brine water ejection and both the stages of compression are shown in Fig. 2.24

This way, the high-energy present in the brine is utilized to increase the pressure of feed water, reducing the workload on the feed pumps, to meet the desired pressure requirements, on its own. This improves the feed pumps' durability, reduces the specific energy consumption and increases the overall efficiency of the RO process.

Configuration of Clark pump in Reverse Osmosis Desalination System

The simple configuration of Clark pump used in Reverse Osmosis Desalination System is shown in Fig. 2.25 wherein the feed water is pumped through the system by the medium-pressure pump. The water is then fed to the pressure intensifying device called Clark pump which utilizes the high-pressure brine to further increase the feed water pressure before supplying it through the reverse osmosis membrane which produces fresh water and brine (waste water) as the by-product. The brine produced is of high-pressure and is again fed back to the Clark pump which again makes use of the high-pressure brine and then pumps it out of the system.

As a result, we see that there is considerable improvement in the overall efficiency of the system and reduction in specific energy consumption as the feed water pump does not have to do all the workload in supplying the required pressure to the feed water.

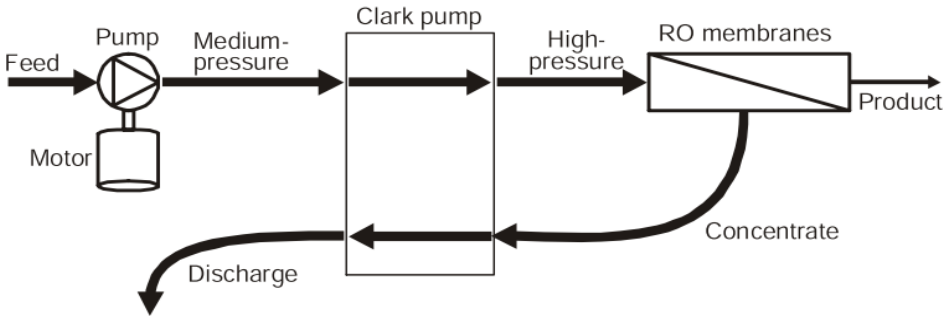

Figure 2.25: Configuration of Clark pump in RO Desalination Systems [34]

Qiblawey et al. [38] presented reverse-osmosis desalination technique which is powered by solar energy for electricity, as part of a project called ADIRA, which is funded by the European Union to promote a common interest called Reverse-Osmosis Desalination using Solar Energy in various rural areas, in accordance with various countries. The two main components are Reverse Osmosis System, to desalinate the water, which is able to produce 500 L of fresh water on a daily basis and the second being, the Photovoltaic Solar panels of 433Wp to provide electricity to run the RO system. As explained in the paper, the system was successful in providing clean drinkable water from salty water which has salt content up to 1700mg/L. The components of the system are PV-Modules (as many as 8) , a solar charge regulator , RO-Membrane (as many as 4, working in parallel) of thin-film type made of polyamide in a spiral wound configuration, High-Pressure Pump with open flow of 89 L/h, Feed-pump (centrifugal type) with output power of 60W and operating flow of 35 L/min, a softener unit, two batteries each of 12V, sensors like feed-pressure sensor, ambient temperature sensor, water temperature sensor, pyranometer sensor and flow meters for measuring the permeate and feed flow. The various parameters which were measured were incident solar radiation (insolation), irradiation, the peak sunshine hours, ambient temperature etc., and various observations were made like the solar radiation and its influence on current and voltage of solar PV modules, the effect of the number of working hours of the system on daily production of fresh water, the effect of temperature of feed water on the salt

rejection (percentage) and permeate recovery keeping the operating pressure constant. The authors have also shown that the specific energy that is consumed decreases with an increase in recovery percentage, keeping the operating pressure. The performance of the system was also studied based on parameters like feed flow, the total dissolved solids in feed flow, the permeate flow and its corresponding dissolved solids. In the end, to sum it up, what the authors have tried to present is to evaluate the performance of PV-RO system wherein the reverse-osmosis system is powered by PV panels and batteries were used to store the extra power that is produced and run the system at night. The system worked fine thereby achieving the goal of providing the supply of usable drinking water to rural areas. The permeate that was produced was in the range of 9.3L/h to 53L/h, based on the operating pressure and water recovery percentage. Based on the performance, the efficiency was calculated to be 12% with permeate being produced is of low TDS, around 30mg/L.

Sobana and Panda [39] presented the literature review on the identification, modeling and the control aspect of Reverse Osmosis Desalination systems and presented a refined paper in 2011, based on their study. They started out by defining desalination as an efficient separation process used for removal of dissolved salts from salty or brackish water to make it usable for household purposes or for drinking. They described Reverse Osmosis as the best technique to achieve the desalination of water not because it is an efficient technique but also because it is very cost effective. The authors have also highlighted the fact that the performance of Reverse Osmosis system depends on various parameters like feed-water temperature and pressure, the amount of dissolved solids in the feed water and also the strength of the RO membrane to withstand the high feed pressure. Next, the authors have discussed the outcomes of the literature survey by throwing light on the parametric identification, the dynamic modeling and the control based on

the obtained models. Most of the dynamic models of Reverse Osmosis systems that are presented are in the form of transfer function matrix and also a dynamic MIMO model based on lumped parameter distribution by Gambier explained below. The various control techniques discussed in this literature survey are either PID controllers or Model Predictive Control. In the end, the authors have mentioned that the main reason behind the extensive research that is been done in Reverse-Osmosis desalination is due to the scarcity of fresh water due to factors like global-warming and deterioration in the quality of underground water. The authors have also mentioned that there are basically three types of mechanistic models of membrane transport process namely porous, non-porous and irreversible thermodynamic models. Membrane fouling is another area that needs to be worked on by improving its maintenance. Also, in order to improve or increase the production of fresh water, the RO system needs to have a good control of the concerned control variables. In the end, this work enables one to understand the reverse osmosis process well and also the modeling and control of it in an easy and unobtrusive manner.

Gambier et al.[40]presented a dynamic model of a reverse-osmosis desalination system for the purpose of control. Since reverse-osmosis is considered a very powerful tool for desalination, it requires an equally good control system to manage the costs. In order to achieve this, modeling of the RO system is very critical. There are various models that one can find related to Reverse Osmosis Desalination based on an identification method called parameter identification but this paper presents lumped dynamic modeling based on certain laws of physics. The model developed is implemented using MATLAB/Simulink so as to try out different plant configurations and test the control that is applied. Various experiments were conducted, first of which was, studying the permeate flow rate and the concentration for a given (constant) feed water temperature but at various valve openings (in percentage). It was observed that as valve

opening is reduced, the permeate flow rate increases thereby decreasing the salt concentration and improving the quality of water. Next experiment involves keeping the valve opening at a constant value and varying the feed temperature. It has been observed that as the temperature of feed water increases, the concentration of permeates first increases but decreases later since more permeate is being produced. Next, both valve opening and feed water temperature are varied simultaneously and the corresponding effects showed the salt concentration of permeate increasing exponentially with the increase of feed water temperature.

Gambier [41] presented a robust PID controller based on multi-objective optimization for the control of desalination plant. Generally, the PID controllers that are used for desalination systems are not well tuned because the system parameters change every time thereby changing the model of RO plant. In this paper, a PID controller for permeate flow rate control is developed using multi-objective optimization so that this control is not very sensitive to changes in plant. The RO plant considered here is a small plant used for purifying the tap water. Therefore, no brine energy recovery device is used and neither is there a need for post-treatment of the permeate. For the study, the plant is considered as a Single-Input-Single-Output system with Brine Valve position as the Input and permeate flow rate as the output. Subspace Identification was carried out to obtain different models of the plant and a random model was also obtained for the purpose of studying the plant. The simulation that was carried out showed that the method gives good performance for long operating conditions.

Chaaben et al.[42] presented a Multi-Input-Multi-Output Model for Solar powered Reverse Osmosis Desalination System. The authors stressed on how important a process reverse-osmosis desalination is, in converting brackish water into pure water by removing the salt through membrane separation and also stressed on the need of a good control system to efficiently

control the plant. Even though there are many models that are presented related to the PV-RO system, this paper presents a new modeling approach by treating the plant as a Multi-Input-Multi-Output System. The system has got two inputs namely, the angular speed of the motor pump and the opening of the reject valve (brine valve) and two outputs namely, the product flow and the salinity in the product flow. Also the salinity in the feed water is considered as a disturbance. The reason why the above-mentioned parameters were selected as inputs and outputs was because the quality of the product (pure water) is highly dependent on these parameters. The models presented are transfer function matrix model and the state-space model of 4th order. Also for validation of the selected models, some experiments were also performed in which one of the two inputs were varied keeping the other input constant. Validation of the models was done by applying the step signal to the inputs and measuring the output variables. This validation proved that the models can very well be used for implementation in process control industry for efficient run and to minimize the operating costs.

Thomson [43] presented an extensive work on Reverse-Osmosis desalination powered by solar but without any batteries, as part of PhD thesis in 2003. The author worked extensively towards the design, construction as well as the testing of PV-RO system. The system basically works towards desalinating the seawater. As mentioned earlier this is a system which does not use batteries, hence the operation of the plant is done only during day and the quantity of fresh water produced varies depending upon the solar radiation on the given day. Another notable aspect here is the use of Clark pump to obtain high pressure of brine stream (concentrated salt solution) to increase the overall efficiency of the system. Other general requirements are the same as in other PV-RO systems like motors, pumps, inverter etc. Maximum Power Point Tracking, abbreviated as MPPT, is also used to obtain the maximum power from the array of solar panels

that are connected. Since the amount of irradiation as well as the temperature varies throughout the day, the power produced by the PV panels also varies, implying that the MPP is not stationary. This controlling of current or voltage to make sure that the system operates at maximum power is what is known as MPPT. The Instrumentation involved is explain in a user-friendly software called Lab VIEW and the modeling and testing part is done using Mat lab/Simulink which was done keeping in mind the basic goal of minimizing the cost of fresh water that is produced. To sum it up, the author was successful in developing a model for the battery less PV-RO system which would help in further enhancing or extending the work done in this thesis. Like for instance, the MPPT algorithm developed could be refined further to be used with other PV-RO systems.

Palacin et al., [44] presented a paper on the initial validation of Reverse Osmosis Simulator. The reverse osmosis desalination plants usually have short operating times and a good control strategy would help to reduce this operating times even further and lowering the costs as well. This paper presents the validation of a simulator (dynamic) of reverse osmosis desalination plants which was developed earlier and this validation is based on the real-time data obtained from a real desalination plant. First, a brief introduction of Reverse Osmosis plant and its various components is given, based on which a simulator of RO plant is designed. Although there are various parameters of the plant that are measured like flow, pressure, pH, temperature, salt concentration etc, for the validation part, only pressure and flow are considered. Comparison of the calculated values and the real-time measured values for different flows like feed flow and permeate flow and different pressures like inlet pressure and outlet pressure, is done for the sake of validation. Hence, this paper actually highlights the importance of having a simulator for

Reverse Osmosis plant and validation of a part of this simulator was done by comparing parameters related to pressure and flow.

Bilton et al., [45] presented a paper on PV-RO systems based on their research, which focused on evaluating and improving the feasibility of PV-RO systems. The authors emphasized that even a small-scale reverse osmosis desalination system can provide fresh water to communities that are deprived of natural resources like water. But for the system to be practically implemented, the economic as well as the technical feasibility is a criteria. Hence the authors did a research to evaluate and improve the feasibility of PV-RO plants. First, the authors through extensive research developed a method to evaluate the feasibility first and then work on it to improve it. They found that location is a very important factor related to feasibility of the PV-RO system. Research also showed that improving the overall efficiency of the system can make it even more feasible. PV-RO system models developed in this paper have also been validated using experimental data. Hence this paper serves as a motivation for the control research work that is being done related to PV-RO. It was concluded that geographic location is an important criteria for PV-RO systems to be feasible which can further be improved by improving the overall system efficiency.

Joyce et al., [46] presented a small-scale reverse osmosis desalination system powered by solar to provide pure water to rural areas. The authors start out by highlighting the large-scale desalination systems and how they are used extensively all around the world to produce several cubic meters of fresh water everyday which requires high amount of energy to run pumps. But what they are presenting here is a small-scale PV-RO system which might prove to be really helpful to provide water to remote areas or during catastrophes when drinking water is not readily available. These systems can be made by employing the commercially available small

RO units which produce fresh water in the range of 100-500 Liters per day with pressures as low as 5 bars. These units can work on brackish water with salt concentration of up to 5000ppm. A series of experiments have been performed on this setup and a key conclusion that was made was that the energy consumption decreases with increase in feed pressure and feed water recovery. The results were used for developing a mathematical model of the system using the current-voltage characteristics of PV-modules. And this model will also be used for estimating the amount of water that will be produced on yearly basis and the related cost.

Suleimani and Nair [47] presented a reverse-osmosis desalination system powered by solar in Oman. The experiment was done to desalinate the brackish water (underground) at a remote location in Oman. The PV-RO system comprises of a pump used for pumping the well-water and pre-treating it to remove hydrogen sulphide, cartridge for filtering, reverse-osmosis unit and waste-water pond along with necessary control and instrumentation. The results related to the amount of water-production, the amount of energy utilized and the operating cost, proved that reverse osmosis desalination systems (solar driven) are highly useful in inaccessible areas that have scarce supply of fresh water. Also the components used in the system are easy to maintain and are very user-friendly. A comparison was also made between the solar energy and diesel alternative and it was observed that in terms of the overall costs, the solar is reasonable compared to diesel alternative and the overall costs of PV-RO is expected to decrease since the costs of PV modules would possible decline in future. To sum it up, it can be concluded that for remote areas PV-RO is a very good and feasible option to provide drinking water.

Abbas [48] presented a paper on Reverse Osmosis Desalination System and its control by a method called Model Predictive Control, abbreviated as MPC, based on Dynamic Matrix Control. It’s an advanced method of control, which is very popular in process industry. There are

many strategies that one can apply in MPC but the one used in this paper is Dynamic Matrix Control (DMC). There were two cases that were considered, first was a Single-Input-Single-Output system with feed pressure as the input and permeate flux as the output. And in the second case, the feed pressure and pH were considered as inputs and permeate flow rate and conductivity, were considered as outputs. Also the performance of MPC was evaluated based on its comparison with standard PI controller, besides investigating the sensitivity of MPC to changes in plant parameters. Results proved that MPC is better than PI controller in terms of the performance and robustness.

Alatiqi et al., [49] presented a paper on Identification and Control of a Reverse Osmosis Desalination system in Kuwait. They started out by highlighting the importance of having an efficient control system not just for Reverse Osmosis desalination but for any other plant to have a long-term and successful operation. In this paper, the control parameters are the permeate flux and its conductivity. The input parameters are the feed pressure and pH of feed pressure. Considering the inputs and outputs, all transfer functions seemed to have dominating first order response with permeates flux response being quicker than the response of conductivity. The membrane configuration used is that of hollow fine fiber. The control techniques used are system identification, Zeigler-Nichols setting and for multivariable case, log modulus tuning technique is used. Upon applying the control techniques, satisfactory results were obtained for set-point tracking.

Greenlee et al., [50] presented the research work on Reverse Osmosis desalination, its technology and the challenges it faces. It's a known fact that RO technology has grown leaps and bounds since last 40 years evident from the fact that close to 80% of the shares of desalination plants come from reverse osmosis membrane technology. Today, we have tailored membrane

systems and pretreatment systems for the application of RO systems. RO desalination is basically done for two types of water sources namely, salt water and brackish water. The basic difference between the two is related to the salinity, brine concentration, membrane fouling, waste-water disposal options and also the location of the plant. However, the options that are available for pre-treatment are more or less the same for both the water sources. Also the recent advances in the renewable energy will allow reverse osmosis desalination to be used in remote rural areas as well. Also the article, presents some of the key parameters related to the two water sources like the contaminants that are present, the membrane fouling and its cleaning, the system design, post-treatment of the product (permeate), disposal of the waste-water, the alternate energy-sources and more importantly the costs related to the two water sources. The authors concluded saying that, though salt and brackish water are heavily used in large-scale plants, several challenges still remain which calls for further improvement in membrane technology, the use of energy and the treatment of the concentrate.

Ghermandi and Messalem [51] discussed reverse osmosis desalination powered by solar, its current state of the art. They start out by saying that solar-driven RO-based desalination systems have the potential to overtake desalination that is done using fossil fuels thereby reducing the overall operational costs and improve the environmental sustainability. The research on solar-powered desalination was done by analyzing 79 experimental design systems related to PV-RO, worldwide. It was proven that it was cost-competitive related to other energy sources that are available, to be employed on a small-scale basis in remote communities. Given any favorable conditions a hybrid system with an additional power source works better or at least as good as a solar-power desalination system. Like for instance, for small-scale applications, solar energy combined with wind energy can achieve lower costs by deriving the best from both the

renewable energy sources. For large scale applications, solar along with fuel-firing can stabilize the overall desalination system especially during nights or when the irradiation is low. Based on their research, the authors conclude that solar-based desalination systems are mature enough and have the potential to see huge advancements in future to be applied to large-scale solar desalination system and also to be able to serve remote areas on a small-scale basis.

Al-Atiqi et al., [52] presented an overview of the process control that is used in the desalination plants. The desalination techniques used were multi-stage flash and reverse osmosis. They explained that currently the classical controls used are the conventional PID and PI controllers. The instrumentation, the indicators and alarms formed the crux of the control system that is used. They concluded that in order to have good control system in place, there should be good co-operation between the desalination industry and research centers.

Chapter 3

THE EXPERIMENTAL SETUP

3.1 The Reverse Osmosis Unit

The battery-powered reverse osmosis desalination system at KFUPM is manufactured by Spectra Water makers and comprises of the following components:

1) Spectra Clark Pump Pressure Intensifier, with a 40-inch spiral wound membrane.

2) Primary feed pump module with fresh water flush valve.

3) Secondary feed pump.

4) Pre-filter.

4) Water Accumulator.

5) Remote Monitoring Panel.

3.1.1 Clark pump- RO membrane module

The Clark pump along with the spiral wound membrane is shown in Fig. 3.1.

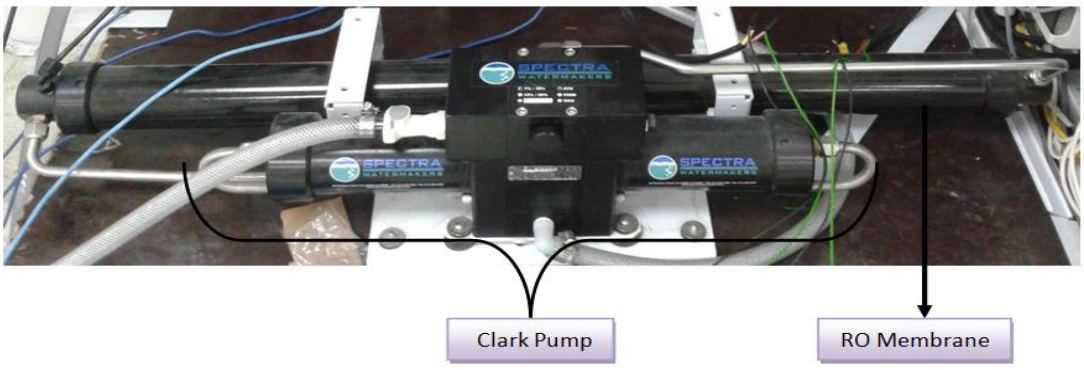

Figure 3.1: Clark Pump with RO Membrane

As mentioned in Section 2.9.7, the Clark pump is a two-stage pressure intensifying device which makes use of the high pressure brine in increasing the feed water pressure to a point where

reverse osmosis can take place, thereby decreasing the specific energy consumption of the system by 75% as compared to other conventional systems. It is made up of composite materials and engineered plastics and is considered to be highly efficient and durable. The Clark pump pumps the feed water to the reverse osmosis membrane which has a spiral wound configuration and is 40-inch in length. The membrane produces the fresh water and feeds the waste water (brine) back to the Clark pump for utilization of its energy in increasing the feed water pressure.

The Clark pump holds proper membrane pressure for a wide range of water temperatures and water quality without any effect on the quantity and quality of product water that is produced. The rugged construction of the Clark pump is to resist any kind of corrosion and requires low maintenance and hence considered to be highly reliable.

For the purpose of easy servicing, the Clark pump is equipped with an easy-to-disconnect fitting on the brine discharge line.

3.1.2 Feed water pumps

The primary feed pump module fitted with fresh water flush valve and the secondary feed pump-pre filter assembly is shown in Fig. 3.2.

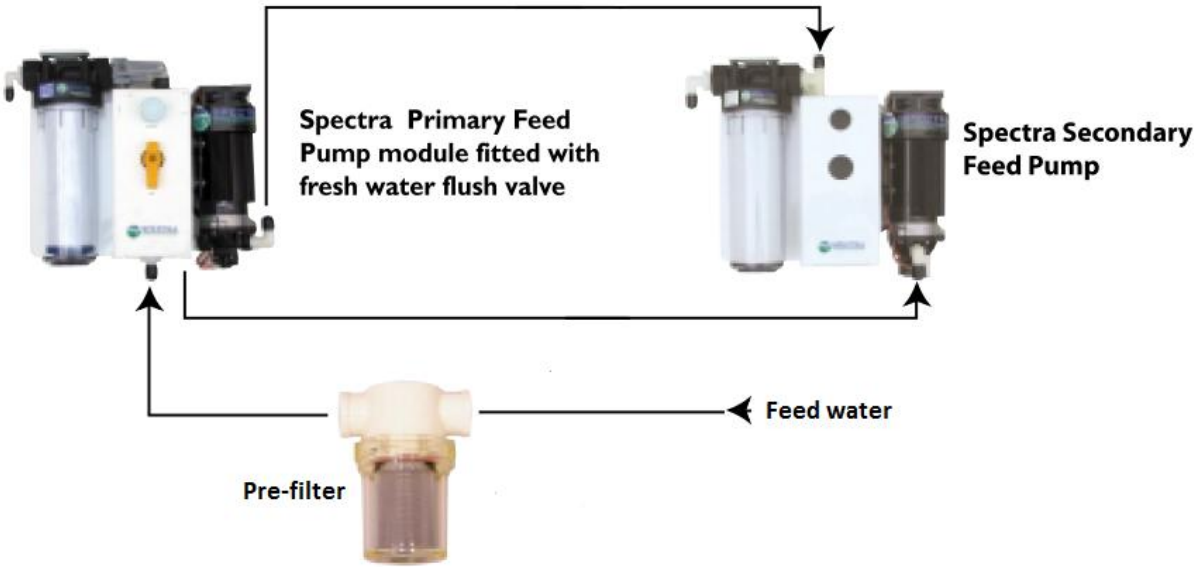

Figure 3.2: Feed water pumps & pre-filter assembly [53]

The two feed pumps are very efficient and at the same time very rugged and cannot be damaged if they are running dry or by feed water intake aeration. The system is so versatile that it can have both pumps to run simultaneously to obtain high quantity of product water and can also run on a single feed pump for obtaining high efficiency. Another advantage of having two pumps is the redundancy factor wherein if one of the two feed pumps goes bad, the unit can still function perfectly on the other pump to produce fresh water. The system has got simple, easy to understand mechanical controls and gauges and there are no complex electronics that are involved. The connections are also straightforward , with basic digital switching and there are only three modules to be mounted namely the two feed water pumps and the Clark pump with the reverse osmosis membrane. Both the pumps are equipped with cooling fans to ease down the heating of the pumps especially during longer runs to improve the efficiency and reliability.

The fresh water production is 7 gallons/31 liters per hour when the system is running on one pump and14 gallons/53 Liters an hour when the system is running on both the feed pumps. The power consumption in the first case is just 120W and 280W in the second case. The complete

unit is capable of running both on 12V and 24V.For effortless servicing and maintenance of the primary feed pump, it has a freshwater flush valve to enable easy flushing of fresh water.

3.1.3 Pre-filter

The reverse osmosis membranes are designed to remove compounds that are soluble like the mineral ions. However, they cannot remove the large amount of suspended particles or solids that are normally present in feed water. If the membrane is kept in the feed water with these suspended particles, then it leads to accumulation of these particles on the membrane surface, leading to membrane fouling i.e. blocking the membrane surface, leading to a discontinuous and unsteady desalination process. Hence, these suspended particles should be removed before the feed water reaches the membrane. For this purpose, a five-micron **pre-filter** is used to remove large particles like seaweed and debris from the feed water before it is fed to both the feed pumps which help in increasing the efficiency and life span of reverse osmosis systems. The pre-filter is shown in Fig. 3.2.

3.1.4 Water Accumulator & Remote Monitoring Panel

The **water accumulator** manufactured by SHURflo [54] is a bladder-type pressure storage vessel designed to hold water under high pressure. It is used just before the water is supplied to the Clark pump, to enable trouble-free and smooth running of Clark pump. It stores certain quantity of water under high pressure and supplies it only when the system demands thereby improving the system efficiency.

The main use of accumulator is the energy conservation. It basically helps in assisting the output flow from the pumps and supplying only when the system demands. This way, it reduces the running time of the pumps and conserves energy.

It is very effective in reduction of noise caused by piston pumps in hydraulic systems. Noise reduction up to 90% can be achieved too in some systems.

The electrical failure can lead to severe damages to the system. Using a fully charged water accumulator can supply the required amount of flow needed for the process to run smoothly.

The **remote monitoring panel** indicates the feed water pressure (bar and psi) and the product water flow (gallon/hour and liter per hour) for continuous monitoring. The water accumulator and the remote monitoring panel are shown in Fig. 3.3.

Figure 3.3: Water Accumulator & Remote Monitoring Panel [53]

Figure 3.4: Reverse Osmosis Unit at KFUPM

The complete reverse osmosis system, manufactured by Spectra Water makers and assembled at KFUPM is shown in Fig. 3.4. Some of the other specifications of the reverse osmosis system manufactured by Spectra Water makers are given in Table 3-1.

Table 3-1: Specifications of Reverse Osmosis system by Spectra Water makers [53]

WATER PRODUCTION	Gallons per day / hour
Output at 25°C Feed water (Rated at 35000 ppm)	336 / 14 (1272 Liters per day / 53 hours)
POWER REQUIREMENTS	
Pump Horsepower	1/8 Each
Watt/Hour per gallon	16
Amp/Hour per gallon (12V)	1.3
Current Draw	18Amps (12V) , 9Amps (24V)
TOTAL SYSTEM WEIGHT	65lbs (29.5kg)

3.2 Instrumentation & Data Acquisition

The purpose of the instrumentation system is to monitor and control the important variables of the process. In order to determine the efficiency of the process and evaluate the quality of the outlet water, one needs to measure some parameters such as the flow rates and salt concentration for inlet and outlet water, water pressure and temperature. In addition, the instrumentation system is necessary to control the water pumps and apply a closed loop control for obtaining the desired flow rates.

3.2.1 Data Acquisition Software -Lab VIEW

LabVIEW software from National Instruments is perhaps the industry standard data acquisition package. There are many other data acquisition softwares available, but LabVIEW was found to be very simple, easy to understand and extremely user-friendly and provides various data acquisition, data analysis and data visualization tools for the user and hence was selected. Based on working experience in using LabVIEW, the choice still seems good.

LabVIEW is a graphical programming language, very different from the text-based languages that most programmers are familiar with. It relies on graphical symbols rather than textual language to describe programming actions [55]. The principle of dataflow, in which functions execute only after receiving the necessary data, governs execution in a straightforward manner. The data appears to flow simultaneously through different parts of the application program, and this, coupled with the fact that data-acquisition is inherently time-critical, can be off-putting, even to well experienced text-based programmers. Data types (integers, real, Booleans, arrays and so on) are represented by line colors and thicknesses, and can seem awkward to programmers used to less strongly-typed languages such as Mat lab, Basic or Perl. As with all programming languages, there are innumerable ways of tackling a particular problem.

Used elegantly, LabVIEW can deliver impressive functionality with minimal programming. Conversely, using LabVIEW as if it were text-based language leads to very clumsy and limited programs. National Instruments provide excellent documentation both for LabVIEW itself and for data acquisition in general.

The programs written in Lab VIEW are known as Virtual Instruments or VIs because visually they mimic the real-time physical instruments such as the knobs, gauges, multi meters etc. In LabVIEW, there are two important screens namely the front panel and its corresponding block diagram. The front panel is built with the help of in-built tools in Lab VIEW. The front panel contains various controls like the dials, toggle switch, slide switch, start and stop buttons etc and indicators like numeric indicators, LEDs, charts and other types of displays. The function of the controls is to give the user-specified input to the instrument and provide the data to the block diagram. The function of indicators is to display the output data from the instruments which are the output devices.

Whenever an object is added to the front panel, its terminus is automatically created on the block diagram window. Hence, if there is an object that is to be deleted, it should be done from the front panel and its terminus on the block diagram will automatically get deleted. However, the vice-versa is not true.

An example of front panel and its corresponding block diagram is shown in Fig. 3.5.

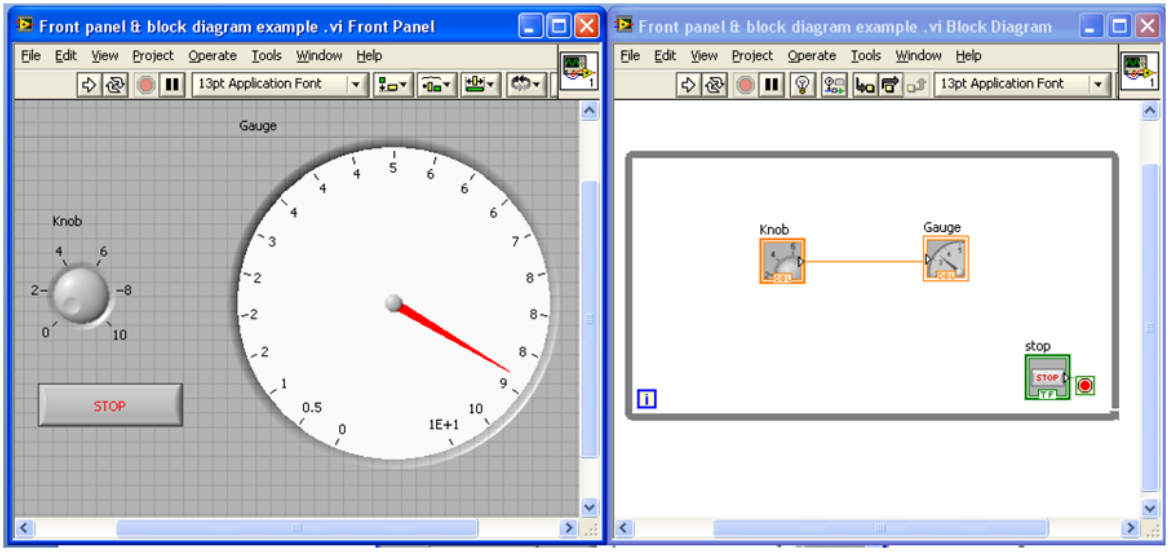

Figure 3.5: Front panel (left) & its block diagram (right) in LabVIEW [55]

3.2.2 Data Acquisition Hardware – NI USB 6009

The data acquisition hardware used is USB-6009 [56] which is a very simple and low-cost multi-functional I/O device from National Instruments. It is considered to be the best I/O device for educational purposes because of its simple structure, the ease it offers to connect devices to its various Analog and Digital I/O ports, its compact size and USB Plug-n-play connection.The device is shown in Fig. 3.6.

Figure 3.6: NI USB-6009 I/O Device [56]

The various options the device offers are shown in Table 3-2, where its specifications are listed. The USB-6009 provides eight analog input channels (single-ended), two analog output channels, twelve digital input/output channels and USB interface with the data acquisition software.

Table 3-2: NI USB-6009 Specifications [56]

NI USB-6009 Specifications	
Analog Inputs	8
Analog Outputs	2
Digital Inputs/Outputs	12
Power supply through USB connection, no additional supply needed	
Provides +5V Power Supply Output	
Provides 32-bit Counter	
Compatible with Data Acquisition software Lab VIEW	

Figure 3.7 shows the pin diagram of USB-6009 I/O Device. The Analog input channels offer two configurations, single-ended analog input and differential analog input. The digital ports can be configured both as input as well as output.

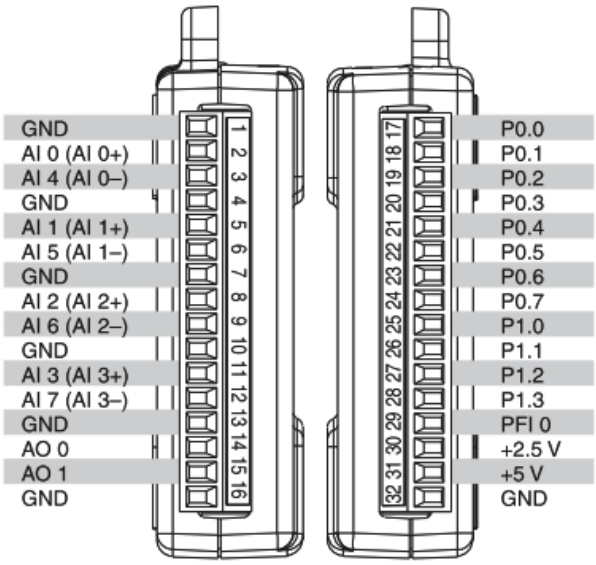

Figure 3.7: USB-6009 Pin Diagram [56]

GND represents the ground for each of the eight single-ended analog input channels, the two analog output channels, the digital I/Os and also the +5V & +2.5V power supply.

AI 0-AI 7 represents the eight single-ended analog input channels with respect to ground. For differential measurement, two AIs combine to form one differential analog input. For eg, AI 0 & AI 4 combine to form one differential analog input channel 0 i.e. AI 0+, AI 0-. Similarly, the other differential analog input pairs are AI 1&5, AI 2&6, AI 3&7. Hence there are four differential analog input channels available in USB-6009.

The analog input voltage range in single-ended configuration is +/-10V and in differential mode it has various ranges like +/-20V, +/-10V, +/-5V, +/-4V, +/-2.5V, +/-2V, +/-1.25V and +/-1V. However, for e.g. +/-20V means that $|(\boldsymbol{AI}+) - (\boldsymbol{AI}-)| \leq \boldsymbol{20V}$. But individually both AI+ and AI- should be within +/-10V.

AO 0-1 represents the two analog output channels and gives the analog output voltage with respect to the ground terminal. The analog output voltage range is 0-5V.

P0.0-7 & P1.0-3 represents the twelve digital input/output channels. They can be used both as digital input as well as digital output channels with respect to ground as the reference.

PFI 0 represents a trigger input or a counter input with respect to the ground.

+5V & 2.5V represent the power supply sources and serve as the output terminals.

3.2.3Acquiring data using NI USB-6009 in Lab VIEW

In order to use NI USB-6009 in Lab VIEW, we need to use a function called NI-DAQmx which is known as Data Acquisition palette, found under the Measurement I/O palette. Fig. 3.8 shows a screenshot wherein the Measurement I/O is highlighted and NI-DAQmx is indicated in a red rounded rectangular box.

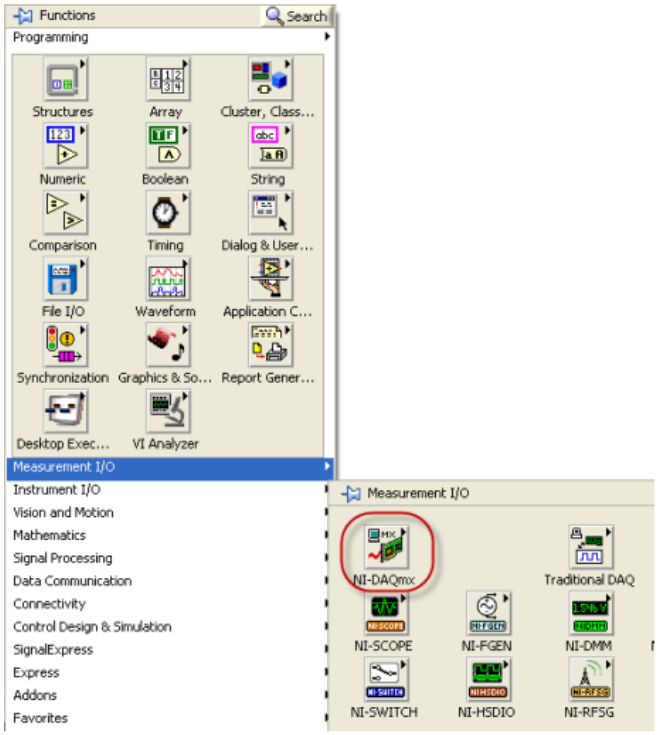

Figure 3.8: NI-DAQmx in Lab VIEW [57]

Inside the Data Acquisition palette i.e. DAQmx, there are various data acquisition functions that are available like read, write, triggering etc as shown in Fig. 3.9. But the easiest of all is the 'DAQ Assistant' function indicated in a black rectangular box in the same figure.

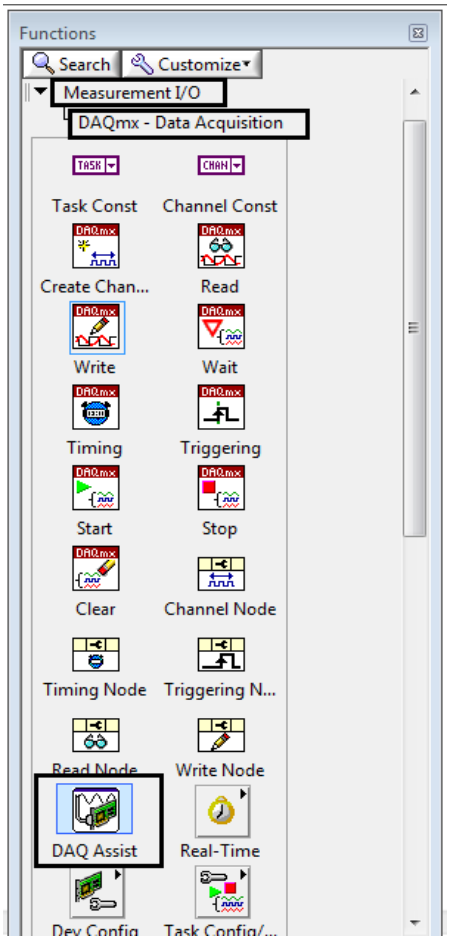

Figure 3.9: DAQ Assistant In Lab VIEW [57]

For each operation, we use a separate DAQ Assistant i.e. for analog input we use one and for analog output we use another. If in case there are two analog inputs, they can be indicated in a single DAQ Assistant. Same is the case for multiple analog output signals.

Once we drag and drop the DAQ Assistant icon on the Block Diagram window, another pop-up screen appears, snapshot of which is shown in Fig. 3.10, wherein we need to mention whether we wish to acquire signals (analog/digital input) or generate signals (analog/digital output).

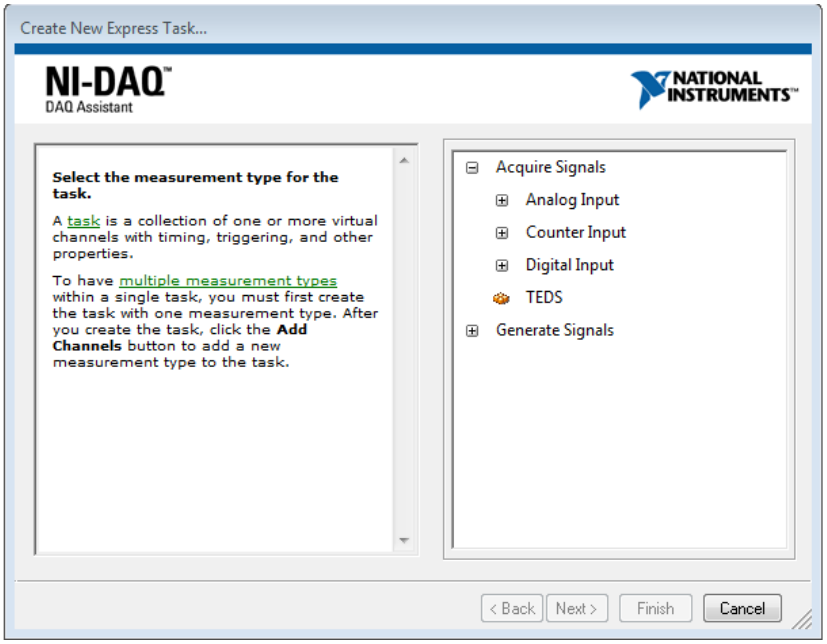

Figure 3.10: DAQ Assistant - Measurement type selection [57]

As seen in Fig. 3.10, we can either acquire analog input, counter input or digital input. The various analog input parameters are voltage, temperature, current etc. In this work, voltage is measured.

For the sake of explanation, consider that we want to acquire analog voltage signal. Therefore, we first click on Acquire Signals ->Analog Input -> Voltage. When we click on voltage, another window appears, wherein we need to mention the analog input channel that is being used for measurement. The analog input channel selection window is shown in Fig. 3.11 where ai0-7 indicate the eight available analog input channels.

For example, if the measurement device is connected to AI 0 with respect to ground (single-ended mode), then ai0 is selected as shown in Fig. 3.11. Suppose if the analog voltage measurement is in differential mode i.e. if the measurement device is connected to AI 0 & 4, then ai0 is selected in the window shown in Fig. 3.11. Similarly, if the measurement device is connected to AI 1&5, for its voltage to be measured in differential mode, then ai1 is selected.

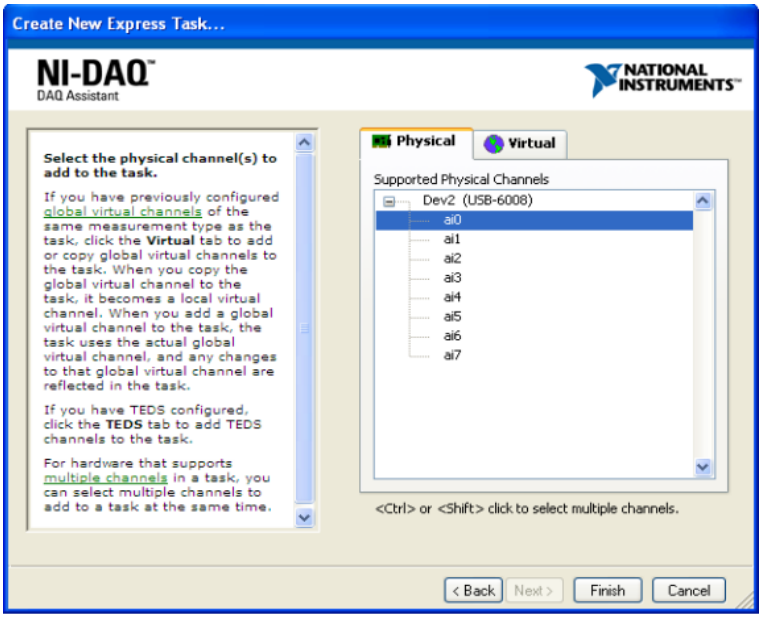

Figure 3.11: Analog Input - Channel selection window [57]

Suppose we have connected the measurement device to analog input channel 0, we select 'ai0' and click on Finish. Another window appears, snapshot of which is shown in Fig. 3.12, wherein we get all the details related to the voltage measurement like the maximum and minimum value within which the voltage is to be measured, the terminal configuration i.e. single-ended or differential mode, the data sampling time and a provision to add more analog input voltage channels. All these important details are indicated in red rounded rectangles in Fig. 3.12.

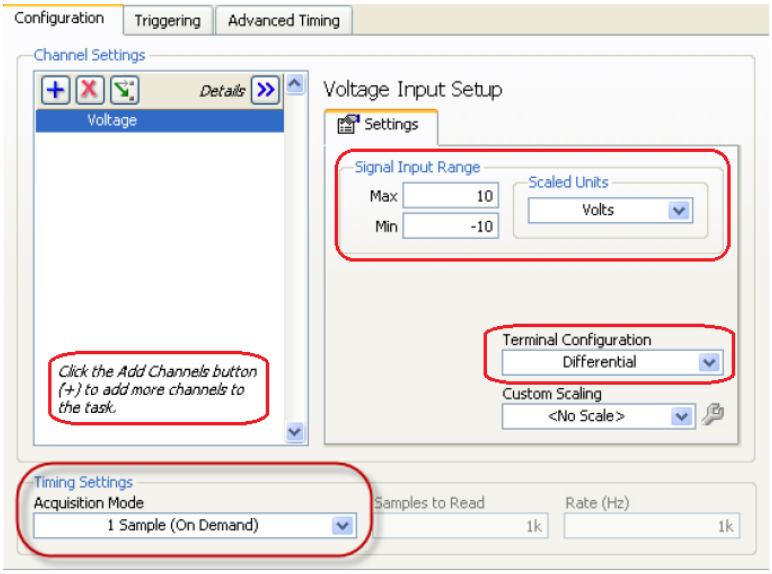

Figure 3.12: Voltage Measurement -Configuration window [57]

The sampling rate was selected as one second for this project work. This concludes the configuration of DAQ Assistant for acquiring of analog input signals. DAQ Assistants for other type of measurements can be configured in the same way. This is how NI USB-6009 is used for data-acquisition in this project.

3.2.4 Logging measurement data to file

It is very important to log the measurement data to a file for further investigation about the system, understand the system better and in this case, the measurement data is logged to an excel file in Lab VIEW, for developing various polynomial models of reverse osmosis desalination system using system identification techniques.

Lab VIEW provides us options to write the measurement data to a file and also read from the measurement file. These functions are 'Write to Measurement File' and 'Read from Measurement File' [58]. The location of these functions in Lab VIEW is as follows:

Functions -> Programming -> File I/O -> Write to Measurement file (For writing data to file)

Functions ->Programming ->File I/O ->Read from Measurement file (For reading data from file)

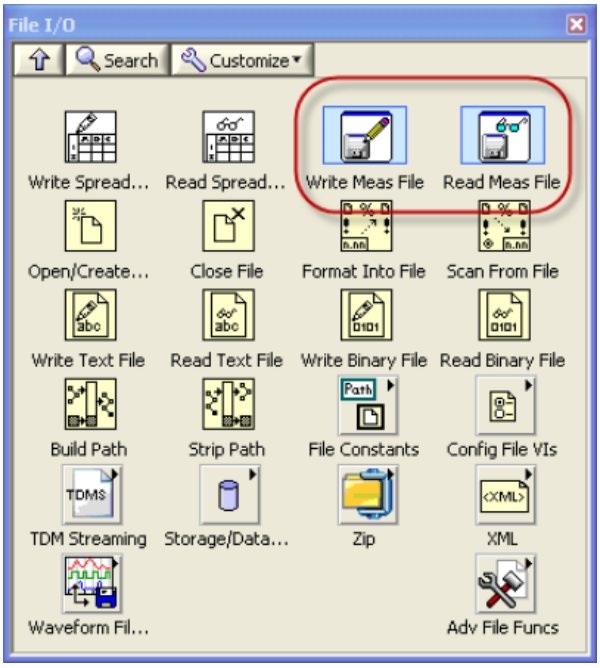

Figure 3.13: Data logging functions in Lab VIEW [57]

The snapshot of Lab VIEW indicating the location of 'Write to Measurement File' function and 'Read from Measurement file' function under File I/O palette is shown in Fig. 3.13 indicated by red rounded rectangular box.

Writing data to measurement file

In order to write data to a file, we drag the 'Write to Measurement File' function and drop it onto the Block Diagram window in Lab VIEW. We get another pop-up window known as the configuration screen, wherein we give all the details like the location of the file (on the hard-drive) to which we intend to write the data to, the filename, the file format (LVM, TDMS) and other options as indicated in Fig. 3.14. Selecting LVM data format will write the data to a notepad file whereas selecting TDMS format will write it to an excel file. Likewise, there are

other options that are available like overwriting an already existing file or to append the data to the existing file keeping the previous data intact. For our project work, we have selected TDMS as the file format.

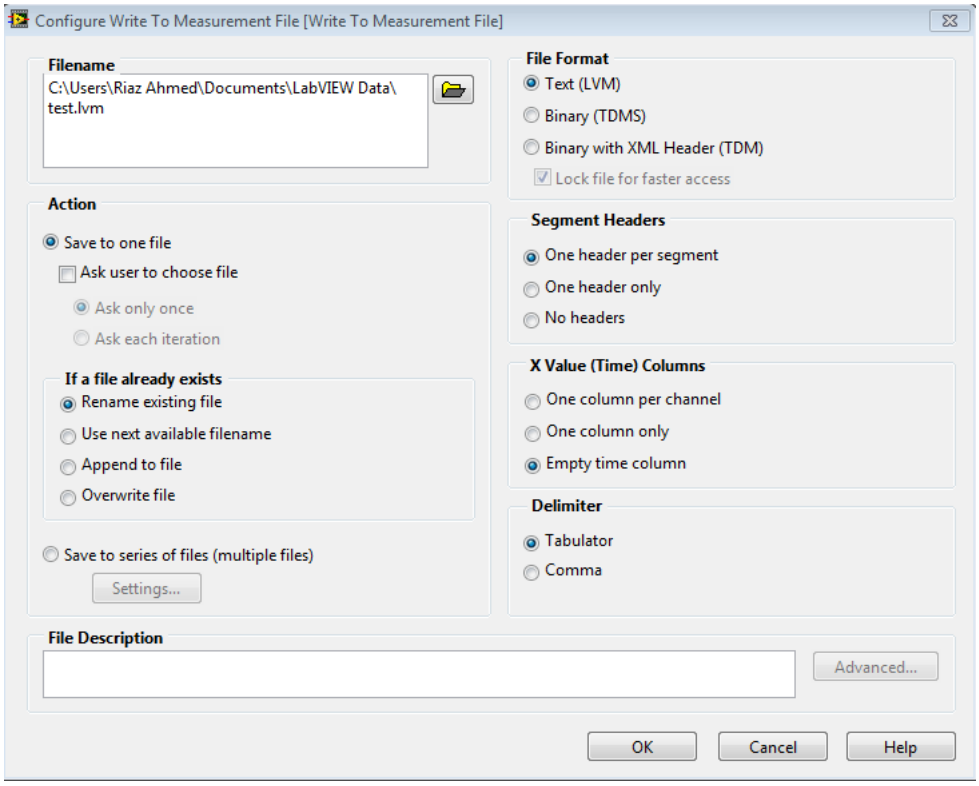

Figure 3.14: Write to Measurement File - Configuration Screen [57]

Reading data from Measurement file

In order to read the measurement data from an existing file, we drag the 'Read from Measurement file' function and drop it onto the block diagram window. We get another pop-up window known as the configuration screen for reading data from measurement file as shown in Fig. 3.15. Since the data writing is done in TDMS file format, we select the same format when reading the data form measurement file, as shown in Fig. 3.15.

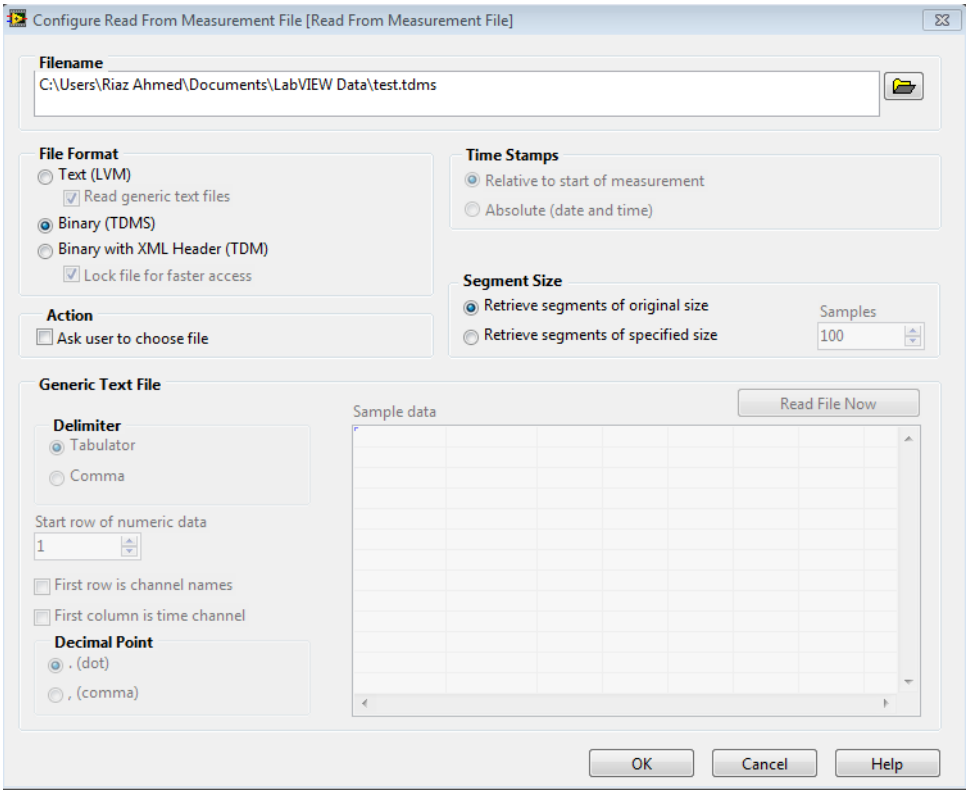

Figure 3.15: Read from Measurement file - Configuration Screen [57]

3.2.5 Flow Measurement

There are two types of flow meters used in this project, but both work on the same principle. One is the impeller type flow meter and the other is turbine flow rate sensor. Both give output in terms of electrical pulses based on which flow rate is determined.

3.2.5.1 Impeller-type flow meter

The flow meters used for the measurement of input flow rate are impeller or paddle-wheel type flow meters manufactured by OMEGA Engineering [59].These types of flow meters consist of a rotor with multiple-blades on its circumference, kept in the direction of liquid-flow. The wheel or the rotor starts spinning as the liquid hits the blade and sets the rotor spinning.The mechanism of these flow meters is such that as the rotor starts spinning, the flow meter gives the electrical pulses as the output. The higher the rotation of the wheel, the greater the number of pulses generated by the flow meter which indicates higher flow-rate.

Fig. 3.16 shows the impeller-type flow meter used in this project.

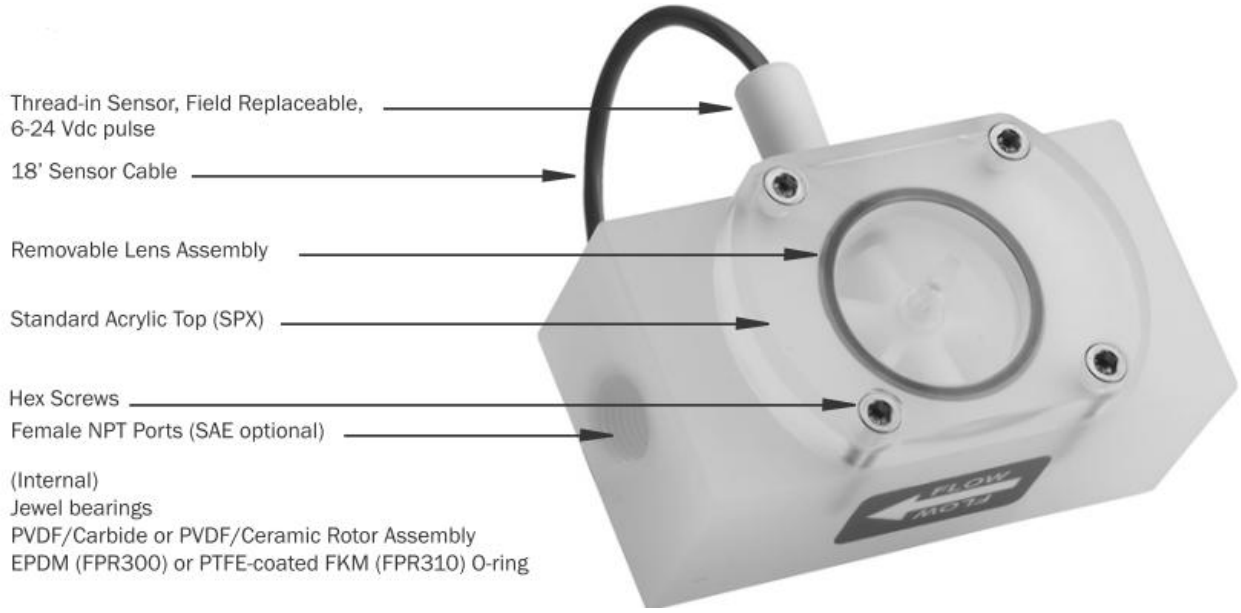

Figure 3.16: FPR-301 Series Low Flow Meter [59]

The maximum pressure that this particular type of flow meter can withstand is 150psi / 10 bar. The accuracy is also very good and is in the range of +/-1% of full scale. The other specifications like the maximum temperature, the material it is made of, the power requirement and the output signal type are listed in Table 3-3. Another important note about these flow meters is that they are factory calibrated and each meter will have its distinct K-factor, which is a numerical value that indicates the number of pulses per gallon flow of water through the meter.

Table 3-3: Specifications of FPR-301 Flow meter [59]

Specifications of FPR-301 Series Flow Meter		
Material	Body	Polypropylene
	Rotor	Polyvinylidene difluoride
	Cover	Acrylic
Maximum Pressure		150psi (10 bar)
Maximum Temperature		160^0F (70^0C)
Power		5-24Vdc, 2mA min
Output		Current sinking pulses

The flow meters are connected to the analog input channels of USB-6009 Data acquisition device as per the connection diagram shown in Fig. 3.17.The red wire is connected to +5V dc voltage supplied by the data acquisition device (USB-6009) and the black wire is connected to the ground terminal of the same device. The white wire which carries the signal can be connected to any one of the analog input channels of the DAQ device.

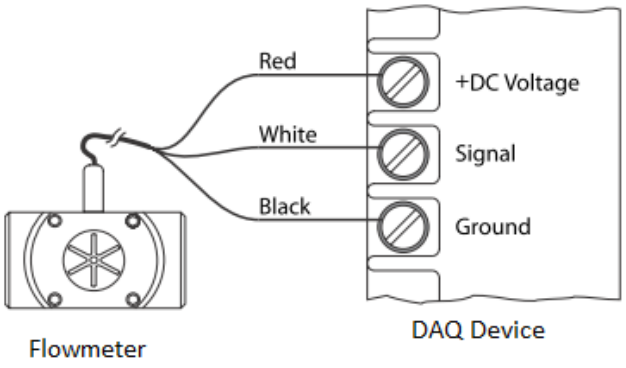

Figure 3.17: Flow meter connections [59]

The analog channel that the flow meter is connected to is then configured in Lab VIEW using the 'DAQ Assistant' function. Another important note is to configure the analog input channel in single-ended mode since the signal is measured with respect to ground. A snapshot of the pulses generated by the two flow meters is shown in Fig. 3.18.

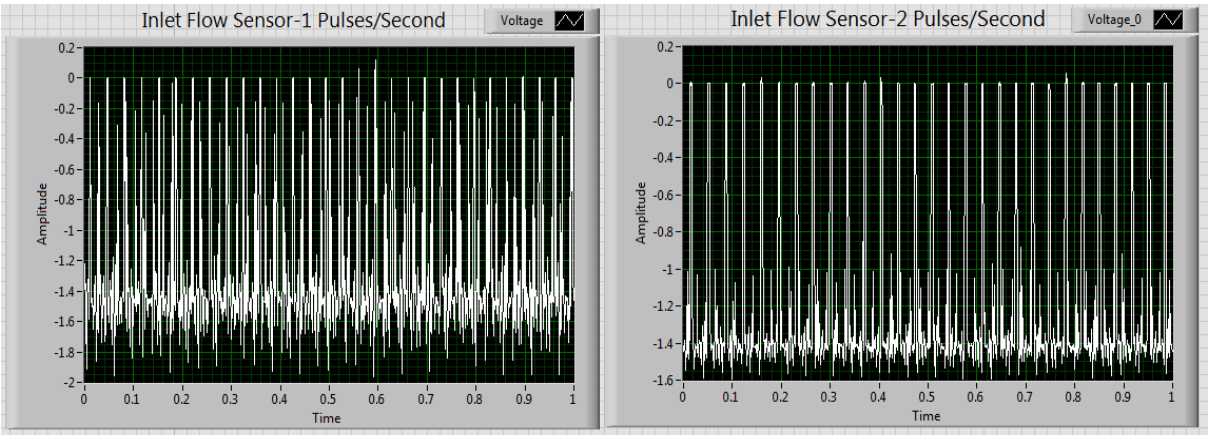

Figure 3.18: Pulses generated by the flow meters in Seconds

3.2.5.2 Turbine Flow rate Sensor

Another type of flow rate sensor called turbine flow rate sensor is used for measuring the product water flow rate. It is also manufactured by OMEGA Engineering and works on the same principle as the impeller-type explained earlier. The picture and the wiring diagram of this flow sensor is shown in Fig. 3.19.The connections are same as impeller flow meter except that an external resistor is connected to ensure open collector current sink is less than 50mA.

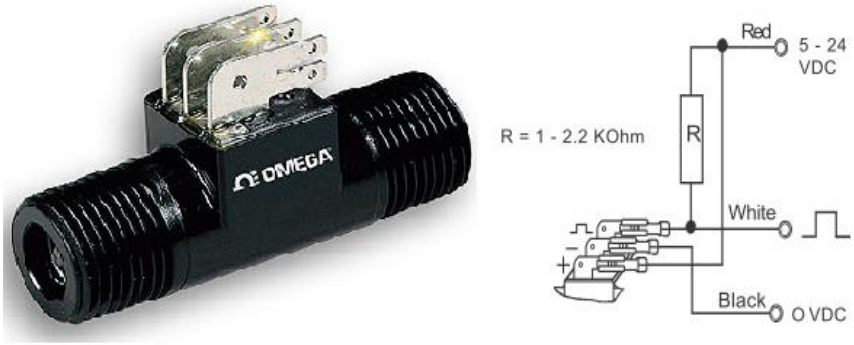

Figure 3.19: Turbine flow rate sensor and its wiring diagram [60]

The analog channel that the flow rate sensor is connected to is configured in the same 'DAQ Assistant' function box as the impeller type flow meters. The pulses generated by the product flow sensor are shown in Fig. 3.20.

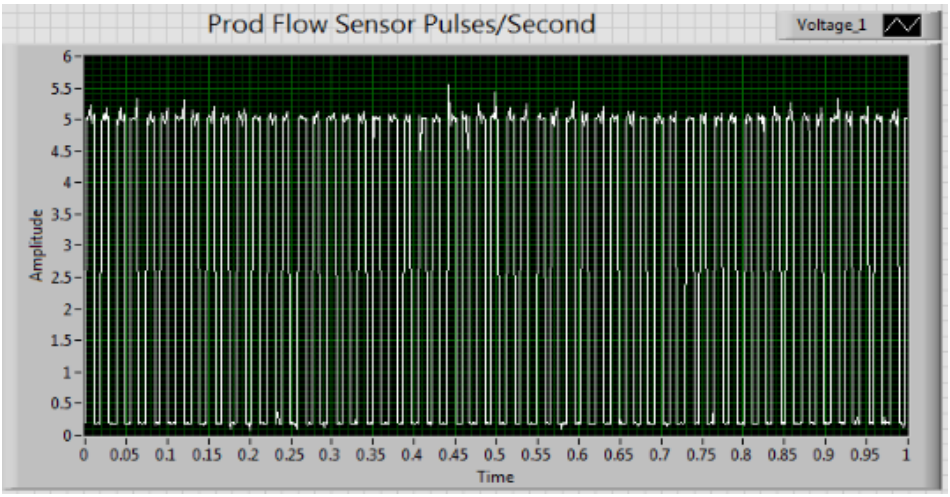

Figure 3.20: Turbine flow rate sensor pulses

3.2.5.3 Flow rate calculation

To measure the actual flow-rate on the basis of number of electrical pulses that are being produced by the flow meters, a code was developed in Lab VIEW, wherein we calculate the number of pulses generated by the flow meters in a second and divide it by the industry-calibrated k-factor of the respective flow meters, which is a numerical value and indicates pulses per gallon.

For the flow meters used in this project, the k-factors are 1385 and 1409 Pulses per Gallon respectively for the two inlet flow sensors (impeller-type). These values are modified to get k-factor in terms of Pulses per liter. For the product flow rate sensor (turbine-type), the k-factor is 3300 Pulses per liter. These k-factors are used in the Lab VIEW code and together with a count of number of pulses generated per second we get an account of the flow rates of the inlet and the product water in liter/second. A snapshot of the code developed to calculate the flow rate based on pulses generated by the flow meters is shown in Fig. 3.21.

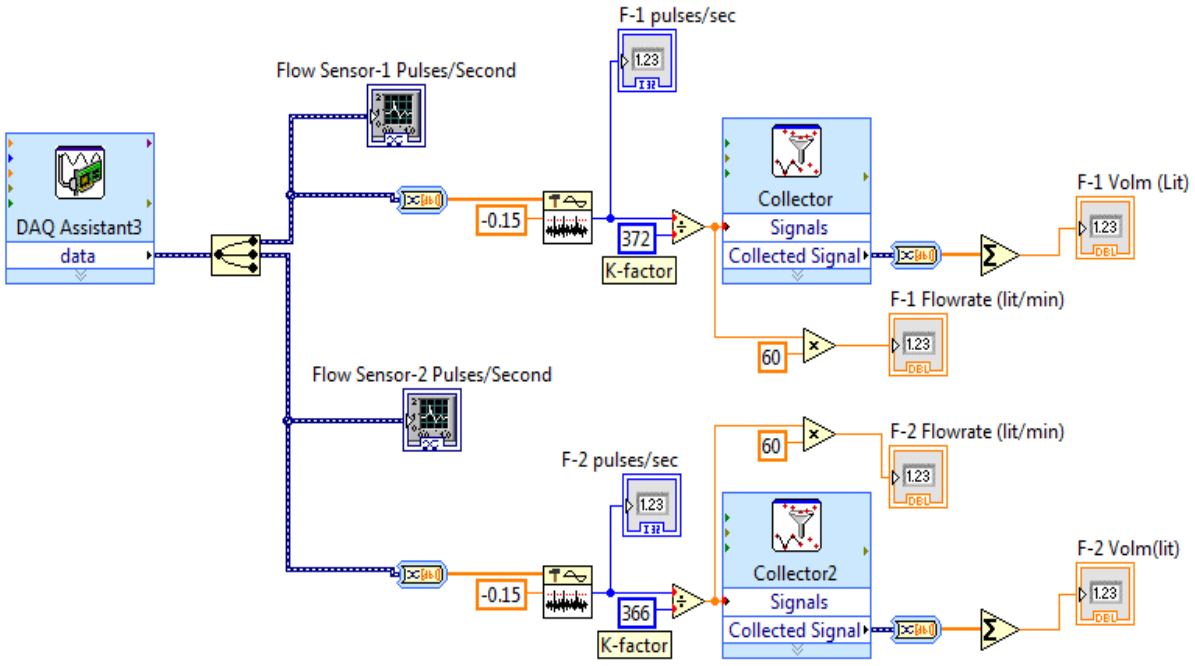

Figure 3.21: Block diagram for flow rate calculation

The DAQ Assistant block is to configure analog input channels the flow meters are connected to. This is connected to a dedicated Lab VIEW in-built function called Threshold Detector (shown in Fig. 3.21) which analyzes the pulse sequence generated by the flow meters, compares it to a threshold value given by the user and keeps a count of peaks that exceed the threshold value. The sampling time is set to one second, therefore, the number of peaks or pulses generated by the flow meter are calculated every second. This is also indicated in Fig. 3.21. This count of pulses per second is divided by the K-factor given in pulses/liter, indicated on the flow meter.This gives the flow rate in liters per second. The value obtained can be modified to get the flow rate in liters per minute, as shown in Fig. 3.21.

Another useful function in Lab VIEW is the Collector Signal, which collects all the pulses generated every second, and gives the volumetric flow passing through the flow meter in Liters

which gives us an indication of the amount of water that has passed through the flow meter. This is also shown in Fig. 3.21.

3.2.6 Pressure Measurement

The pressure sensor used for pressure measurement is MSP 300 Pressure Transducer manufactured by Microfused^{TM} is highly popular device because its cost is on the lower side, and is an ideal choice for processes involving polluted water such as reverse osmosis process. The main advantage of this type of pressure transducer is that there is no welding involved and hence is considered to be highly durable. The pressure transducer is shown in Fig. 3.22.

Figure 3.22: MSP 300- Pressure Transducer [61]

Some of the main features of MSP 300 Pressure transducer are listed in Table3-4.

Table 3-4: Specifications of FPR-301 Flow meter [59]

Features of MSP 300 Pressure Transducer	
1) Construction	Solid and Rugged Stainless Steel
2) Pressure Range	Up to 10000 psi or 700 bars
3) Accuracy	Excellent
4) Output	mV or Amplified Output

Apart from its top-notch accuracy and wide pressure ranges, it has also got a wide range of operating temperatures, no leakages, no O-Rings involved and no silicon oil involved too. The dimension diagram of the pressure transducer used in this project is shown in Fig. 3.23.

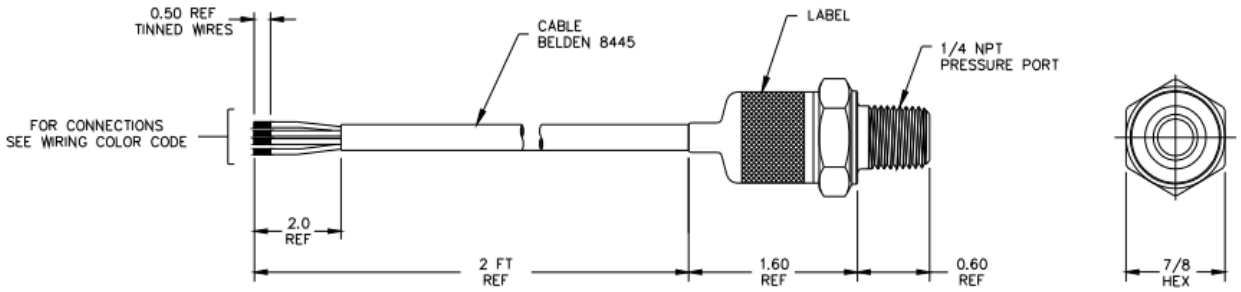

Figure 3.23: Pressure Transducer Dimensions [61]

These pressure transducers have got different output ranges based on different codes. Also the wiring connections vary according to these codes. Hence the output ranges and the wiring connections for these codes are listed in Table 3-5.

In our case, the pressure transducer used is of code 3.

Table 3-5: MSP-300 - Output range & wiring connections [61]

Output Options				
Code	**Output**	**Supply (Min)**	**Supply (Typ)**	**Supply (Max)**
2	0 – 100mV	2.5	5	12
3	0.5 – 4.5V	4.75	5	5.25
4	1 – 5V	8		30
5	4 – 20 mA	9		30
Wiring Color Code				
Code	**+Supply**	**-Supply**	**+Output**	**-Output**
2	Red	Black	Green	White
3	Red	Black	White	N/A
4	Red	Black	White	N/A
5	Red	Black	N/A	N/A

3.2.7 Temperature Measurement

The temperature measurement is done with the help of surface-mount thermistor sensor manufactured by OMEGA Engineering. The surface mount or stick-on thermistor sensor used in this project for the measurement of water temperature is shown in Fig. 3.24.

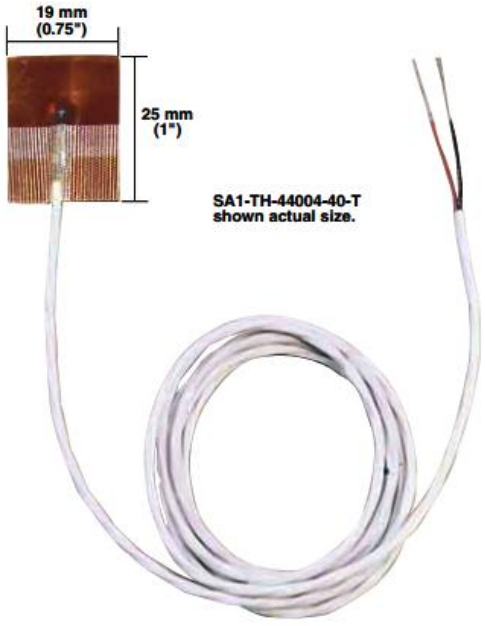

Figure 3.24: Thermistor Sensor [62]

As seen in Fig. 3.24, the sensor has an adhesive material on the bottom of its surface. For the temperature measurement, the peel strip should be removed and the sensor should be pasted to any surface for measurement purpose.

These sensors are very easy-to-use, simple in design and easy to install. Hence they are the best choice for temporary measurements. Because of its small-size, it has an advantage of measuring temperature at points which are out of reach of other conventional temperature measuring devices. The features of this type of temperature sensor are listed in Table 3-6.

Table 3-6: Features of surface-mount temperature sensor [62]

Features of Surface-Mount Temperature Sensor
1) Available in five different designs each with a different resistor value.
2) Can easily be applied to surfaces that are flat or curved.
3) Operating temperature range of -80 to 120^{o}C
4) 1 meter of 26 AWG Standard insulated and jacketed cable with stripped leads
5) Phone plug connector – Optional

The various models of this thermistor sensor based on resistance values, maximum working temperatures and the preferred storage temperatures are shown in Table 3-7.

Table 3-7: Temperature Sensor - Various models [62]

Model Number	Resistance (at 25^{o}C)	Maximum Working Temperature	Interchangeability @ 0 to 70^{o}C	Storage and Working Temperature
SA1-TH-44004-40-T	2252 Ω	150^{o}C	+/- 0.2^{o}C	-80 to 120^{o}C
SA1-TH-44005-40-T	3000 Ω	150^{o}C	+/- 0.2^{o}C	-80 to 120^{o}C
SA1-TH-44007-40-T	5000 Ω	150^{o}C	+/- 0.2^{o}C	-80 to 120^{o}C
SA1-TH-44006-40-T	10000 Ω	150^{o}C	+/- 0.2^{o}C	-80 to 120^{o}C
SA1-TH-44008-40-T	30000 Ω	150^{o}C	+/- 0.2^{o}C	-80 to 120^{o}C

The third and fourth model (resistance 5000 Ω and 10000 Ω) are the most popular. Another point to be noted is that since the thermistor gives the output in terms of voltages, it should later be converted to the corresponding temperature value based on specifications in the data sheet.

3.2.8 Conductivity Measurement

Conductivity is defined as the ability of a solution to conduct current. The amount of conductivity of a solution is proportional to the amount of dissolved salts in water. In other words, higher the amount of dissolved salts, higher would be the conductivity of water. Hence, the amount of dissolved salts would give us an idea about conductivity. Based on this theory, one can say that clean water is not a good conductor of electricity.

The amount of salts dissolved in water is known as Total Dissolved Solids (TDS) and is usually measured in terms of parts per million (ppm) which gives an indication of the mount of impurities that are present in one million unit of water.

In this project, the TDS in water is measured with the help of a digital handheld TDS meter from Spectra shown in Fig. 3.25. The meter comes with a separate carrying case shown in Fig. 3.25 and also a belt clip making it extremely useful to carry in pockets at all times and for checking the salinity of water on the spot. The TDS meter is considered to be the ideal choice for a process like reverse osmosis and other consumer or commercial applications and hence was selected for this project too for monitoring the salinities of feed water and the product water.

Figure 3.25: TDS Meter [63]

The main features of this hand-held TDS Meter are [63]:

1) Considered to be highly-efficient and accurate.

2) Has a built-in thermometer too for measuring the liquid temperature.

3) Large LCD Display makes it easier to read.

4) PPM Measurement range is 0 to 9990ppm. Since the digital display has three digits, 0 to 999 ppm is indicated with resolution of 1ppm and 1000 to 9990 the resolution is in steps of 10ppm.

5) Has the option of holding the measurement value even after taking the meter out of the solution,to make it easy for recording purpose.

6) The meter also has the option of auto turn off if it is kept idle for 10 minutes or more thereby preserving and increasing the life of the batteries.

7) Meter is factory calibrated and hence can readily be used for measurements.

8) Because of all these advantages, it is highly preferred for consumer as well as commercial applications.

The specifications of the TDS Meter are listed in Table 3-8.

Table 3-8: TDS Meter Specifications [63]

Specifications of hand-held TDS Meter	
TDS Range	0 to 9990 ppm
TDS Resolution	1ppm (0 to 999), 10ppm (1000 to 9990)
Temperature Range	0 to 80^{o}C
Temperature Resolution	0.1^{o}C
Power	Button cell batteries (2 x 1.5V)
Battery life	1000 hours
Accuracy	+/-2%
Dimensions	15.5 x 3.1 x 2.3 cm
Weight	76.5gms (with case), 56.7gms(without)

However, when the measurements are made, the meter would show different readings for the same water. This is attributed to various reasons such as:

1) The TDS meter would measure the ions that conduct electricity. However these ions are constantly on the move. Due to this reason, there would always be variations in the reading.

2) Even a slightest change in water temperature would bring in changes in the conductivity.

3) The air bubbles that have held on to the meter sensor can also vary the TDS reading.

4) The material holding the water can also vary the conductivity. For example, a plastic cup can hold the electric charges even after removal of water. Hence, if the sensor touches the walls of the plastic cup, it would pick these electric charges bringing about a change in conductivity.

5) Same water with different quantities will have different conductivity readings. Water that is displaced or moved will also alter the reading.

Following are the steps one needs to follow to get perfect measurements:

1) Before measuring the TDS of a new sample, it is good to remove the excess water that has stayed on the meter probe.

2) The air bubbles can vary the reading too as explained above, hence it is better to stir the TDS meter in the sample gently and tap it on the containers' walls to make sure there are no bubbles on the sensor.

3) It is advisable to keep the sensor immersed in the sample for a longer time as it gives us the accurate reading.

4) If one is to test the high TDS and low TDS waters one after the other, it is suggested that we wash off the sensor with pure water in between the two measurements to get the accurate readings of both the samples.

5) To get the accurate readings, the measurements should be done at room temperature or $25^{o}C$ is preferred.

3.2.9 Motor Driver

The two feed water pumps have their voltages being controlled by a single 24Volts 20Amps H-bridge Motor Driver manufactured by Devantech. The motor driver and its corresponding connection diagram are shown in Fig. 3.26.

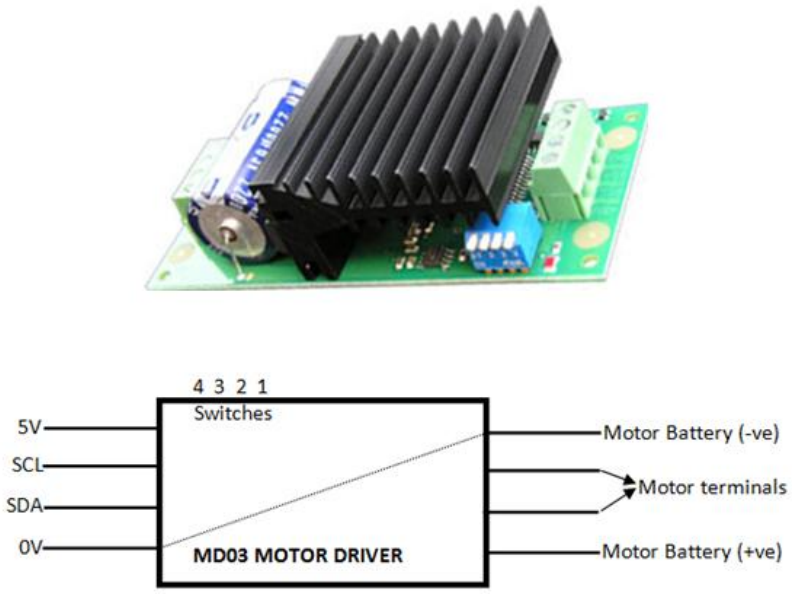

Figure 3.26: MD03 Motor Driver and Connection Diagram [64]

The motor driver has four mode switches (ON/OFF) installed on the board which enables the motor driver to operate in different modes. Since we are using the motor driver for 0 – 5V analog supply mode, the four switches have the following configuration: Switches 1&4 are OFF and Switches 2&3 are ON. For other modes available and their corresponding switch positions, the motor driver datasheet can be referred.

For the analog supply mode, the motor connected to motor terminals is controlled by 0 to 5V supply, with zero corresponding to motor being OFF and 5V corresponds to motor running at full speed. Pin SDA (data line) is connected to the analog output channel of DAQ USB-6009. We configure this analog output channel in Lab VIEW, to control the motor voltages from 0 to 5V.

Pin SCL (dock line) represents the motor direction. Since our motors run in forward direction, it is connected to +5V supply on the motor driver itself. The 0V Logic ground and ground of motor battery are internally connected as indicated by the dotted lines in Fig. 3.26.

3.3 Measurements, Results & Discussion

The circuit diagram implemented for the calculation of current and voltage measurements for the reverse osmosis desalination system is shown in Fig. 3.27.

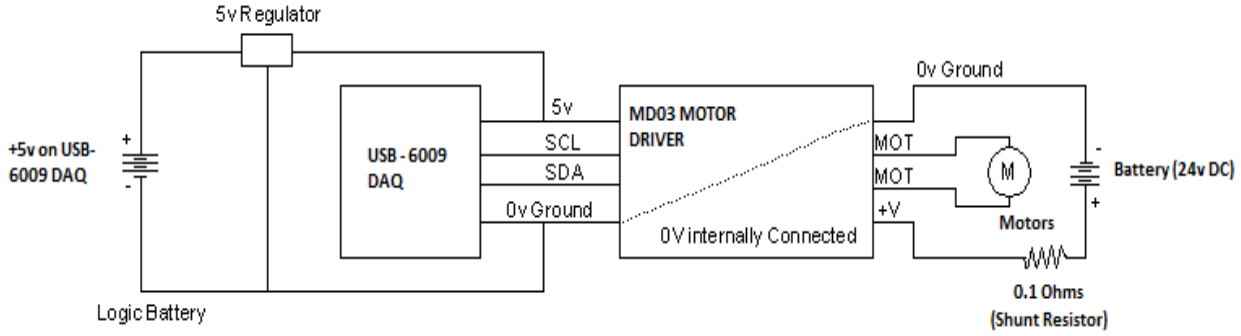

Figure 3.27: Current and Voltage Measurements Circuitry

The two pumps, namely the primary feed pump and secondary feed pump are connected together across the terminals marked "MOT" on the motor driver. The power supply for the motors i.e. the 24Vdc battery is connected across the terminals marked +V and 0V on the motor driver. A standard 5V supply, required for the control logic, is provided by USB-6009 which has separate terminals that provide +5V supply. SDA is the I2C bus data line and is connected to the Analog Output port of the USB-6009. SCL is the I2C bus dock line and decides the running direction of the motor. Since in this case, the motors are operated in forward direction, they are connected to logic 1 (+5V).

The USB-6009 DAQ Device measures the differential voltage across the shunt resistor of value 0.1Ohms, which enables us to measure the current taken by the setup. Similarly the voltage

across the motor terminals of the motor driver is also measured using a voltage divider circuit because the USB-6009 cannot measure voltages in excess of 20V. Hence 1.2kOhm and 3.6KOhm resistors form the voltage divider circuit and voltage across 1.2kOhm resistor is used for measuring the motor voltage. Using the current and voltage measurements, the Specific Energy Consumption is calculated in kWh/m3.

A snapshot of the Front panel of the LabVIEW file for the reverse osmosis desalination system, is shown in Fig. 3.28. Motor Voltage control on the extreme left of the front panel enables us to vary the pump motor voltages. The flow sensors are not designed to directly measure flow rate and it only gives output in the form of pulses. The numbers of pulses generated are calculated every second and using the flow sensors' K-factor given in datasheet, the flow-rate is calculated and simultaneously the total volumetric flow through each flow sensor. Hence for each flow sensor, three details are indicated namely, the flow rate in liters/min, the volumetric flow through the flow sensor, increasing with each passing second and the pulses generated by the flow sensor every second. The operating temperature and pressure are also indicated. The total inlet flow, the total outlet flow and the brine flow is also indicated numerically on the front panel. As explained earlier, for the current measurements, the voltage across the shunt resistor is measured, based on which the current taken by the setup is calculated. Hence, both, these values are indicated as well on the front panel. For measuring the voltage across the motors, as explained earlier, we use a voltage divider circuit. Hence the voltage across the 1.2kOhm resistor of the voltage divider circuit and the motor voltage are also indicated on the front panel. The specific energy consumption, measured every second, in kWh/m3 is also indicated numerically.

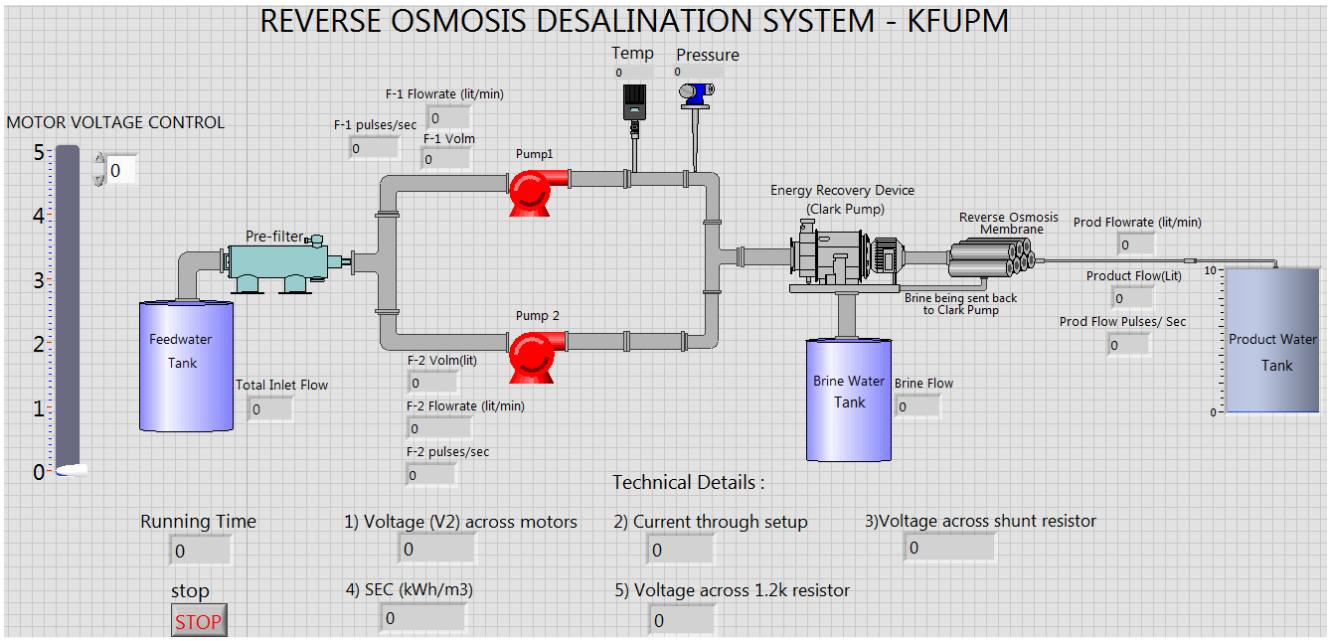

Figure 3.28: RO Process - Front panel in LabVIEW

With the feed water salinity at 2130 ppm and the feed water temperature at 28.6degC, the setup is run at maximum motor control voltage of 5V and the corresponding values of current through the setup, the voltage across the motor, the product water flow rate and the specific energy consumption are monitored and recorded every second from the Lab View's front panel. Also monitored, is the product water salinity using a TDS meter.

The variation of all the recorded parameters is shown in Fig. 3.29 through 3.33. As seen from the graphs, a lot of noise was encountered in the voltage across the motors, the current and the product flow rate due to the inherent characteristics of the system. Hence for this reason, data smoothing was done using a 5-point moving average filter. Hence, we see both the raw data and their filtered versions in the graphs.

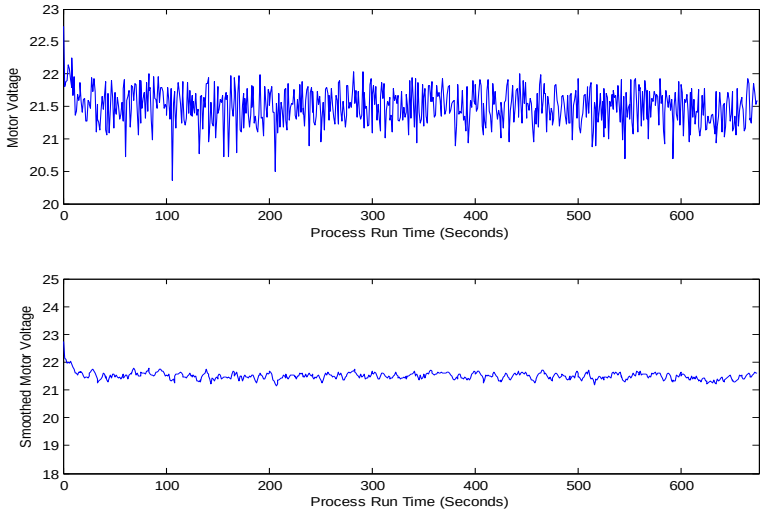

Figure 3.29: Voltage and its smoothed version

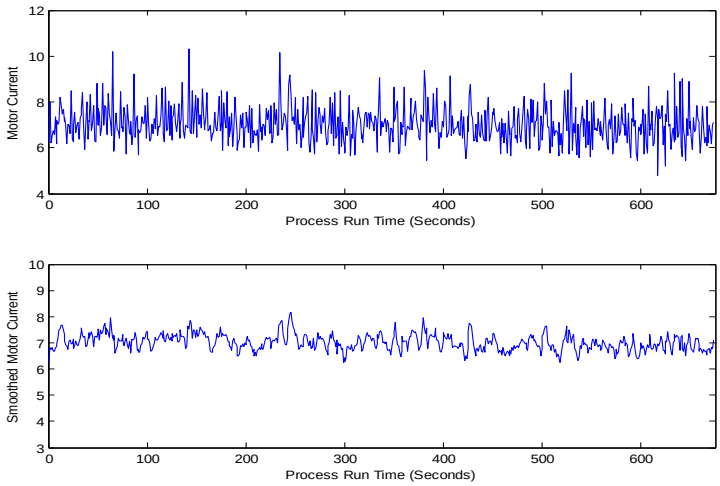

Figure 3.30: Current and its smoothed version

However at the sampling time of one second, the exact current pattern is not observed. Hence, upon changing the sampling time to 1milli second, and collecting the data for duration of 32 seconds we obtain a definite and clear pattern of the current taken by the setup. As seen in Fig. 3.31, the current taken by the setup follows a definite pattern which can be explained by understanding the working principle of Clark pump explained in detail in Section 2.9.7.1. In

short, the Clark pump has two reciprocating cylinders which switch between driving and pressurizing as shown in Fig. 2.24. The switching occurs with the help of a reversing valve. The peaks obtained in the current amplitude graph indicate the activation of reversing valve in the Clark pump to allow the cylinders to switch roles.

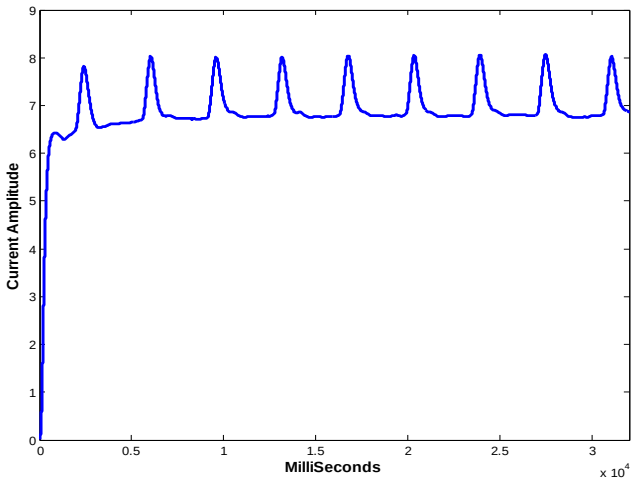

Figure 3.31: Current Amplitude at millisecond sampling

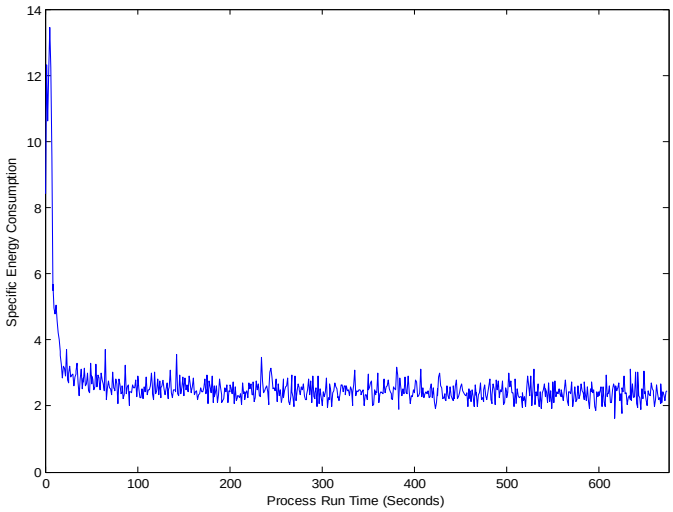

Figure 3.32: Specific Energy Consumption (kWh/m3)

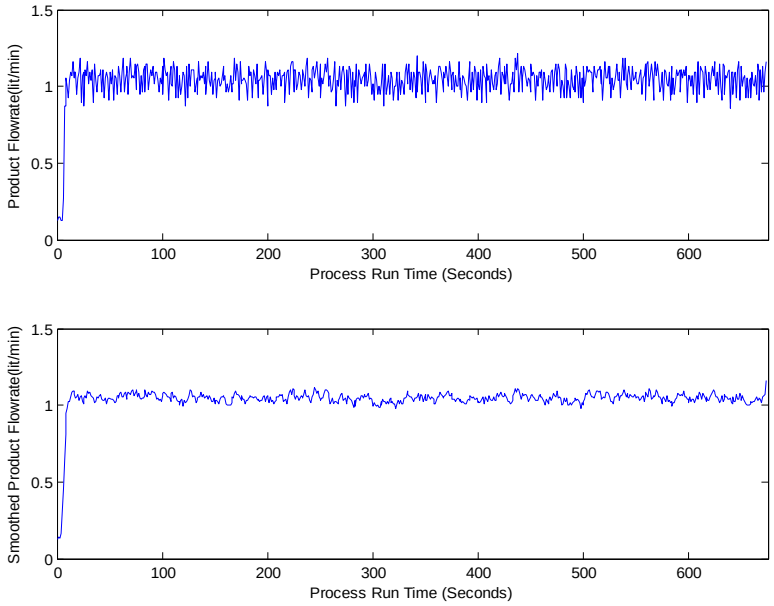

Figure 3.33: Product Flow rate (lit/min)

Observing the graphs, it can be concluded that the average current taken by the setup was found to be 7.022Amps, the average voltage across the motors was 21.481V, the average Specific Energy Consumption was 2.585kWh/m^3, and the average product flow rate was 1.03lit/min. The product water salinity was 106 ppm, 30seconds after the start of the experiment and later settled at 25 ppm till the end of the experimental run.

The salt rejection is calculated using the product water salinity and the feed water salinity as:

$$Salt\ Rejection = 100\% \left(1 - \frac{Product\ \ Salinity}{Feedwater\ \ Salinity}\right) = 100\% \left(1 - \frac{25}{2130}\right) = \ 98.8\% \qquad (6)$$

Similarly, using the feed water flow rate, obtained by adding the flow rates at the primary and the secondary feed pumps respectively and the product water flow rate, one can calculate the Recovery or Conversion ratio of feed water to product water, as

$$Recovery\ Ratio = 100\% \left(\frac{Product\ \ flowr\ ate}{Feedwater\ \ flowrate}\right) = \ 100\% \left(\frac{1.03}{4.84+4.92}\right) = 10.55\% \qquad (7)$$

For the performance evaluation done by Qiblawey et al., [38], the recovery ratio is 9% for salt rejection rate of 98%. The results obtained for our system is better because the recovery ratio is 10.55% for salt rejection rate of 98.8%. Also the specific energy consumption for the desalination system given in [38] was 45kWh/m3 for recovery ratio of 14% and would be even higher if recovery ratio of 10% were to be considered. For the system presented in this work, the specific energy consumption is only 2.585kWh/m3 for recovery ratio of 10.55%. The reason for the specific energy consumption being so low for our system is because of the energy recovery device called Clark pump which makes use of the high-pressure brine in improving the overall efficiency of the system by decreasing the specific energy consumption. Hence the Clark pump is considered to be the main feature of the desalination system considered in this work. Also, the specific energy consumption of 2.585 kWh/m3 hold good in accordance with the desalination system given in [45] where the specific energy consumption with Clark pump was found to be between 2.5 and 4 kWh/m3.

Advantage of Clark pump (Energy recovery device)

Let power supplied by the two feed pumps is given by P_f*Q_f where P_f is the feed pressure and Q_f is the feed flow rate. Let P_m be the membrane pressure (pressure across the membrane). Let power lost in brine flow be denoted by E_b and given as P_b*Q_b where P_b is the brine pressure and Q_b is the brine flow rate.

When Clark pump is used, it utilizes the high energy of the brine by pumping it back into the system to boost the feed pressure across the membrane. In other words, the brine water pressure adds to the feed pressure provided by the two pumps thereby increasing the pressure of feed water across the membrane.

$$\text{Power lost in brine } (E_b) = P_b*Q_b = (P_m - P_f)*Q_f \quad \text{(a)}$$

Since the recovery ratio was found to be 10.5%, the brine flow rate will be 89.5% of feed flow rate i.e. $Q_b = 0.895 * Q_f$. Substituting the value of Q_b in above equation we get,

$$(P_m - P_f)*Q_f = P_b*0.895Q_f \quad \text{(b)}$$

$$P_m = P_f + 0.895*P_b \quad \text{(c)}$$

In ideal case scenario, the membrane pressure P_m is roughly equal to the brine pressure P_b.

It follows that,

$P_m (1 – 0.895) = P_f$

Membrane pressure (P_m) = 9.52 * P_f (Feed pressure) (d)

Equation. (d) shows that the membrane pressure increases by 9.52 times the feed pressure provided by the pumps, with the help of the high energy of brine using the Clark pump.

During the steady-state run of the experimental setup, the feed water pressure provided by the two inlet pumps, indicated on the remote monitoring panel shown in Fig. 3.3 was 5 bar. With the help of Clark pump, we reuse the high energy of brine in increasing the feed water pressure to approximately 48bar using Eqn. (d). Because majority of the feed water pressure is provided by brine, the specific energy consumption of the desalination system is significantly less as compared to the case where the energy recovery device such as Clark pump is not used.

Suppose E_m is the power required to produce certain quantity of water say 'W' m^3, with Clark pump. Let E_b be the power going to the brine water which is reused in the system because of Clark pump. If there is no Clark pump, then the power going to the brine (E_b) is lost. Therefore to produce the same quantity of water i.e. W m^3, without the Clark pump, the total power required would be $E_m + E_b$.

Therefore the Specific Energy Consumption (SEC) (Without Clark pump) = $(E_m + E_b) / W$. (e)

And the Specific Energy Consumption (SEC) (With Clark pump) = $(E_m) / W$. (f)

Comparing Eqns (e) & (f), we see that the Energy Consumption with Clark pump is substantially less compared to the case where Clark pump is not used because the value of 'E_b' is very large.

Also, the performance evaluation results show that the system meets the design specifications in delivering the product flow rate of 1 lit/min (or 60 liters of fresh water per hour) and achieving the salt rejection close to 99% given in the technical specifications [53] which indicates that the system is working fine and the data collected from the system can be used for further analysis. In this case, the data collected from the system is used for system identification and control.

Chapter 4

SYSTEM IDENTIFICATION AND CONTROL

4.1 Introduction to System Identification

The System Identification basically deals with estimating a model of a system based on the system's observed input-output data. System identification provides a lot of models that can be estimated for a given system based on its experimental real-time data. But, the procedure that is followed to compute the model from observed data has three basic requisites:

• **The input-output data**: The input-output data or the experimental data are recorded during an experiment that is specially designed for collecting data for system identification, where it is the user's choice to identify which signals to measure and when to measure and may also choose the input signals. The main reason for such an experimental design is to have the data become maximally informative, subject to constraints that may be at hand. In other cases the user may not have the option of modifying the experiment for system identification, but can use the data directly from the normal operation of the system.

• **A set of candidate models**: A set of candidate models is obtained by specifying within which collection of models we are going to look for a suitable one. This is no doubt the most important and, at the same time, the most difficult choice of the system identification procedure. It is here that a priori knowledge and engineering intuition and insight have to be combined with formal properties of models. Sometimes the model set is obtained after careful modeling. In other cases standard linear models may be employed, without reference to the physical background. Such a model set, whose parameters are basically viewed as vehicles for adjusting the fit to the data and do not reflect physical considerations in the system, is called a black box. Model sets with adjustable parameters with physical interpretation may, accordingly, be called gray boxes.

• **A rule by which candidate models can be assessed using the data**: This step involves determining the "best" model in the set, guided by the data. The assessment of model quality is typically based on how the models perform when they attempt to reproduce the measured data.

4.2 Model Validation

After having settled on the preceding three choices, we have, at least implicitly, arrived at a particular model: the one in the set that best describes the data according to the chosen criterion. It then remains to test whether this model is "good enough," that is, whether it is valid for its purpose. Such tests are known as model validation. They involve various procedures to assess how the model relates to observed data, to prior knowledge, and to its intended use. Deficient model behavior in these respects makes us reject the model, while good performance will develop a certain confidence in the model. A model can never be accepted as a final and true description of the system. Rather, it can at best be regarded as a good enough description of certain aspects that are of particular interest to us.

4.3 System Identification Loop

The system identification procedure has a natural logical flow: first collect data, then choose a model set, then pick the "best" model in this set. It is quite likely, though, that the model first obtained will not pass the model validation tests. We must then go back and revise the various steps of the procedure.

The model may be deficient for a variety of reasons:

1) The numerical procedure failed to find the best model according to our criterion.

2) The criterion was not well chosen.

3) The model set was not appropriate, in that it did not contain any “good enough” description of the system.

4) The data set was not informative enough to provide guidance in selecting good models.

The major part of an identification application in fact consists of addressing these problems, in particular the third one, in an iterative manner, guided by prior information and the outcomes of previous attempts. Fig. 4.1shows the system identification loop and the basic steps involved in system identification problem. It is an iterative process which involves going back to previous steps if desired results are not obtained, as indicated by the arrows.

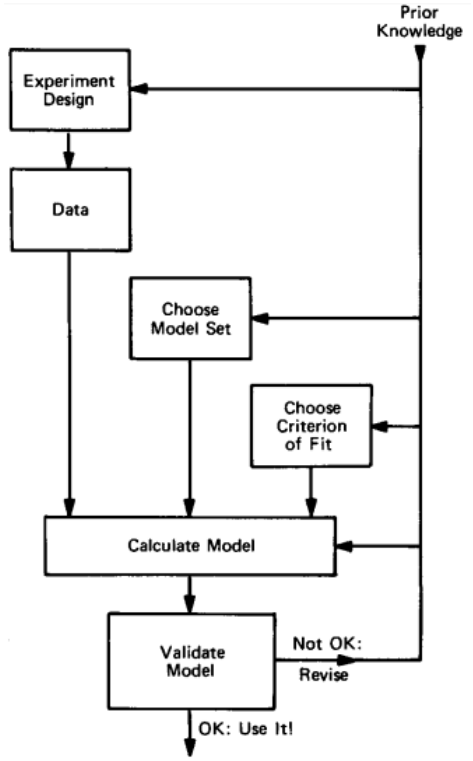

Figure 4.1: System Identification loop [65]

As seen in Fig. 4.1, the steps involved are:

1) The first step is to design an experiment and collect the input-output data [66] from the process that is to be identified. In this case, the process is reverse osmosis desalination system.

2) The next step would be to polish the data like removing trends and outliers, and select useful portions of the original data. Possibly apply filtering to eliminate the unwanted noise from the data.

3) Select and define a model structure (a set of candidate system descriptions) within which a model is to be found.

4) Compute the best model in the model structure according to the model fittings with the input-output data.

5) No model is good enough until it is validated with a separate dataset. A good model is one which gives good fit percentages with validation data.

6) If the model is good enough, then stop; otherwise go back to Step 3 to try another model.

4.4 Polynomial Models

In this research work, three polynomial models namely ARX (Auto Regressive eXogenous input), ARMAX (Auto Regressive Moving Average eXogenous input), OE (Output Error) are estimated, validated and compared against each other based on a fixed model order. All the three models are subsets of a general polynomial model which uses the transfer function notion to express the relationship between the input *(u(t))*, output *(y(t))* and the noise *(e(t))* using Equation .8:

$$A(q)y(t) = \sum_{i=1}^{nu} \frac{B_i(q)}{F_i(q)} u_i(t - nk_i) + \frac{C(q)}{D(q)} e(t) \quad (8)$$

Where A, B, C, D and F are the polynomials expressed in terms of the time shift operator q^{-1}. u_i is the i^{th} input, n_u represents the total number of inputs.

MATLAB has an in-built toolbox called System Identification Toolbox for estimating these polynomial models wherein the user specifies the model order which also corresponds to the number of coefficients for each polynomial term included in the selected model structure.

Table 4-1 illustrates the model structures for the ARX, ARMAX and OE models. An important point here is that the both the dynamic model and the noise model have common poles in A(q).

Table 4-1: System Identification Model structures

Model structure	Equation
1) ARX	$A(q)y(t) = B(q)u(t) + e(t)$
2) ARMAX	$A(q)y(t) = B(q)u(t) + C(q)e(t)$
3) OE	$y(t) = \frac{B(q)}{F(q)}u(t) + e(t)$

ARX Model is probably the most simplest of all, describe the input-output relationship as a simple linear differential equation shown in Table 4-1. It is also known as the Equation Error Model. The 'AR' refers to the autoregressive element A(q)y(t) and 'X' refers to the extra input 'B(q)u(t)'. The ARX Model is given as:

$$y(t) + a_1\, y(t-1) + \cdots + a_{n_a} y(t-n_a) = b_1 u(t-1) + \cdots + b_{n_b} u(t-n_b) + e(t) \qquad (9)$$

The ARMAX Model is similar to the ARX Model but also describes the properties of the disturbance term e(t). In other words, in ARMAX Model, we add the flexibility of including the moving average of white noise. Hence we see an additional polynomial term 'C(q)' in ARMAX Model as seen in Table 4-1. The ARMAX Model is given as:

$$y(t) + a_1\, y(t-1) + \cdots + a_{n_a} y(t-n_a) = b_1 u(t-1) + \cdots + b_{n_b} u(t-n_b) + e(t) +$$

$$c_1 e(t-1) + \cdots + c_{n_c} e(t-n_c) \quad (10)$$

Considering the ARMAX Model, if we replace the polynomial C(q) with A(q), we get the 'Output Error' Model as given in Eqn.11.

$$A(q)y(t) = B(q)u(t) + C(q)e(t)\ (The\ ARMAX\ Model)$$

$$A(q)(y(t) - e(t)) = B(q)u(t) \quad (11)$$

The difference between the output y(t) and white noise e(t) is the undisturbed output say w(t). Hence the Output Error Model gives the relationship between the undisturbed output w(t) and the input u(t).

Continuing from Eqn. 11, let $y(t) - e(t) = w(t)(Undisturbed\ Output)$. Also let F(t) represent the polynomial term for the undisturbed output w(t). Then the output-error model would look like Eqn. 12:

$$w(t) + f_1\, w(t-1) + \cdots + f_{n_f} w\left(t - n_f\right) = b_1 u(t-1) + \cdots + b_{n_b} u(t-n_b) \quad (12)$$

where $w(t) = y(t) - e(t)$ and the polynomial term $F(q) = 1 + f_1 q^{-1} + \cdots + f_{n_f} q^{-nf}$.

Finally, substituting the value of w(t) in equation (12) and re-arranging terms , we get the final equation for Output Error Model as:

$$y(t) = \frac{B(q)}{F(q)} u(t) + e(t) \quad (13)$$

First, the experimental data was collected for the product flow rate by varying the motor driver control voltage in steps and around 855 samples of data were collected. This data was detrended

to remove means, offsets from the regularly sampled data. Now the models developed based on the detrended data will describe how changes in input gives changes in output but doesn't explain the actual signal levels which is completely normal. The data was also filtered to remove the unwanted noise, to obtain a dataset which is good for system identification.

The first half of the collected data was used for developing models and the second half was used for validating the models. For comparison purpose third order polynomial models were estimated and compared against each other to find the best model amongst the model set. The system identification results and the comparison of the third order models with the actual data is shown in Fig. 4.2. No model is good enough until it is validated with a separate dataset. Hence Fig. 4.3 shows the comparison of validation data and the three model outputs. From the figures, it is clear that when third order polynomial models are estimated, all the three models are good at replicating the actual data but the Output Error Model has the highest fit percentage when compared to the data used for system identification and also the data used for validation.

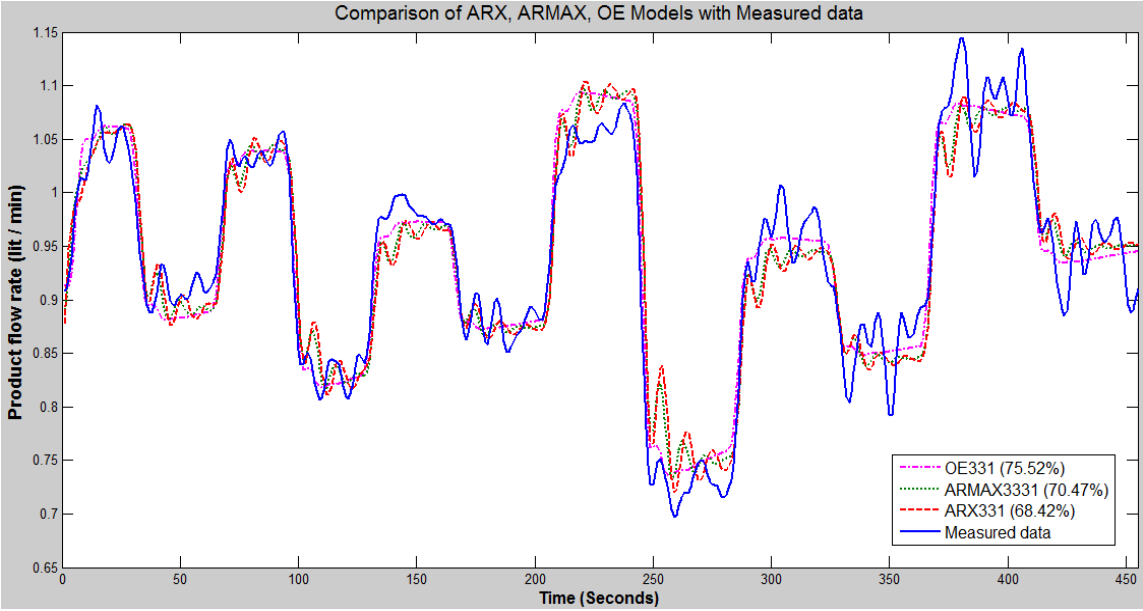

Figure 4.2: Comparison of ARX, ARMAX, OE Models with Measured data

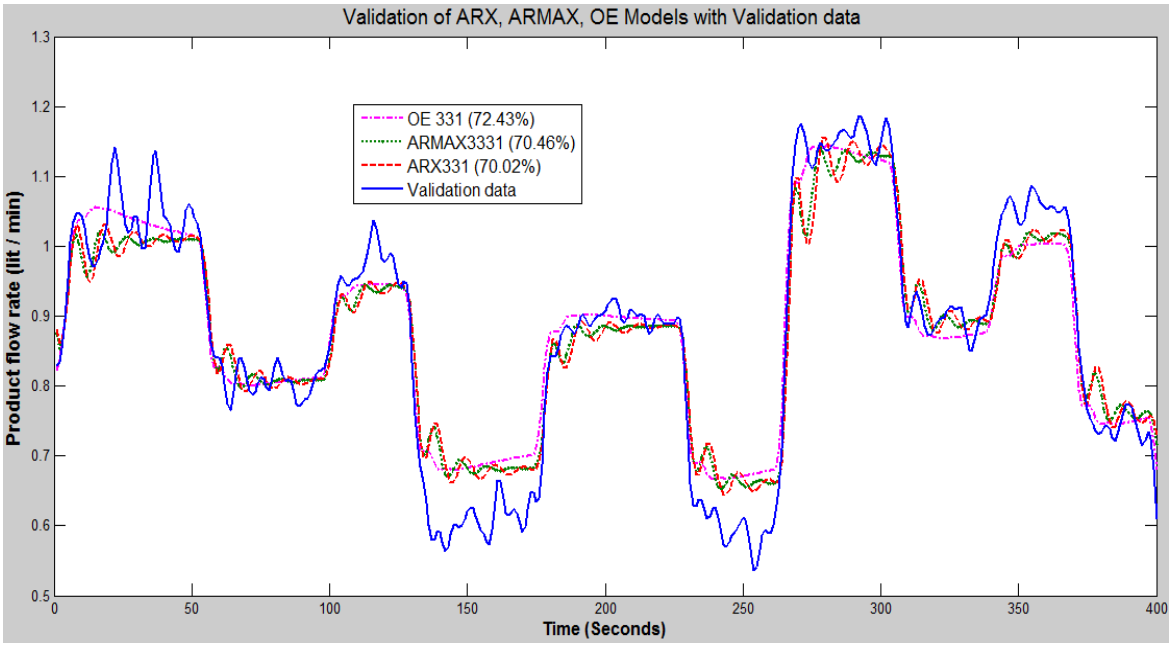

Figure 4.3: Validation of ARX, ARMAX, OE Models with Validation data

The third order polynomial equations obtained from system identification and the respective fit percentages for the three models are shown in Table 4-2.

Table 4-2: Polynomial models, their equations and fit percentages

Model structure	3rd Order Model Equations	Fit Percentages
1) ARX	$A(q)y(t) = B(q)u(t) + e(t)$ where, $A(q) = 1 - 2.369\ q^{-1} + 2.142\ q^{-2} - 0.7169\ q^{-3}$ $B(q) = 0.05271\ q^{-1} - 0.07145\ q^{-2} + 0.03055\ q^{-3}$	With Measured data: 68.42% With Validation data: 70.02%
2) ARMAX	$A(q)y(t) = B(q)u(t) + C(q)e(t)$ where, $A(q) = 1 - 2.229\ q^{-1} + 1.958\ q^{-2} - 0.6546\ q^{-3}$ $B(q) = 0.05807\ q^{-1} - 0.07422\ q^{-2} + 0.03185\ q^{-3}$ $C(q) = 1 + 2.949\ q^{-1} + 2.899\ q^{-2} + 0.9503\ q^{-3}$	With Measured data: 70.47% With Validation data: 70.46%

3) OE	$y(t) = (B(q)/F(q))\,u(t) + e(t)$ where, $B(q) = 0.1966\ q^{-1} - 0.3073\ q^{-2} + 0.1126\ q^{-3}$ $F(q) = 1 - 0.9594\ q^{-1} - 0.657\ q^{-2} + 0.6279\ q^{-3}$	With Measured data: 75.52% With Validation data: 72.43%

The chart depicting the fitness percentage levels for the three polynomial models, with the data used for modeling and the validation data is shown in Table 4-3.

Table 4-3: Fit percentages of ARX, ARMAX, OE models with experimental data

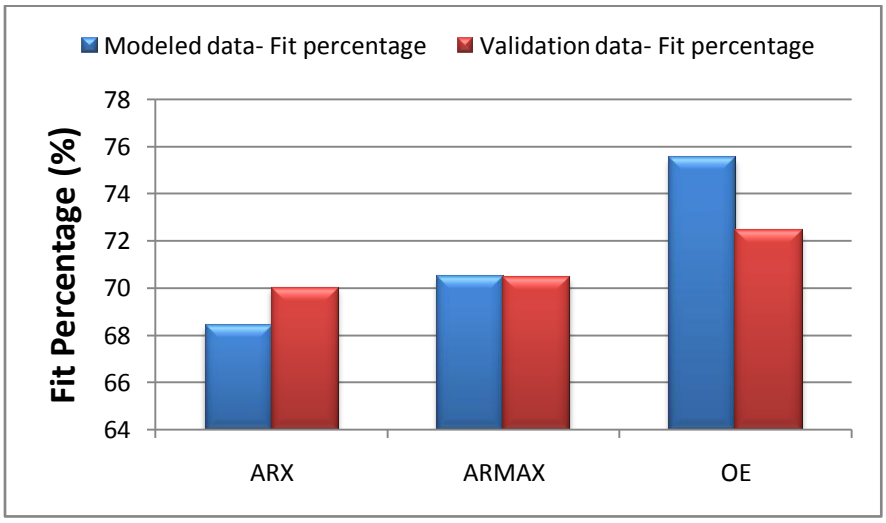

4.5 State-space System Identification

Another type of system identification is to estimate the state-space models from the experimental data. There are two methods of system identification by which state-space models can be computed based on experimental data. They are subspace identification and prediction error method.

The subspace identification method [67] is a non-iterative method of estimating discrete time state-space models and prediction error method is an iterative estimation method that minimizes

prediction error. These models can be estimated in MATLAB environment using the commands *n4sid* and *pem*. The general format of the discrete state-space model is given in Eqn. 14 as:

$$x(t + Ts) = Ax(t) + Bu(t) + Ke(t) \quad (14)$$

$$y(t) = Cx(t) + Du(t) + e(t)$$

Where 'x' represents the state vector, 'u' represents the input vector and 'y' represents the output vector. A, B, C, D and K matrices are state-space matrices estimated by system identification. They represent the system dynamics and are known as model coefficients.

4.5.1 Subspace Identification

The subspace identification method was developed in eighties and is based on the QR factorization and the Singular Value Decomposition (SVD) [68]. Some of the key features of subspace identification are [69]:

1) It gives the minimum realization of the model in the state-space form.

2) The state-space model is estimated using the experimental data and doesn't require to construct a priori parameterization. The only detail required for subspace identification is the model order, which is determined by means of the inspection of the dominant singular values of a matrix that is calculated during the identification process.

3)Subspace Identification is a non-iterative procedure and do not require any non-linear optimization. Hence they do not pose problems related to convergence, local minima or sensitivity to the parameter values (initial values). Also they have less computation as compared to other techniques like Prediction Error Minimization (PEM) [70] method.

4) There is no criterion for the initial condition to be mentioned and can be considered as zero.

The subspace identification algorithms present the next common steps [71]:

Construct the input and output Hankel matrices, which are formed using the input and output measurements, $\{u_k\}_{k=1}^{N}$ and $\{y_k\}_{k=1}^{N}$ [69] as given by Eqn. 15.

$$U_{0|k-1} = \begin{bmatrix} u(0) & u(1) & \dots & u(N-1) \\ u(1) & u(2) & \dots & u(N) \\ \vdots & \vdots & \ddots & \vdots \\ u(k-1) & u(k) & \dots & u(N-k+2) \end{bmatrix} \tag{15}$$

The block Hankel matrix for output data ($Y_{0|k-1}$) is constructed in a similar fashion as in Eqn. 15 and QR decomposition is realized from these matrices [68]. The singular value decomposition (SVD) is performed on the low dimensional rank-deficient R-component to find the extended observability matrix.

The two state-space identification methods differ from each other in terms of how these steps are computed. After these three common steps, the procedure followed for determining the matrices A, B, C, D and K is completely different and varies according to the method used [71].

The subspace identification is based on the work done by Van Overschee and De Moor [69].

For notational convenience, let p and f denote the past and future respectively. Hence we define the past-data as $U_p := U_{0|k-1}$ and $Y_p := Y_{0|k-1}$ and future-data as $U_f := U_{k|2k-1}$ and $Y_f := Y_{k|2k-1}$. The joint past data is denoted by $W_p := \begin{bmatrix} U_p \\ Y_p \end{bmatrix}$ and the joint future data is denoted by $W_f := \begin{bmatrix} U_f \\ Y_f \end{bmatrix}$.

Let the LQ decomposition be given by

$$\begin{bmatrix} U_f \\ W_p \\ Y_f \end{bmatrix} = \begin{bmatrix} R_{11} & 0 & 0 \\ R_{12} & R_{22} & 0 \\ R_{13} & R_{23} & R_{33} \end{bmatrix} \begin{bmatrix} \bar{Q}_1^T \\ \bar{Q}_2^T \\ \bar{Q}_3^T \end{bmatrix} \tag{16}$$

where $R_{11} \in R^{km \times km}$, $R_{22} \in R^{k(m+p) \times k(m+p)}$ and $R_{33} \in R^{kp \times kp}$ are diagonal elements and Q_i (i=1, 2, 3) are orthogonal matrices.

Let the oblique projection of Y_f onto joint-past W_p along future U_f is given by,

$$\xi = \hat{E}_{||Uf}\{Y_f \,|W_p\} = R_{32}R_{22}^{+}W_p \tag{17}$$

where $(.)^{+}$ denotes the pseudo inverse. We can show that ξ can be factored as a product of extended observability matrix O_k and future state vector $X_f := [\, x(k) \;\; \ldots \; x(k+N-1)] \in R^{nxN}$. It thus follows that,

$$\xi = O_k X_f = R_{32}R_{22}^{+}W_p \tag{18}$$

Suppose the Singular-value decomposition (SVD) of ξ is given by

$$\xi = U\sum V^T \tag{19}$$

with rank($\sum$) = n. Thus we can take the extended observability matrix as

$$O_k = U\sum^{1/2} \tag{20}$$

Substituting the value of ξ and O_k from Equations .19 and .20 in Equation .18, it follows that the value of state vector X_f is obtained as

$$X_f = O_k^{+}\xi = \sum^{1/2} V^T \tag{21}$$

We define the following matrices with N-1 columns as,

$$\bar{X}_{k+1} := [x_{k+1} \quad \ldots \quad x_{k+N-1}] \tag{22}$$

$$\bar{X}_{k} := [x_{k+1} \quad \ldots \quad x_{k+N-2}] \tag{23}$$

$$\bar{U}_{k|k} := [u_k \quad \ldots \quad u_{k+N-2}] \tag{24}$$

$$\bar{Y}_{k|k} := [y_k \quad \ldots \quad y_{k+N-2}] \tag{25}$$

The matrices A, B, C and D are obtained by solving the system of linear equations given in Eqn .26 by using the least squares method.

$$\begin{bmatrix} \bar{X}_{k+1} \\ \bar{Y}_{k|k} \end{bmatrix} = \begin{bmatrix} A & B \\ C & D \end{bmatrix} \begin{bmatrix} \bar{X}_k \\ \bar{U}_{k|k} \end{bmatrix} \tag{26}$$

However, the state-space model based on subspace identification can be computed using the built-in MATLAB command called *'n4sid'*.

The results obtained from subspace identification using MATLAB command *n4sid* are:

$$\mathrm{A_n} = \begin{pmatrix} 0.87683 & 0.37628 & 0.080327 \\ -0.30702 & 0.75622 & 0.543 \\ 0.071741 & -0.42791 & 0.43535 \end{pmatrix}, \mathrm{B_n} = \begin{pmatrix} -0.12017 \\ -0.037478 \\ 0.077239 \end{pmatrix} \tag{27}$$

$$\mathrm{C_n} = (-0.55846 \quad -0.086395 \quad -0.02042), \quad \mathrm{D_n} = 0, \quad \mathrm{Kn} = \begin{pmatrix} -2.8498 \\ -6.1621 \\ -1.3933 \end{pmatrix}$$

4.5.2 Prediction Error Minimization Method

Prediction Error Methods is a broad family of parameter estimation methods that is applied to quite arbitrary model parameterizations. These methods are closely related to Maximum Likelihood method, originating from [72] and were used for the computation of dynamical models and time series by [73] and [74].

The basic idea behind the prediction error approach is very simple:

1) Describe the model as a predictor of the next output.

$$\hat{y}_m(t|t-1) = f(Z^{t-1}) \tag{28}$$

Where $\hat{y}_m(t|t-1)$ denotes the one-step ahead prediction of the next output and f is arbitrary function of the past observed data.

2) Parameterize the predictor in terms of finite dimensional parameter vector θ:

$$\hat{y}_m(t|\theta) = f(Z^{t-1}, \theta) \tag{29}$$

3) Determine an estimate of θ (denoted as $\hat{\theta}_N$) from the model parameterization and the observed dataset Z^N so that the error between y and $\hat{y}$ is minimized.

In this way, the unknown model parameters can be estimated using iterative prediction error minimization method. MATLAB has a built-in command called *'pem'* to estimate the state-space model based on prediction error minimization principle.

And the results obtained from prediction error method using MATLAB command *pem* are:

$$\mathrm{A_p} = \begin{pmatrix} 1.0875 & 0.95424 & -0.05579 \\ -0.20333 & 0.87083 & 0.65852 \\ 0.058277 & -0.45471 & 0.23723 \end{pmatrix}, \mathrm{B_p} = \begin{pmatrix} -0.052475 \\ 0.0073884 \\ -0.00025989 \end{pmatrix} \tag{30}$$

$$\mathrm{C_p} = (-1.1992 \quad -0.27203 \quad 0.0070498), \qquad \mathrm{D_p} = 0, \mathrm{Kp} = \begin{pmatrix} -2.9053 \\ -6.2221 \\ -1.4286 \end{pmatrix}$$

4.6 Comparison of State-Space Models

The performances of the two state-space models are demonstrated by applying optimal control scheme called linear quadratic regulator to both the models and comparing their control performance.

The optimal control is used to compare the performance of two state-space models developed by system identification presented in the preceding section. The performance of a control system can be quantified in many applications by a quadratic cost function. A cost function is in general, a scalar, real-valued, non-negative function of the system, or of the time histories of the state, reference output and control input, subject to a given set of initial conditions and inputs. The cost can be used to evaluate the performance of a system, where superior performance is indicated by a smaller cost [75].

The quadratic cost function is given by,

$$J = \int_0^\infty x^T(t)Q(t)x(t) + \rho\, u^T(t)R(t)u(t)dt \qquad (31)$$

The integral is from zero to infinity to ensure we have a controller that works well for all the duration of time. x is the state vector, u is the input vector, both evolving with time, Q(t) is a positive semi-definite state-weighting matrix, and R(t) is the weighting on the control, used to impose a penalty on the use of excessive amounts of control. Changing the values of Q and R matrices will change the relative weighting of one state against the other. In other words, it is the diagonal elements of the Q matrix that penalize the states i.e. the first element on the diagonal will penalize the first state and so on and the diagonal elements of R matrix penalize the control inputs. Hence proper trial and error of Q and R matrices needs to be done, to get the best control.

The feedback control law that is implemented is given by

$$u(t) = -K_{LQR} * x(t) \quad (32)$$

where the controller gain $K_{lqr} = R^{-1}B^{T}P$ where R is the weight on the control input, B is the input matrix and P is the solution to the Algebraic Ricatti Equation given by:

$$A^{T}P + PA - PBR^{-1}B^{T}P + Q = 0 \quad (33)$$

Substituting the value of feedback control law into the state space equation given in Eq .14, we get a new closed-loop system which looks like:

$$x(t + Ts) = (A - BK)x(t) + Ke(t) \quad (34)$$

the matrix (A-BK) will have stable eigen values. Hence we get a stabilizing controller that minimizes the quadratic cost function J, previously defined.

Fig. 4.4 shows the comparison of the two state-space models based on their optimal control performance in controlling the product flow rate for a set point of 1.1 lit/min.

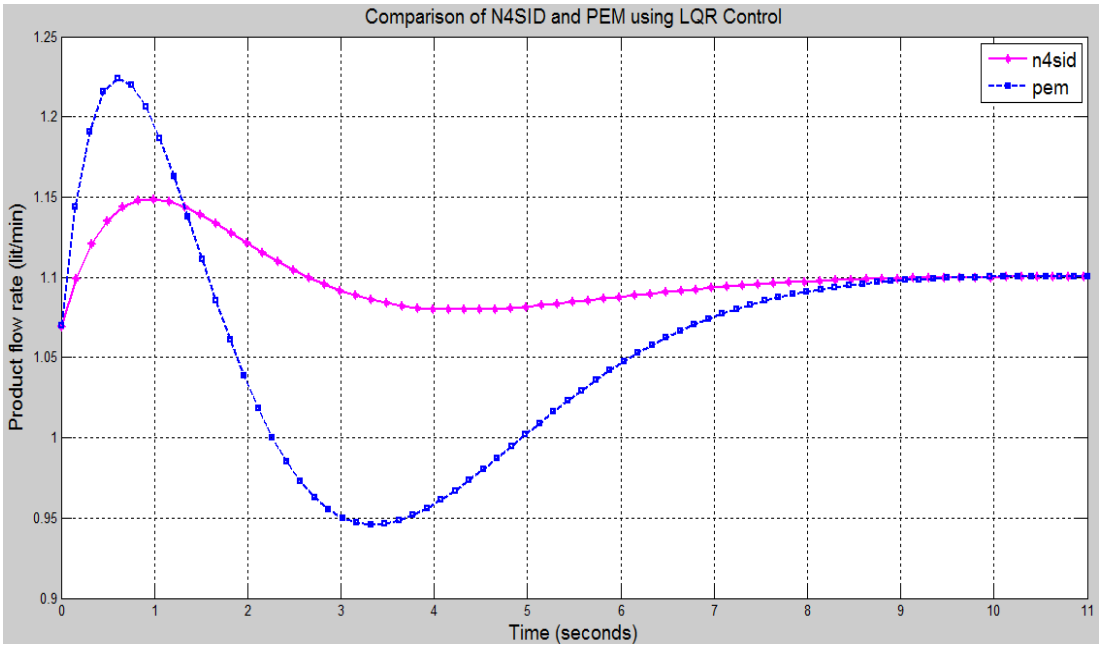

Figure 4.4: Comparison of N4SID and PEM using LQR Control

The subspace based optimal control does better performance compared to prediction error method based optimal control in terms of the rise time, settling time and the overshoot.

Hence, further investigation in terms of different control penalties on input is done for subspace identification. Eqn. 31 can be re-written as:

$$J = \int_0^\infty z^2(t) + \rho\, u^2(t)dt \qquad (35)$$

where 'ρ' is the penalty on the control input.

Choosing different values of this penalty can provide us with pole locations that achieve a balance between FAST RESPONSE and LOW CONTROL EFFORT. In other words, smaller value of ρ implies low penalty on control, smaller value of $\int_0^\infty z^2(t)dt$ but gives faster response. And higher value of ρ implies high penalty on control input, smaller value of $\int_0^\infty u^2(t)dt$, low

control effort and slower response. Hence we see in Fig. 4.5 that as the penalty on control input is decreased, the response keeps getting better and faster.

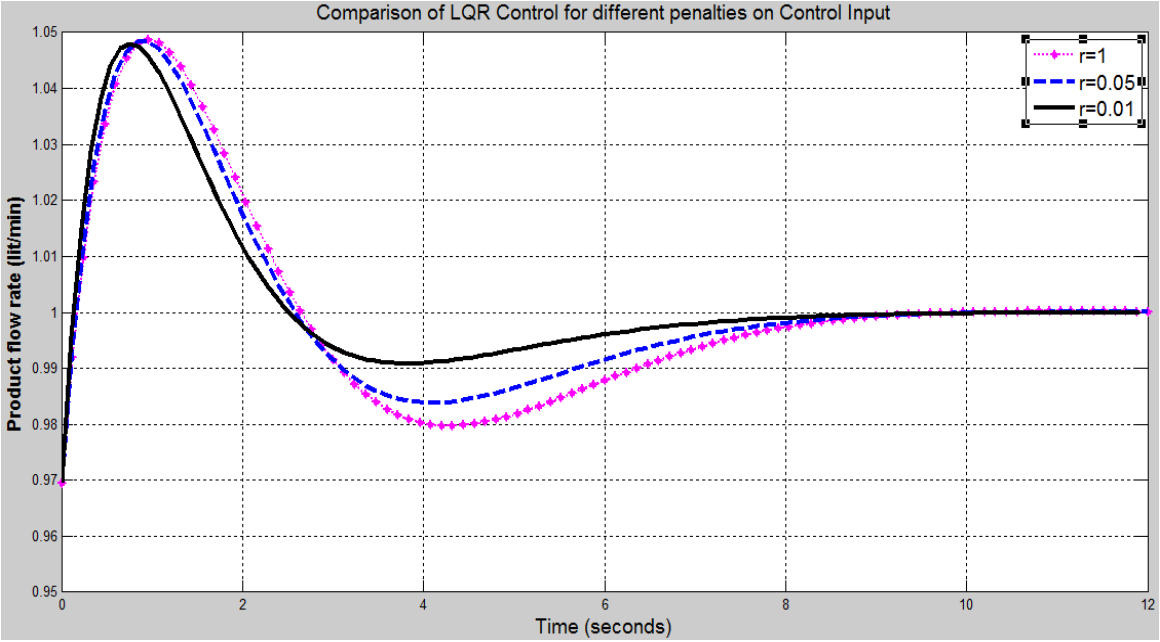

Figure 4.5: Comparison of LQR for different control penalties for Subspace based state-space model

Hence, optimal control scheme called linear quadratic regulator indicates that the performance of subspace identification is better compared to prediction error method.

Further investigation in terms of model predictive control, presented in the next sub section, is done for state-space model obtained from subs-space identification.

4.7 State-space Model Predictive Control

Another important type of controller presented is the model predictive controller (MPC). It is a relatively recent type of controller design technique that makes explicit use of a model to obtain a control signal. In other words, the objective of model predictive control is to compute the future values of the manipulated variable or the control signal in order to optimize the future

behavior of the output variable of the plant and minimize the objective function [76] shown in Eqn. 36, subject to constraints on input and output variables.

$$\min\left\{\sum_{k=0}^{N-1}\|y(t+k)-r(t)^2\|+\rho\|u(t+k)-u(t)\|^2\right\} \quad (36)$$

This optimization is performed within a limited time window by giving the plant information or the plant model at the start of the window. This methodology of obtaining the control signal is known as Receding Horizon Principle. The performance of the controller depends on how well the dynamics of the system are captured by the plant model to be used in the design of controller. The main reason for the popularity of MPC is its ability to handle constraints on both input and output variables and the ease with which it provides the optimization.

The strategy called 'Receding Horizon' wherein the horizon is moved one step towards the future but involves the application of only the first control signal from the computed control sequence is shown in Fig. 4.6 [77].

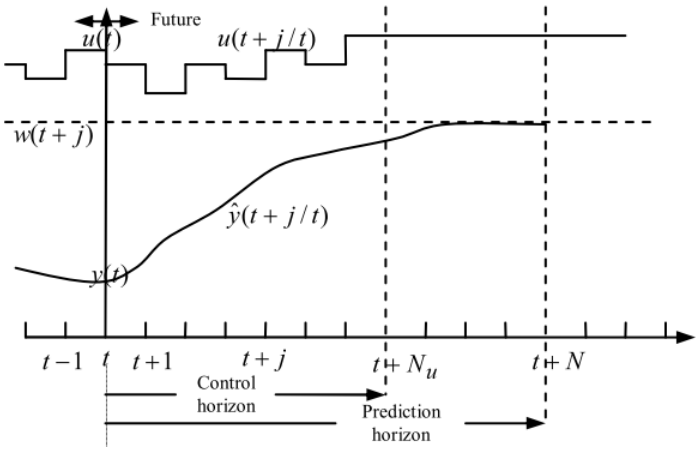

Figure 4.6: Receding Horizon Philosophy [77]

The process model calculates the predicted future outputs $\hat{y}(t+j)$ for the prediction horizon 'N' at each time instant. The calculation of the future control signals for the control horizon 'N_u' is

computed to minimize the objective function. However the current signal u(t) is sent to the process. At the next sampling instant y(t+1) is measured and the same process is repeated wherein now the control signal u(t+1) is calculated using receding horizon concept and sent to the process.

4.7.1 Models used in MPC Design

MPC Control is done in a variety of ways which differ on the basis of the model that is used in the control design. During the initial times when MPC was developed, FIR models and step response models were used. The usage of these models for MPC design is referred to as Dynamic Matrix Control. The choice of selection of one of these two models is based on the application they are used for. FIR models are used for plants which are stable and those which require the models to be of large order whereas step response models can be used for both unstable as well as stable plants. However in recent times, it is the used of state-space models for MPC formulation that has become very popular. In this work also, the state-space models in discrete time are used for MPC Control and the principle it is based on is known as the Receding Horizon Control.

4.7.2 Optimization

For optimization, we need a condition to decide on how to achieve the control objective using MPC control. One basic rule is to measure the difference between the target value and the actual process value in terms of an objective function and then finding ways and means to optimize the control action in reducing the cost function to as minimum value as possible. However, all this is to be done inside the prediction horizon.

Let us assume that $r(k_i)$ is the desired value of the output variable at sample time k_i (discrete case). The goal would now be to find best control action in terms of ΔU which minimizes the gap

between desired value and actual value of the process variable being controlled. Consider the data vector containing the desired value, is given by Eqn. 37.

$$R_s^T = \overbrace{[1\ 1\ \ldots 1]}^{N_p} r(k_i) \tag{37}$$

We define the cost function J that reflects the control objective given in Eqn.38.

$$J = (R_s - Y)^T (R_s - Y) + \Delta U^T \bar{R} \Delta U, \tag{38}$$

The first term is linked to the objective of minimizing the errors between predicted output and set-point signal while the second term reflects the consideration given to the size of ΔU when the objective function J is made small. $\bar{R}$ is a diagonal matrix in the form that $\bar{R} = r_w I_{Nc\ x\ Nc}$($r_w \geq 0$) where r_w is used as a tuning parameter for the desired closed-loop performance.

When r_w is zero, the objective function (38) is seen as the position wherein we are not interested in what ΔU is (large or small) but our objective is to reduce the error between the desired value and the actual value given by $\left(R_s - Y\right)^T (R_s - Y)$as small as possible. When r_w is large, the function (38) is seen as the situation where we are concerned about how large or small ΔU is and at the same time we would very carefully work towards reducing the error between desired and the actual value. We have the predictor equation for output Y given by Eqn.39 as,

$$Y = Fx(k_i) + \Phi \Delta U \tag{39}$$

To find the optimal ΔU that will minimize J, by substituting (39) in (38), J is expressed as:

$$J = \left(R_S - Fx(k_i)\right)^T \left(R_S - Fx(k_i)\right) - 2\Delta U^T \Phi^T \left(R_S - Fx(k_i)\right) + \Delta U^T (\Phi^T \Phi + \bar{R}) \Delta U \tag{40}$$

From the first derivative of the cost function J given in (40), with respect to control signal ΔU:

$$\frac{\partial J}{\partial \Delta U} = -2\Phi^T\left(R_S - Fx(k_i)\right) + 2(\Phi^T\Phi + \bar{R})\Delta U, \quad (41)$$

the necessary condition of the minimum J is obtained as $\frac{\partial J}{\partial \Delta U} = 0$, from which we get the optimal solution for the control signal as,

$$\Delta U = (\Phi^T\Phi + \bar{R})^{-1}\Phi^T\left(R_S - Fx(k_i)\right) \quad (42)$$

with the assumption that $(\Phi^T\Phi + \bar{R})^{-1}$ exists. The matrix $(\Phi^T\Phi + \bar{R})^{-1}$ is called the Hessian Matrix. Note that R_s is a data vector that contains the set point information expressed as,

$$R_s^T = \overbrace{[1\ 1\ \ldots 1]^T}^{N_p} r(k_i) = \bar{R}_s r(k_i), \text{ where } \bar{R}_s = \overbrace{[1\ 1\ \ldots 1]^T}^{N_p} \quad (43)$$

The optimal solution of the control signal is linked to the set-point signal $r(k_i)$ and the state variable $x(k_i)$ via the following equation:

$$\Delta U = (\Phi^T\Phi + \bar{R})^{-1}\Phi^T\left(\bar{R}_s r(k_i) - Fx(k_i)\right) \quad (44)$$

Hence the model predictive control problem is to minimize the cost function modified as:

$$\left\{\sum_{k=0}^{N-1} \|y_{t+k} - r(t)\|^2 + \rho\|u_{t+k} - u_r(t)\|^2\right\} \quad (45)$$

subject to constraints on input and output given as: $u_{min} \leq u_{t+k} \leq u_{max}$,$y_{min} \leq y_{t+k} \leq y_{max}$.

MATLAB provides an in-built toolbox called Model Predictive Control Toolbox [78, 79] for a system whose model is given in state-space form. In this work, the controller is designed for the third order state-space model of desalination system estimated by sub-space identification. The controller is discussed for unconstrained case and the constrained case respectively.

4.7.3 MPC Control – Unconstrained Case

The variation of the output variable which is the product flow rate with the manipulated variable which is the motor control voltage for unconstrained case is shown in Fig. 4.7 and 4.8.

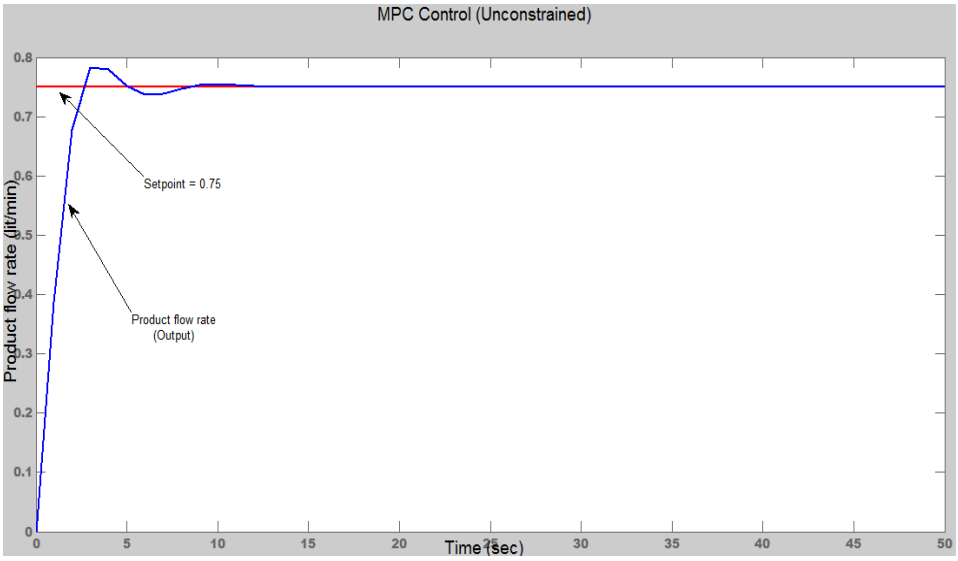

Figure 4.7: MPC Control (UNCONSTRAINED CASE)

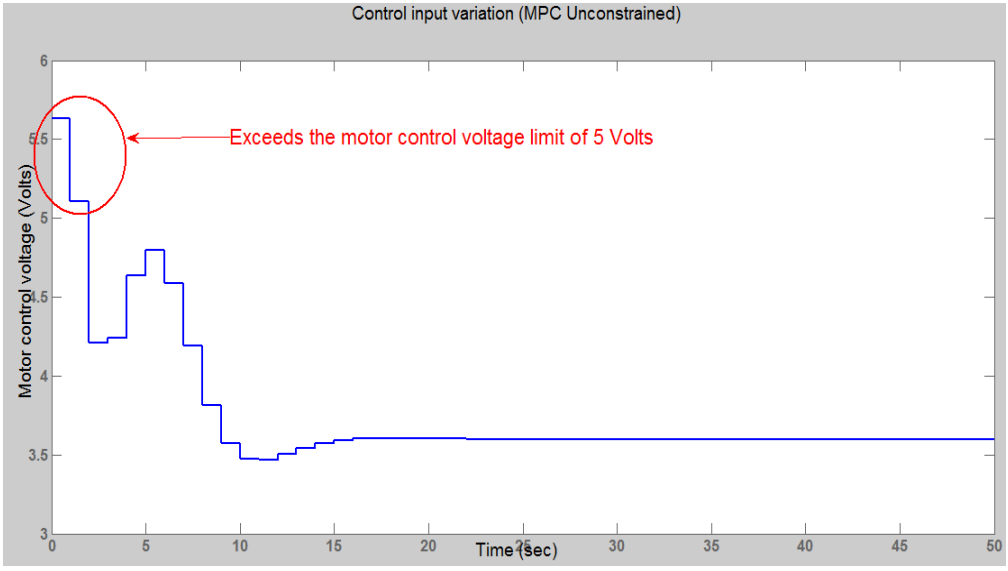

Figure 4.8: Control signal variation (UNCONSTRAINED CASE)

The problem with the unconstrained case is circled in red in Fig. 4.8 wherein the control signal exceeds the motor control voltage limit of 0-5V which is not possible for the proposed system.

4.7.4 MPC – Constrained Case

The simulation result for the constrained case is shown in Fig. 4.9 and 4.10.

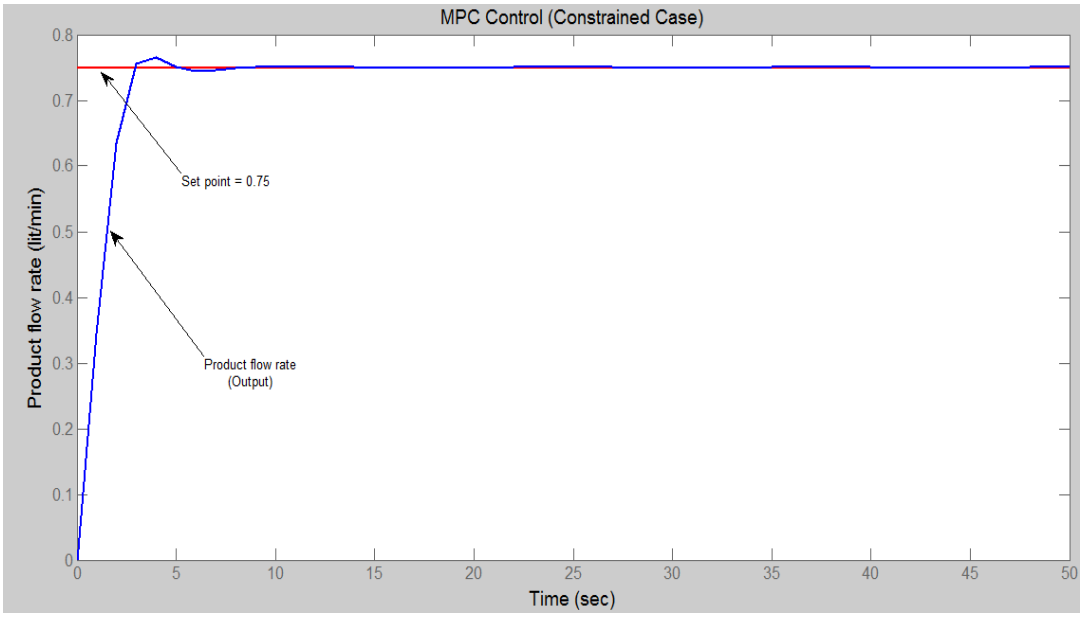

Figure 4.9: MPC Control (CONSTRAINED CASE)

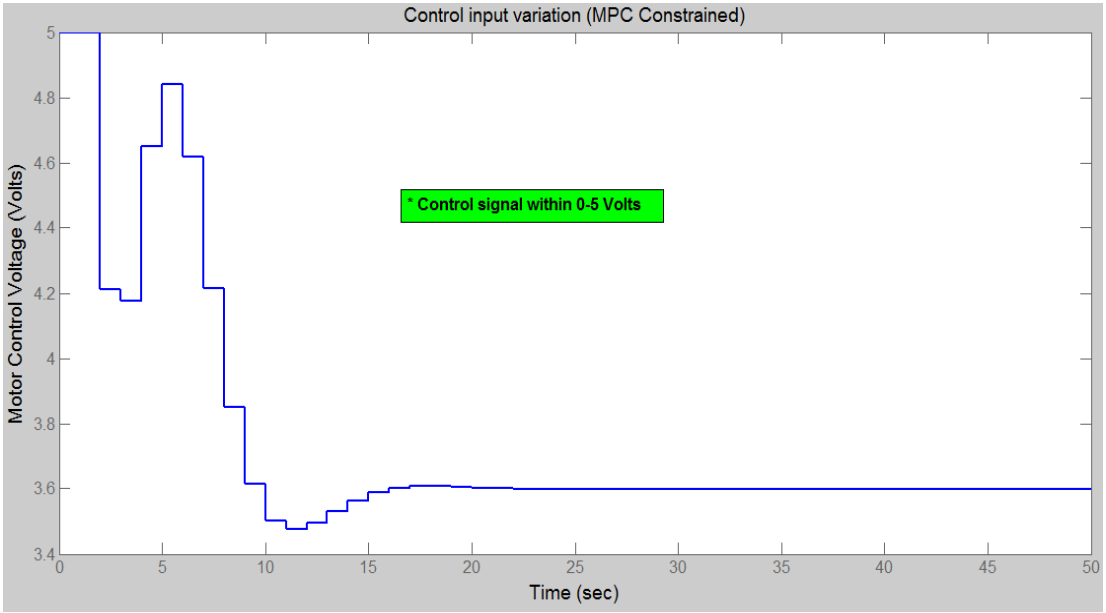

Figure 4.10: Control signal variation (CONSTRAINED CASE)

The constrained case gave better results compared to the unconstrained case in terms of satisfying the constraints, the settling time and the overshoot as seen in Fig. 4.9 and 4.10. Fig. 4.11 and 4.12 illustrate the robustness of the constrained model predictive control which does well even in the presence of a disturbance injected at t=20 seconds signifying its robustness.

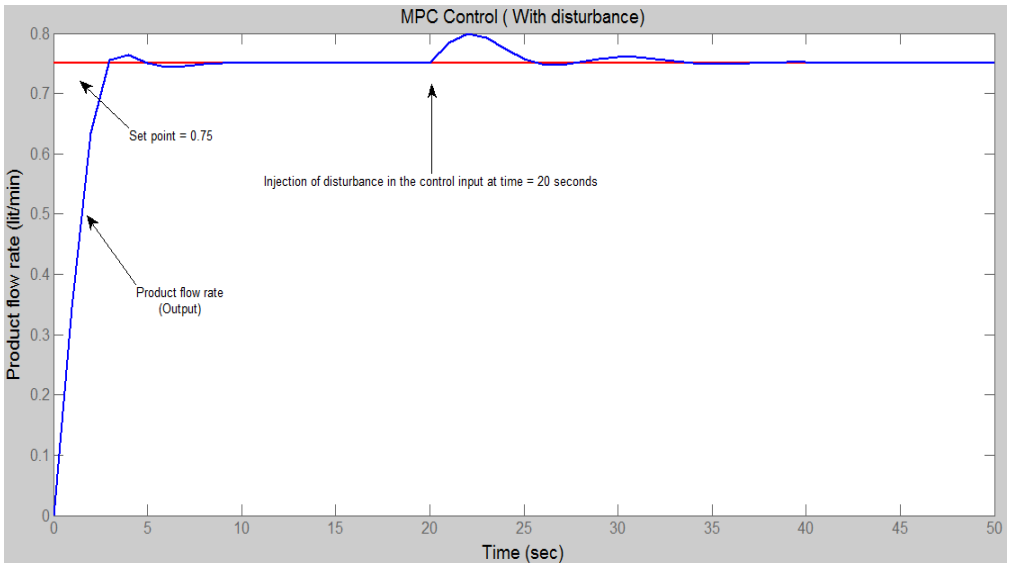

Figure 4.11: MPC Control (CONSTRAINED CASE WITH DISTURBANCE)

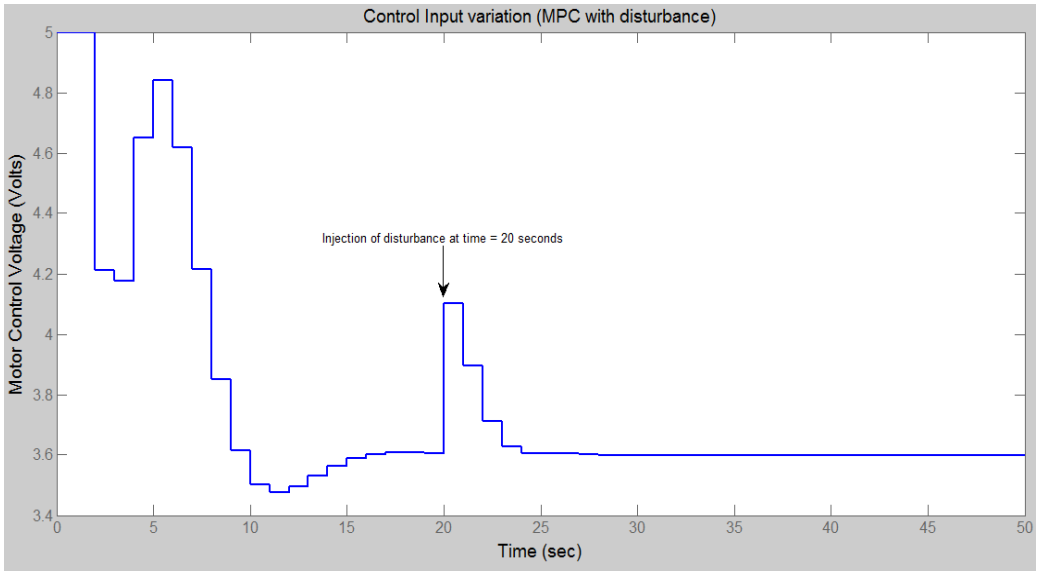

Figure 4.12: Control signal variation (CONSTRAINED CASE WITH DISTURBANCE)

Chapter 5

DISCUSSION, RESULTS AND CONCLUSION

5.1 Results and Discussion

This thesis work presents the various approaches to identify the small-scale reverse osmosis desalination system which is powered by batteries and develop appropriate control strategies. The desalination system being studied is also intended to be used with solar panels but the solar energy is utilized to charge the batteries with MPPT (Maximum power point tracking). The RO system then operates on batteries at night, at steady pressure. This ensures smooth and trouble-free operation of the system which is not guaranteed when solar energy is used as direct power source. For instance, when there is cloud cover, the solar energy might be insufficient in providing the required electricity to the system due to which the operating pressure might fall below osmotic pressure. This would halt the system and therefore doesn't ensure continuous trouble-free operation. Another important component of the system being studied is the energy recovery device called Clark Pump used to recover the energy from high pressure waste water called brine and reuses this energy in the system to increase system's efficiency.

The system was not in fully functional state due to malfunction of some of the sensors and pumps. First these problems were corrected to have the system in fully operational state and necessary additional instrumentation was done to monitor and control some of the critical parameters of the desalination system like flow meters for measuring the input and output flow rates, a temperature sensor for monitoring the temperature of water circulating through the system, as a safety indicator, a pressure transducer for monitoring the pressure of water in pipes to identify blockages in the system and a motor driver for controlling the speeds of the two inlet

pumps. The data acquisition system used is from National Instruments which is used with Lab VIEW software which provides visual medium for monitoring all the process parameters.

First objective is to evaluate the performance of the desalination system for which the setup is run at steady state and the data is collected for certain duration of time. The input water salinity at the start of experiment was 2130 ppm. The data collection is done for the current taken by the setup, the voltage across the motors based on which the specific energy consumption is calculated. Other important performance evaluation parameters like the salt rejection rate which is based on feed water and product water salinities and the recovery ratio using the feed water and product water flow rates, are also computed. Based on the collected data, the average current taken by the setup was 7.022Amps, the average voltage was 21.481V, the average Specific Energy Consumption was 2.585kWh/m3, the average product flow rate was 1.03lit/min and the product water conductivity settled at around 25ppm. The salt rejection rate was 98.8% and the recovery ratio of feed water to product water was found to be 10.55%. It can be concluded from this experiment that the system is working fine as it meets the design specifications of the system in terms of the current taken by the setup, salt rejection rate of the membrane and the flow rate.

The second objective was to identify system characteristics by evaluating polynomial and state-space models of the desalination system using system identification. The models were developed based on the experimental data collected from the system and were also validated using a separate experimental dataset. First, three polynomial models namely ARX, ARMAX and Output Error model were computed and compared based on a fixed model order (order-3) and fit percentages with the measured data. Two state-space models were also estimated based on subspace identification and prediction error method.

The third objective was to evaluate the performances of the two state space models estimated using system identification based on optimal control scheme called linear quadratic regulator. The state-space model based on subspace identification was further investigated for different penalties on the control input.

Another important controller called Model predictive control based on receding horizon principle was also applied to state-space model based on subspace identification for the unconstrained case and the constrained case respectively. The robustness of the model was also studied by injecting a small disturbance in the input variable and observing how the developed model predictive controller would react to it and fulfill the necessary control action.

5.2 Conclusion

The results obtained from performance evaluation of the small-scale reverse osmosis desalination system reveal that the system meets all the design specifications and can be used for further analysis such as system identification and subsequent control. The system identification results reveal that a third order output error model is better compared to ARX and ARMAX model of the same order. Two state-space models based on subspace identification and prediction error method were compared based on their optimal control simulation results which revealed that subspace identification is better in terms of the overall performance and hence was further investigated for different control penalties. It was observed that a decrease in control penalty would result in an improved performance. Since subspace identification was found to be better, it was considered for model predictive control. The simulation results reveal that a constrained model predictive control is more suited for the given system as compared to the unconstrained case. Also the constrained model predictive controller was found to be robust in presence of a small disturbance in the input variable.

REFERENCES

[1] Mohamed, E.S., et al., A direct coupled photovoltaic seawater reverse osmosis desalination system toward battery based systems - a technical and economical experimental comparative study. Desalination, 2008. 221(1-3): p. 17-22.

[2] Eltawil, M.A., Z. Zhengming, and L.Q. Yuan, A review of renewable energy technologies integrated with desalination systems. Renewable & Sustainable Energy Reviews, 2009. 13(9): p. 2245-2262.

[3] Vengosh, A., Salinization and Saline Environments. Treatise on Geochemistry, 2003. 9.

[4] Insights from the Comprehensive Assessment of Water Management in Agriculture, in World Water Week, C. International Water Management Institute (IWMI), Sri Lanka, Editor. 2006: Stockholm.

[5] http://en.wikipedia.org/wiki/Salinity (Date accessed: 3 July 2013)

[6] Voutchkov, N, Introduction to Reverse Osmosis Desalination. www.SunCam.com Copyright 2010 Nikolay Voutchkov.

[7] Sabine Lattemann, I.E., Andrea Schafer, Chapter 2, Global Desalination Situation., Vol. 2. 2010 :Elsevier.

[8] Mohamed, A.E., Zhengming, Z., Liquiang, Y, A review of renewable energy technologies integrated with desalination system. Renewable & Sustainable Energy Reviews, Vol. 13, Issue 9, Dec. 2009, Pages 2245-2262.

[9] Lattemann, S., Schafer, A, Global Desalination Situation . Vol. 2. 2010: Elsevier.

[10] www.hydrotec.co.uk/InfoCentre/Filtration/tabid/138/Default.aspx (Date accessed: 3 July 2013).

[11] Went, J., Kroemke, F., Schmoch, H. and Vetter, M. (2009). Energy demand for desalination with solar powered reverse osmosis units. Proceedings of the European Desalination Society Conference Desalination for the Environment - Clean Water and Energy, Baden-Baden, Germany, 17-20 May 2009, European Desalination Society.

[12] http://www.spectrawatermakers.com/technology/clark-pump.html (Date Accessed: 3 July 2013)

[13] Pankratz., T, IDA desalination yearbook 2008-2009. Global Water Intelligence. Oxford.

[14] El-Dessouky, H.T., Ettouney, H.M, Fundamentals of Salt Water Desalination. Amsterdam, Elsevier (2002).

[15] Spiegler, K.S., El-Sayed, Y.M, A Desalination Primer: Introductory Book for Students and Newcomers to Desalination. Balaban Desalination Publications (1994).

[16] Dow, Dow Chemical Company (2009). http://www.dow.com/. (Accessed: 13 July 2013).

[17] Koch, Koch Membrane Systems (2009). http://www.kochmembrane.com/. (Accessed: 23 July 2013).

[18] Toyobo, Toyobo Group (2009). http://www.toyobo.co.jp/. (Accessed: 14 July 2013).

[19] Toray, Toray Group (2009). http://www.toray-membrane.com. (Accessed: 16 July 2013).

[20] Reid, C.E., Breton, E.J, Water and ion flow across cellulosic membranes. Journal of Applied Polymer Science 1(2): 133-143. (1959).

[21] Buros, O.K., El-Nashar, A.M., Bakish, R, The U.S.A.I.D. Desalination Manual. International Desalination and Environmental Association (IDEA). (1981).

[22] Wilf, M., Awerbuch, L., Bartels, C., Mickley, M., Pearce, G., Voutchkov, N, The guidebook to membrane desalination technology: reverse osmosis, nano-filtration and hybrid systems process, design, applications and economics. L'Aquila, Italy, Balaban Desalination Publications. (2007).

[23] Greenlee, L. F., Lawler, D. F., Freeman, B. D., Marrot, B. and Moulin, P, Reverse osmosis desalination: Water sources, technology, and today's challenges. Water Research 43(9): 2317-2348. (2009).

[24] Van der Bruggen, B., Vandecasteele, C, Distillation vs. membrane filtration: overview of process evolutions in seawater desalination. Desalination 143(3): 207-218. (2002).

[25] Van der Bruggen, B, Desalination by distillation and by reverse osmosis -- trends towards the future. Membrane Technology 2003(2): 6-9. (2003).

[26] MacHarg, J., Truby, R, West Coast researchers seek to demonstrate SWRO affordability. International Desalination and Water Reuse Quarterly 14(3). (2004).

[27] MacHarg, J., Seacord, T. F., Sessions, B, ADC baseline tests reveal trends in membrane performance. International Desalination and Water Reuse Quarterly 18(2): 30-39. (2008).

[28] Medina San Juan, J. A, Desalación de aguas salobres y del mar: Osmosis inversa. Madrid, Mundi-Prensa. (2000).

[29] http://14.139.160.15/courses/103105060/Sde_pdf/Module-3.pdf (Accessed: 20 July 2013)

[30] H.T. El-Dessouky., H.M. Ettouney, Fundamentals of Salt Water Desalination, Elsevier Science B.V, Amsterdam, The Netherlands, 2002.

[31] http://www.synderfiltration.com/services/membrane-filtration-solutions (Date Accessed: 18 July 2013).

[32] Schippers, J.C, One-day intensive course on membrane fouling and pre-treatment in RO technology. Theory and practice. European Desalination Society. (2007).

[33] Doujak, E., List, B, Application of PIV for the Design of Pelton Runners for RO-Systems. Proceedings of the Renewable Energy Sources for Islands, Tourism and Water Desalination Conference, Crete, Greece, 26-28 May 2003, EREC (European Renewable Energy Council), 533-540. (2003).

[34] Bermudez-Contreras, A., Thomson, M, Modified operation of a small scale energy recovery device for seawater reverse osmosis. Proceedings of the European Desalination Society Conference Desalination for the Environment - Clean Water and Energy, Baden-Baden, Germany, European Desalination Society. (2009).

[35] Oklejas, R.A., Oklejas, E, Power recovery pump turbine. United States Patent 4966708. (1990).

[36] Andrews, W. T., Laker, D.S, A twelve-year history of large scale application of work-exchanger energy recovery technology. Desalination 138(1-3): 201-206. (2001).

[37] http://www.energyrecovery.com (Date Accessed: 26 July 2013)

[38] Qiblawey, H., Banat, F., Al-Nasser, Q, Performance of reverse osmosis pilot plant powered by Photovoltaic in Jordan. Renewable Energy. (2011).

[39] Sobana, S., Panda, R.C, Identification, Modeling and Control of Continuous Reverse Osmosis Desalination System: A Review. Separation Science and Technology. (2011).

[40] Gambier, A., Dynamic Modeling of a Simple Reverse Osmosis Desalination Plant for Advanced Control Purposes. American Control Conference. (2007).

[41] Gambier, A., Control of a Reverse Osmosis Plant by Using a Robust PID Design Based on Multi-objective Optimization. IEEE Conference on Decision and Control. (2011).

[42] Chaaben, A.B., Andoulsi, R., Sellami, A., Mhiri, R, MIMO Modeling Approach for a Small Photovoltaic Reverse Osmosis Desalination System. Journal of Applied Fluid Mechanics, Vol 4, No. 1, 35-41. (2011).

[43] Murray Thomson, Reverse-Osmosis Desalination of Seawater powered by Photo-voltaics Without Batteries. (2003).

[44] Palacin, L., Tadeo, F., Salazar, J., Initial Validation of a Reverse Osmosis Simulator. University of Valladolid, Dept. of Systems Engineering and Control. (2010)

[45] Bilton, A.M., Kelley, L.C., Dubowsky, S, Photovoltaic reverse osmosis – Feasibility and a pathway to develop technology. Desalination and Water Treatment. (2011).

[46] Joyce, A., Loureiro, D., Rodrigues, Carlos., Castro, S, Small reverse osmosis units using PV systems for water purification in rural places. Desalination 137 39-44. (2001).

[47] Suleimani, Z.A., Nair, V.A, Desalination by solar-powered reverse osmosis in a remote area of Sultanate of Oman. Applied Energy 65 367-380. (2000).

[48] Abbas, A, Model Predictive Control of a reverse osmosis desalination unit. Desalination 194 268-280. (2006).

[49] Alatiqi, I.M., Ghabris, A.H., Ebrahim, S, System Identification and Control of Reverse Osmosis Desalination. Desalination 75 119-140. (1989).

[50] Greenlee, L.F., Lawler, D.F., Freeman, B.D., Marrot, B., Moulin, P, Reverse Osmosis Desalination: Water sources, technology and today's challenges. Water Research 43 2317-2348. (2009).

[51] Ghermandi, A. and R. Messalem, Solar-driven desalination with Reverse Osmosis: the state of the art. Desalination and Water Treatment, 7(1-3): p. 285-296. (2009).

[52] Alatiqi, I., Ettouney, H., El-Dessouky, H, Process control in water desalination industry: An Overview. Desalination 126 15-32. (1999).

[53] CLARK PUMP: http://www.spectrawatermakers.com. (Accessed: May 23 2013)

[54] WATER ACCUMULATOR: http://www.shurflo.com. (Accessed: May 23 2013)

[55] LabVIEW: http://www.ni.com/gettingstarted/labviewbasics (Accessed: May 22 2013)

[56] USB-6009 DAQ Datasheet: http://www.ni.com/pdf/manuals/371303m.pdf (Accessed: July 24 2013)

[57] LabVIEW Software. http://www.ni.com/labview.

[58] Data-logging Basics: http://www.ni.com/academic/students/learn/ (Accessed: May 23 2013)

[59] Flow meter Datasheet: http://www.omega.com/Green/pdf/FPR301_302_303_304.pdf (Impeller type) (Accessed: May 21 2013)

[60] Flow meter Datasheet: http://www.omega.com/Green/pdf/FTB2000.pdf (Turbine-type) (Accessed: May 21 2013)

[61] Pressure Transducer Datasheet: http://www.meas-spec.com/downloads/MSP300.pdf (Accessed: May 24 2013)

[62] Temperature Sensor Datasheet: http://www.omega.com/Temperature/pdf/SA1-TH-44000.pdf (Accessed: May 27 2013)

[63] Salinity Meter Datasheet: http://www.tdsmeter.com/products/tds3.html (Accessed: May 12 2013)

[64] Motor Driver Datasheet: http://www.robot-electronics.co.uk/htm/md03tech.htm (Accessed: 29 May 2013)

[65] L. Ljung, System Identification: Theory for the user, Prentice Hall Information and System Sciences Series. (1999).

[66] L. Ljung, System Identification Toolbox: User Guide, Math Works, Inc., Natick, 2012b.

[67] F.Huerta., S.Cobreces., F.J.Rodriguez., M.Moranchel., I.Sanz, State-space black box model identification of a voltage-source converter with LCL filter, 3rd IEEE International Symposium on Power Electronics for Distributed Generation Systems. (2012).

[68] T. Katayama, Subspace Methods for System Identification. London: Springer-Verlag. (2005).

[69] P. V. Overschee., B. D. Moor, N4SID: Subspace Algorithms for the Identification of Combined Deterministic-Stochastic Systems, Automatica, Vol. 30, pp.75-93. (1994).

[70] L. Ljung, System Identification: Theory for the User. Englewood Cliffs, NJ: Prentice-Hall, (1987).

[71] W. Favoreel., S. VanHuffel., B. DeMoor., V. Sima., M. Verhaegen, Comparative study between three subspace identification algorithms, Simulation, pp. 1-6. (1998).

[72] R.A. Fisher, On an absolute criterion for fitting frequency curves. Mess. Math., 41:155. (1912)

[73] G.E.P. Box., D.R.Jenkins, Time-series analysis, Forecasting and Control. Holden-Day, San Francisco. (1970).

[74] K.J.Astrom., T. Bohlin, Numerical Identification of linear dynamic systems from normal operating records. IFAC Symposium on Self-Adaptive systems, Teddington, England (1965).

[75] Donald E. Kirk, Optimal Control Theory: An Introduction, Dover Publications, Inc., Mineola, New York. (2012).

[76] K.S.Holkar., L.M.Waghmare, “Discrete Model Predictive Control for DC drive Using Orthonormal Basis function”, UKACC International Conference on CONTROL, Coventry, UK, pp. 435-440 (2010).

[77] E. F. Camacho., C. Bordons, Model Predictive Control, Springer Publication, London. (2007).

[78] A. Bemporad., M. Morari., N.L. Ricker, Model Predictive Control Toolbox: Getting Started Guide, The Math Works, Inc., Natick, 2012a.

[79] A. Bemporad., M. Morari., N.L. Ricker, Model Predictive Control Toolbox: User Guide, The Math Works, Inc., Natick, 2012a.

VITAE

Name: Mohammed Riaz Ahmed

Nationality: Indian

Date of Birth: 28th April, 1988

Permanent Address: H. No.: 16-2-41/8,

Akberbagh, Malakpet,

Hyderabad – 500028, Andhra Pradesh, INDIA

Email: riaza471@gmail.com

Phone: +966-534339721

Education: 1) Bachelor of Engineering (B.S),

Instrumentation Engineering, Osmania University (2005-2009)

2) Intermediate,

Nalanda Junior College, Hyderabad (2003-2005)

3) High School,

Madina High School, Hyderabad, (1993-2003)

Experience: Worked as PROJECT ASSISTANT in Bharat Heavy Electricals Limited (BHEL), Hyderabad, India in Instrumentation and Control Engineering Department. (Sept. 2010 to Sept. 2011).

Skills & Strengths: 1) Determined to learn and adapt to new opportunities and challenges.

2) Excellent inter-personal and communication skills.

3) Team-oriented individual with strong commitment to work.

Other Activities: 1) Attended seminars and workshops on PLC, DCS and SCADA at Advanced Training Institute (ATI), Hyderabad, India.

2) Participated in "Symposium on Industrial Systems & Control" conducted by Systems Engineering Dept. at KFUPM.

3) Participated in a 3-day training on "Instrumentation and Data Acquisition" conducted by National Instruments (NI) at KFUPM.

3) Delivered seminars at Bachelors' and Masters' level on various topics like "Finger-print based attendance monitoring system", "Wearable Health Monitoring System and Instrumentation" and "Modeling & Identification of a Boiler", among others.

Honors & Achievements: 1) Ranked amongst top 5 in Bachelors' program.

2) Presented with the best communication and process trainee awards at DELL International, Hyderabad, India